Spectroscopy of Strange Mesons with COMPASS and AMBER

Stefan Wallner for the COMPASS and AMBER collaborations
(swallner@mpp.mpg.de)

Technical University of Munich, present address Max Planck Institute for Physics

XVI$^{\text{th}}$ Quark Confinement and the Hadron Spectrum Conference
August 21, 2024

COMPASS

AMBER
Apparatus for Meson and Baryon Experimental Research

MAX PLANCK INSTITUTE FOR PHYSICS

TUM

The Strange-Meson Spectrum

Understanding the light-meson spectrum

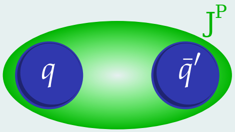

- Completing $\mathrm{SU(3)_{flavor}}$ multiplets
- Identifying supernumerary states
  - ➥ Search for exotic strange mesons

Input to other fields of physics

- Strange mesons appear as resonances in multi-body hadronic final states with kaons
- Searches for CP violation
- Searches for physics beyond SM

The Strange-Meson Spectrum

Understanding the light-meson spectrum

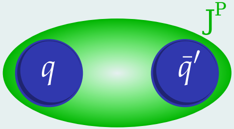

- Completing $\mathrm{SU(3)_{flavor}}$ multiplets
- Identifying supernumerary states
  - ➥ Search for exotic strange mesons

Input to other fields of physics

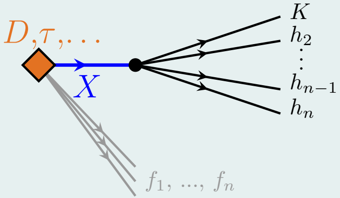

- Strange mesons appear as resonances in multi-body hadronic final states with kaons
- Searches for CP violation
- Searches for physics beyond SM

The Strange-Meson Spectrum

[SW PhD]

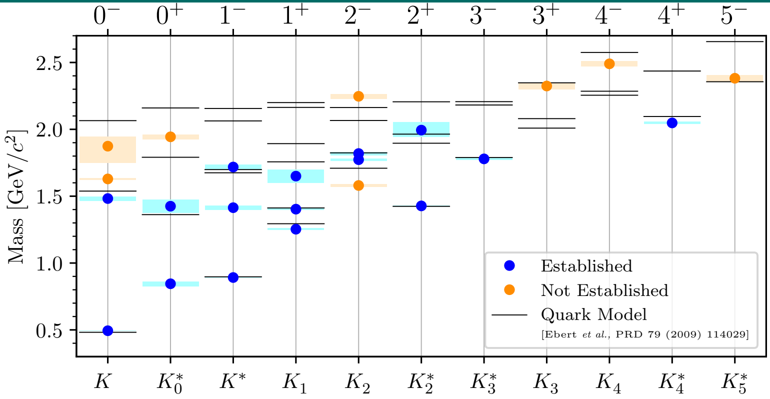

PDG lists 25 strange mesons (2022)

- 16 established states, 9 need further confirmation
- Missing states with respect to quark-model predictions
- Many measurements performed more than 30 years ago

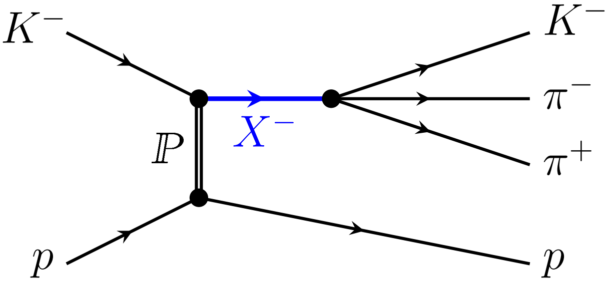

- Diffractive scattering of high-energy kaon beam
- Strange mesons appear as intermediate resonances X^-
- $K^-\pi^-\pi^+$ final state
  - Study in principle all strange mesons
  - Study a wide mass range
  - Study different decay modes

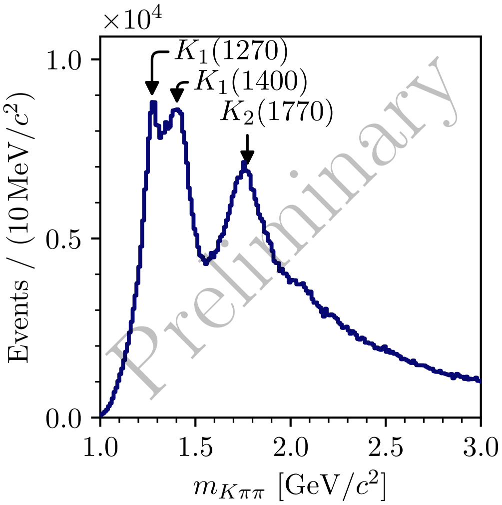

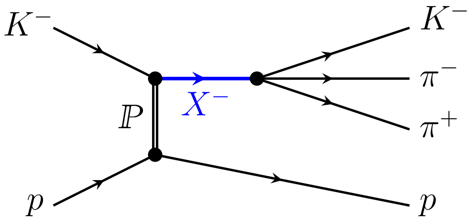

- World's largest data set of about 720 k events
- Rich spectrum of overlapping and interfering X^-
  - Dominant well-known states
  - States with lower intensity are "hidden"

Partial-Wave Analysis of the $K^-\pi^-\pi^+$ Final State

Partial wave: $J^P\, M^\varepsilon\, \xi\, b^-\, L$

- J^P spin and parity
- M^ε spin projection
- ξ isobar resonance
- b^- bachelor particle
- L orbital angular momentum

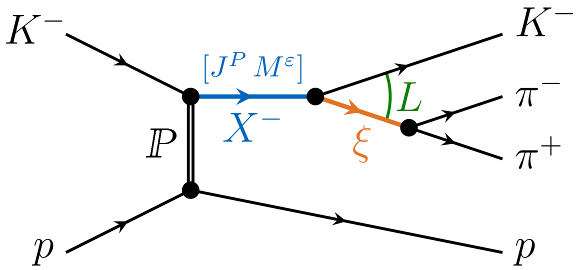

Partial-Wave Analysis of the $K^-\pi^-\pi^+$ Final State

Partial wave: $J^P\, M^\varepsilon\, \xi\, b^-\, L$

- J^P spin and parity
- M^ε spin projection
- ξ isobar resonance
- b^- bachelor particle
- L orbital angular momentum

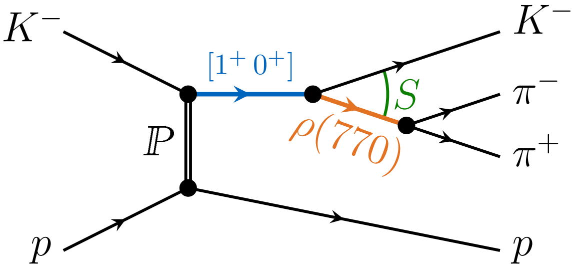

Data: 720 k diffractively produced $K^-\pi^-\pi^+$ candidates

Data: 720 k diffractively produced $K^-\pi^-\pi^+$ candidates

(I) Partial-Wave Decomposition

Performed independently in narrow $(m_{K\pi\pi}, t')$ cells

No assumption about $K\pi\pi$ resonances

Partial waves: Intensities and relative phases as a function of $(m_{K\pi\pi}, t')$

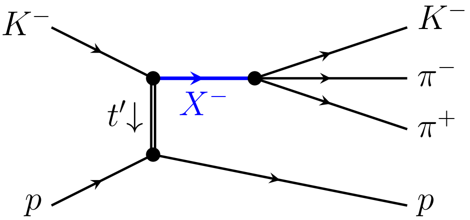

Partial-Wave Analysis of the $K^-\pi^-\pi^+$ Final State

Data: 720 k diffractively produced $K^-\pi^-\pi^+$ candidates

(I) Partial-Wave Decomposition
Performed independently in narrow $(m_{K\pi\pi}, t')$ cells
No assumption about $K\pi\pi$ resonances

Partial waves: Intensities and relative phases as a function of $(m_{K\pi\pi}, t')$

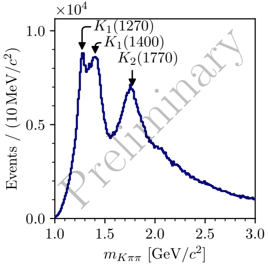

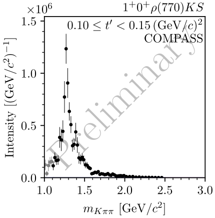

Partial-Wave Analysis of the $K^-\pi^-\pi^+$ Final State

Data: 720 k diffractively produced $K^-\pi^-\pi^+$ candidates

(I) Partial-Wave Decomposition
Performed independently in narrow $(m_{K\pi\pi}, t')$ cells
No assumption about $K\pi\pi$ resonances

Partial waves: Intensities and relative phases as a function of $(m_{K\pi\pi}, t')$

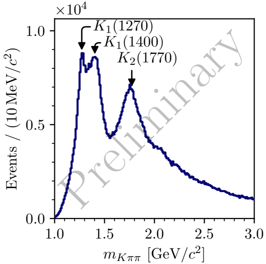

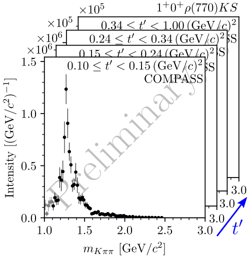

Data: 720 k diffractively produced $K^-\pi^-\pi^+$ candidates

(I) Partial-Wave Decomposition

Performed independently in narrow $(m_{K\pi\pi}, t')$ cells

No assumption about $K\pi\pi$ resonances

Partial waves: Intensities and relative phases as a function of $(m_{K\pi\pi}, t')$

(II) Resonance-Model Fit

Model $m_{K\pi\pi}$ dependence of partial waves

$K\pi\pi$ resonances and background

Resonance parameters: Masses and widths of the strange-meson resonances

Partial-Wave Analysis of the $K^-\pi^-\pi^+$ Final State

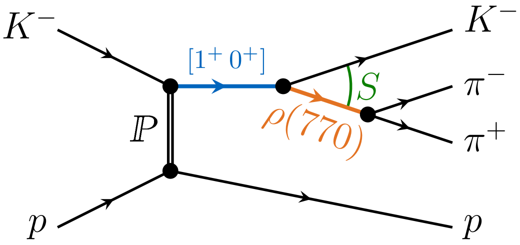

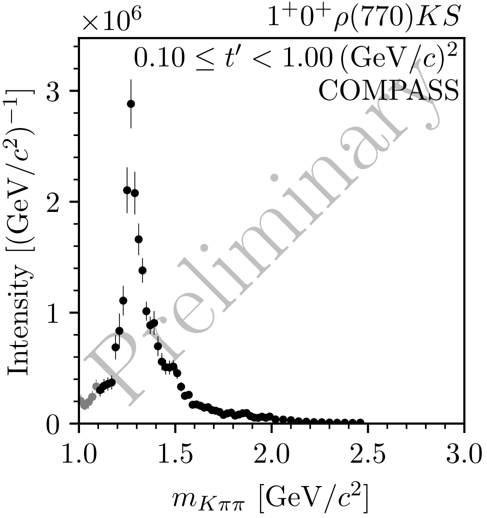

- Partial-wave amplitudes in $(m_{K\pi\pi}, t')$ bins
  - Inferred wave set from data using regularization-based model-selection techniques
  - Bootstrap resampling to improve uncertainty estimates
  - Detailed Monte-Carlo input-output studies
- Model $m_{K\pi\pi}$ dependence of partial-wave amplitudes
- Breit-Wigner amplitudes for $K^-\pi^-\pi^+$ resonance components
- Coherent non-resonant component parameterizing other $K^-\pi^-\pi^+$ production mechanisms
- Developed scheme to handle incoherent backgrounds
  - Incoherent background from π^- diffraction to $\pi^-\pi^-\pi^+$ explicitly modeled by COMPASS $\pi^-\pi^-\pi^+$ analysis
  - Incoherent effective background component parameterizing other background processes

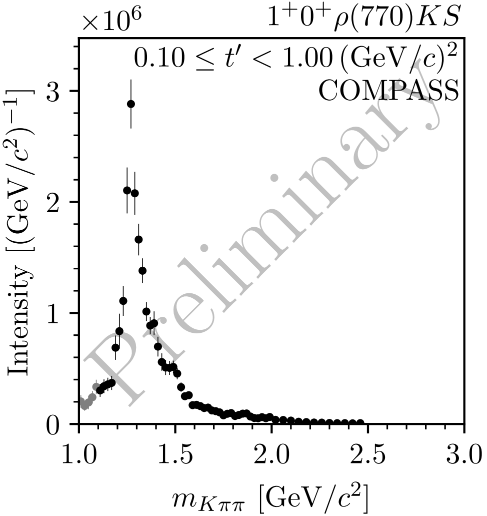

Partial-Wave Analysis of the $K^-\pi^-\pi^+$ Final State

[SW PhD]

- Partial-wave amplitudes in $(m_{K\pi\pi}, t')$ bins
  - Inferred wave set from data using regularization-based model-selection techniques
  - Bootstrap resampling to improve uncertainty estimates
  - Detailed Monte-Carlo input-output studies
- Model $m_{K\pi\pi}$ dependence of partial-wave amplitudes
- Breit-Wigner amplitudes for $K^-\pi^-\pi^+$ resonance components
- Coherent non-resonant component parameterizing other $K^-\pi^-\pi^+$ production mechanisms
- Developed scheme to handle incoherent backgrounds
  - Incoherent background from π^- diffraction to $\pi^-\pi^-\pi^+$ explicitly modeled by COMPASS $\pi^-\pi^-\pi^+$ analysis
  - Incoherent effective background component parameterizing other background processes

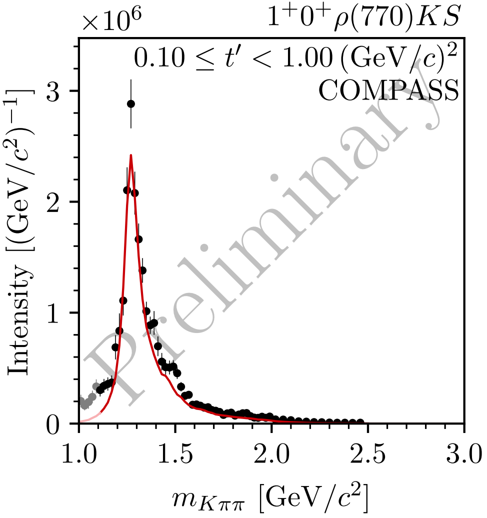

Partial-Wave Analysis of the $K^-\pi^-\pi^+$ Final State

[SW PhD]

- Partial-wave amplitudes in $(m_{K\pi\pi}, t')$ bins
  - Inferred wave set from data using regularization-based model-selection techniques
  - Bootstrap resampling to improve uncertainty estimates
  - Detailed Monte-Carlo input-output studies
- Model $m_{K\pi\pi}$ dependence of partial-wave amplitudes
- Breit-Wigner amplitudes for $K^-\pi^-\pi^+$ resonance components
- Coherent non-resonant component parameterizing other $K^-\pi^-\pi^+$ production mechanisms
- Developed scheme to handle incoherent backgrounds
  - Incoherent background from π^- diffraction to $\pi^-\pi^-\pi^+$ explicitly modeled by COMPASS $\pi^-\pi^-\pi^+$ analysis
  - Incoherent effective background component parameterizing other background processes

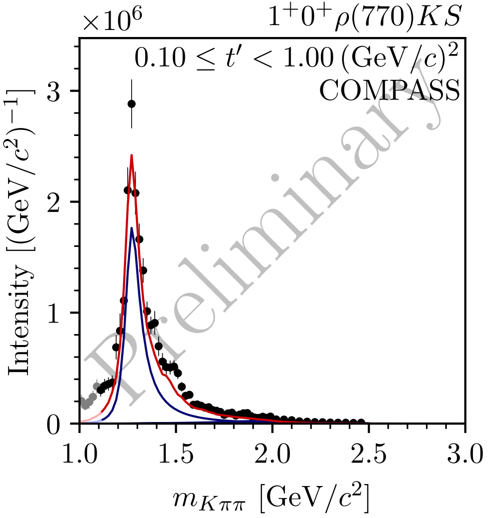

Partial-Wave Analysis of the $K^-\pi^-\pi^+$ Final State

- Partial-wave amplitudes in $(m_{K\pi\pi}, t')$ bins
  - Inferred wave set from data using regularization-based model-selection techniques
  - Bootstrap resampling to improve uncertainty estimates
  - Detailed Monte-Carlo input-output studies
- Model $m_{K\pi\pi}$ dependence of partial-wave amplitudes
- Breit-Wigner amplitudes for $K^-\pi^-\pi^+$ resonance components
- Coherent non-resonant component parameterizing other $K^-\pi^-\pi^+$ production mechanisms
- Developed scheme to handle incoherent backgrounds
  - Incoherent background from π^- diffraction to $\pi^-\pi^-\pi^+$ explicitly modeled by COMPASS $\pi^-\pi^-\pi^+$ analysis
  - Incoherent effective background component parameterizing other background processes

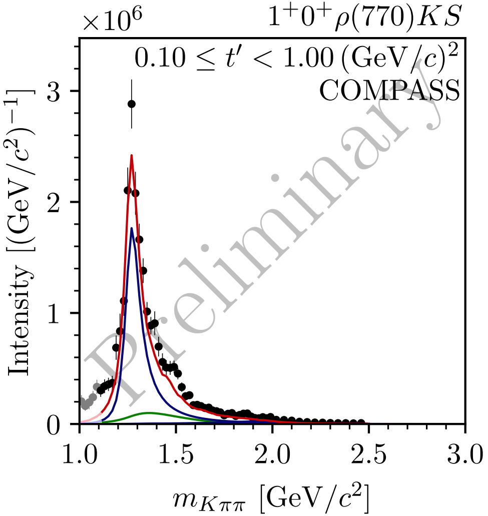

[SW PhD]

- Partial-wave amplitudes in $(m_{K\pi\pi}, t')$ bins
  - Inferred wave set from data using regularization-based model-selection techniques
  - Bootstrap resampling to improve uncertainty estimates
  - Detailed Monte-Carlo input-output studies
- Model $m_{K\pi\pi}$ dependence of partial-wave amplitudes
- Breit-Wigner amplitudes for $K^-\pi^-\pi^+$ resonance components
- Coherent non-resonant component parameterizing other $K^-\pi^-\pi^+$ production mechanisms
- Developed scheme to handle incoherent backgrounds
  - Incoherent background from π^- diffraction to $\pi^-\pi^-\pi^+$ explicitly modeled by COMPASS $\pi^-\pi^-\pi^+$ analysis
  - Incoherent effective background component parameterizing other background processes

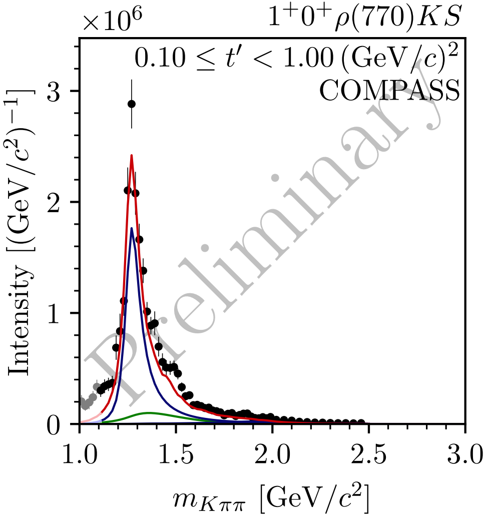

Partial-Wave Analysis of the $K^-\pi^-\pi^+$ Final State

- Partial-wave amplitudes in $(m_{K\pi\pi}, t')$ bins
  - Inferred wave set from data using regularization-based model-selection techniques
  - Bootstrap resampling to improve uncertainty estimates
  - Detailed Monte-Carlo input-output studies
- Model $m_{K\pi\pi}$ dependence of partial-wave amplitudes
- Breit-Wigner amplitudes for $K^-\pi^-\pi^+$ resonance components
- Coherent non-resonant component parameterizing other $K^-\pi^-\pi^+$ production mechanisms
- Developed scheme to handle incoherent backgrounds
  - Incoherent background from π^- diffraction to $\pi^-\pi^-\pi^+$ explicitly modeled by COMPASS $\pi^-\pi^-\pi^+$ analysis
  - Incoherent effective background component parameterizing other background processes

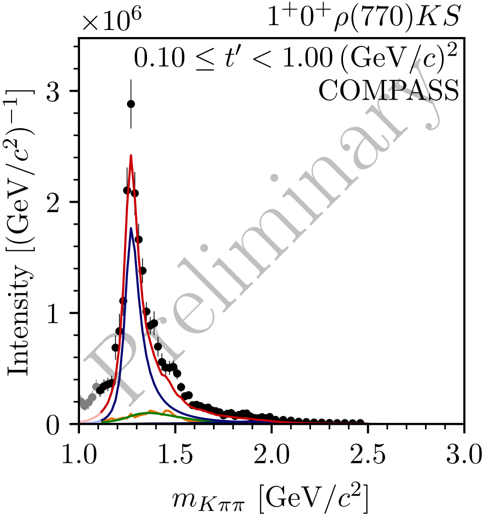

- Partial-wave amplitudes in $(m_{K\pi\pi}, t')$ bins
  - Inferred wave set from data using regularization-based model-selection techniques
  - Bootstrap resampling to improve uncertainty estimates
  - Detailed Monte-Carlo input-output studies
- Model $m_{K\pi\pi}$ dependence of partial-wave amplitudes
- Breit-Wigner amplitudes for $K^-\pi^-\pi^+$ resonance components
- Coherent non-resonant component parameterizing other $K^-\pi^-\pi^+$ production mechanisms
- Developed scheme to handle incoherent backgrounds
  - Incoherent background from π^- diffraction to $\pi^-\pi^-\pi^+$ explicitly modeled by COMPASS $\pi^-\pi^-\pi^+$ analysis
  - Incoherent effective background component parameterizing other background processes

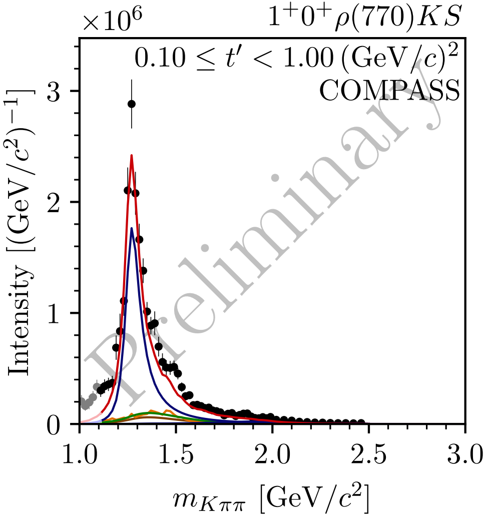

Partial-Wave Analysis of the $K^-\pi^-\pi^+$ Final State

- Simultaneously included 14 partial waves in resonance-model fit
- Modeled by 13 strange-meson resonance components
- Using measured intensities and interference terms (relative phases)

Partial-Wave Analysis of the $K^-\pi^-\pi^+$ Final State

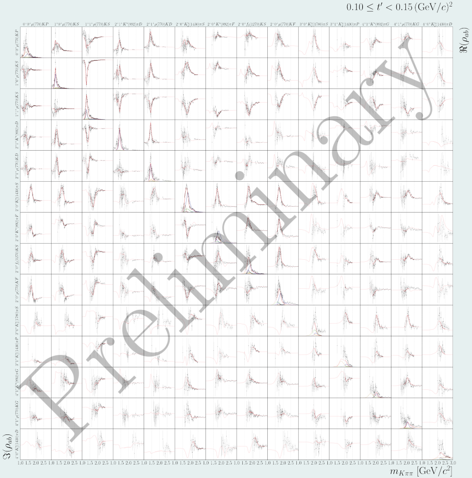

Partial-Wave Analysis of the $K^-\pi^-\pi^+$ Final State

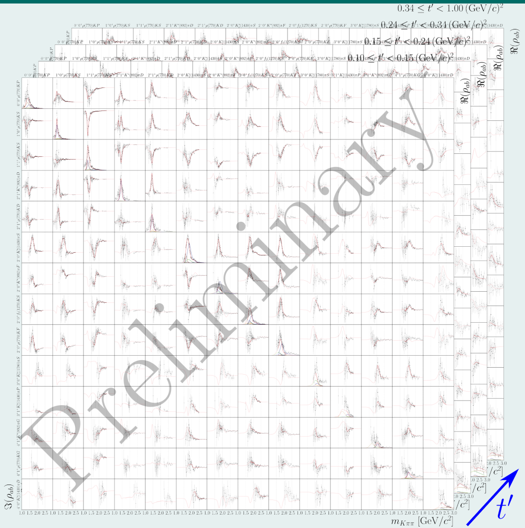

Partial Waves with $J^P = 1^+$

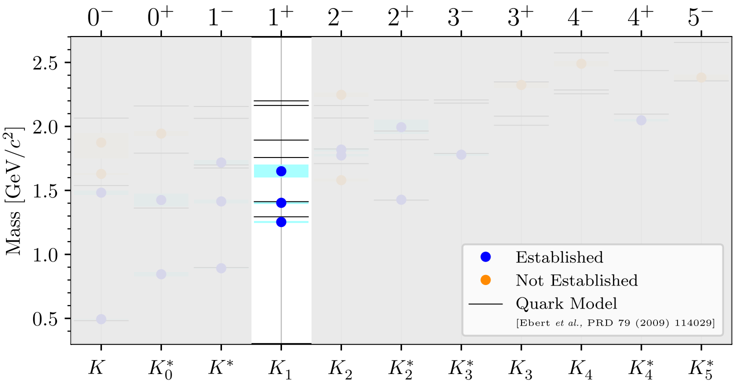

PDG
(2022)

- Two near-by states $K_1(1270)$ and $K_1(1400)$
- Excited $K_1(1650)$

Partial Waves with $J^P = 1^+$

- Study K_1 states in $\rho(770)K$ decay with $M^\varepsilon = 0^+$
- Dominated by $K_1(1270)$
- Similar spectrum also in $M^\varepsilon = 1^+$ wave
- Indications for excited K_1' mainly in $M^\varepsilon = 1^+$ wave

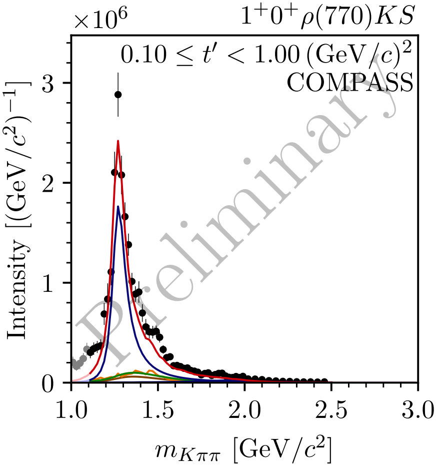

Partial Waves with $J^P = 1^+$

- Study K_1 states in $\rho(770)K$ decay with $M^\varepsilon = 0^+$
- Dominated by $K_1(1270)$
- Similar spectrum also in $M^\varepsilon = 1^+$ wave
- Indications for excited K_1' mainly in $M^\varepsilon = 1^+$ wave

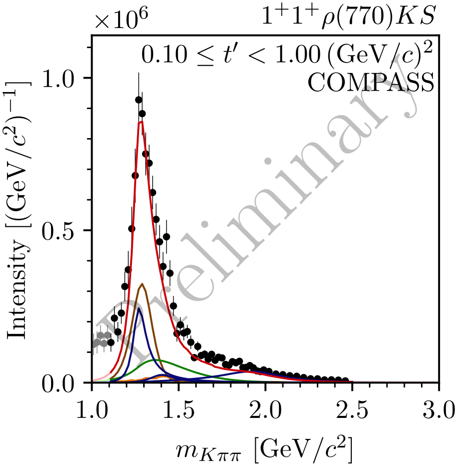

Partial Waves with $J^P = 1^+$

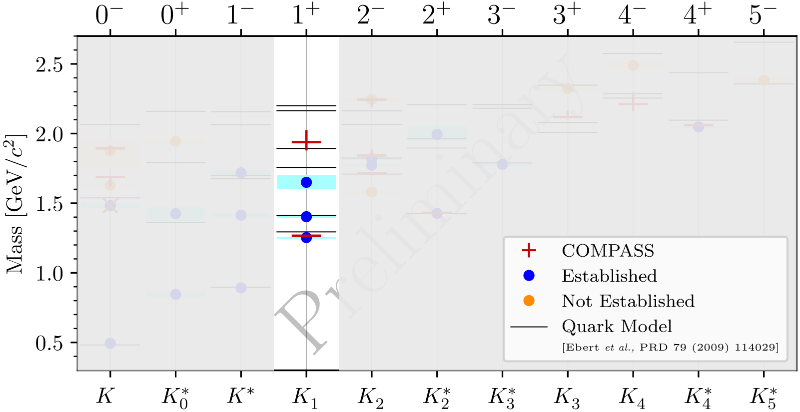

$K_1(1270)$

- Resonance parameters in agreement with previous measurements

Partial Waves with $J^P = 1^+$

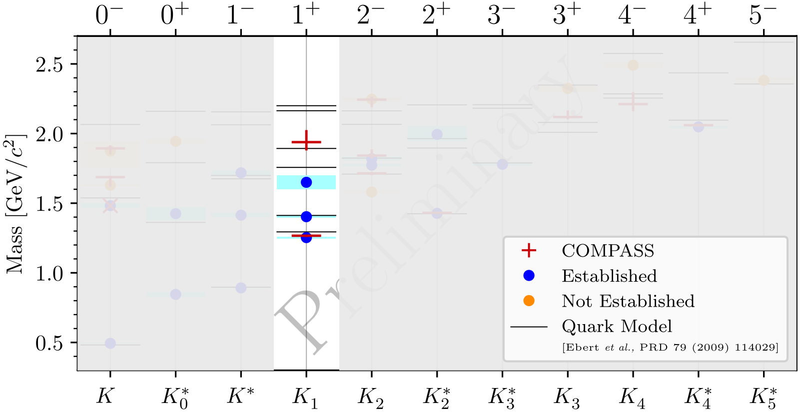

K_1'

- Larger mass and width compared to PDG average of $K_1(1650)$
- PDG average from single measurement; fit to intensity spectrum only [NPB 276 (1986) 667]
- Our estimates consistent with recent measurement in $B^+ \to J/\psi\phi K^+$ at LHCb [PRL 127 (2021) 082001]

K_3 and K_4 Mesons

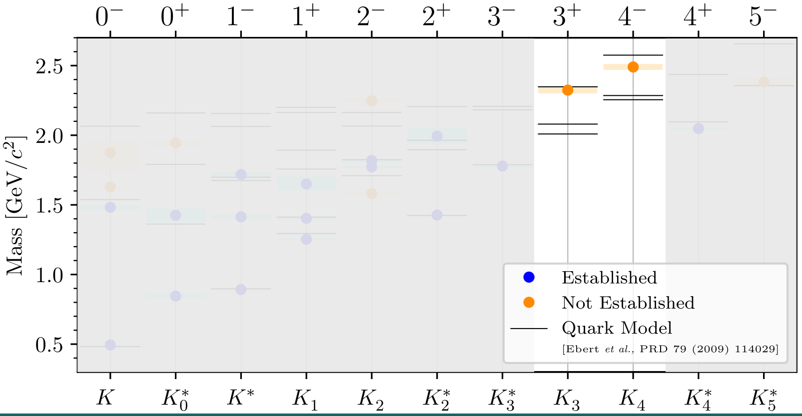

- $K_3(2320)$ and $K_4(2500)$ listed by the PDG
- Need further confirmation
- Seen only in $\Lambda\bar{p}$ final state by few experiments

K_3 and K_4 Mesons

- Observe K_3 signal at about 2.1 GeV/c^2
  - in $K_3^*(1780)\pi$ and $K_2^*(1430)\pi$ decays
- Evidence for K_4 signal at about 2.2 GeV/c^2
  - in $K_2^*(1430)\pi$ decay

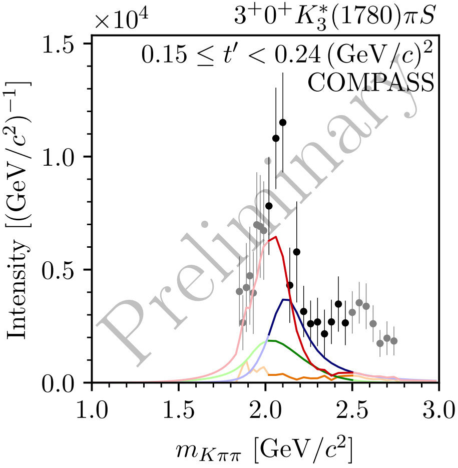

K_3 and K_4 Mesons

- Observe K_3 signal at about 2.1 GeV/c^2
  - in $K_3^*(1780)\pi$ and $K_2^*(1430)\pi$ decays
- Evidence for K_4 signal at about 2.2 GeV/c^2
  - in $K_2^*(1430)\pi$ decay

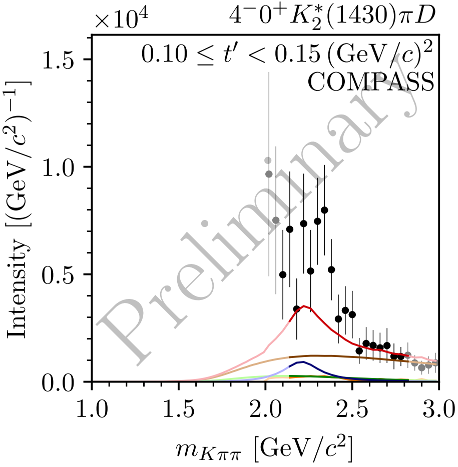

K_3 and K_4 Mesons

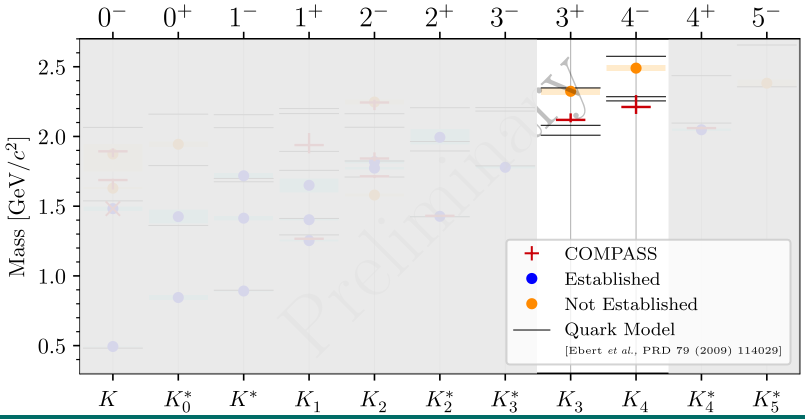

- Width of both states in agreement with previous observations
- Mass significantly lower, however in good agreement with quark-model predictions for ground states
  - ➥ Potential first observation of K_3 and K_4 ground states, while excited states observed in $\Lambda\bar{p}$ decay

K Mesons

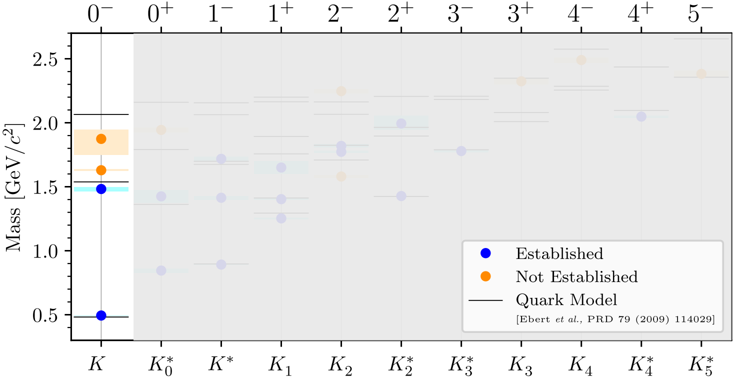

PDG (2022)

- $K(1460)$ and $K(1830)$
- "$K(1630)$"
  - Unexpectedly small width of only $16\,\mathrm{MeV}/c^2$
  - J^P of "$K(1630)$" unclear

K Mesons

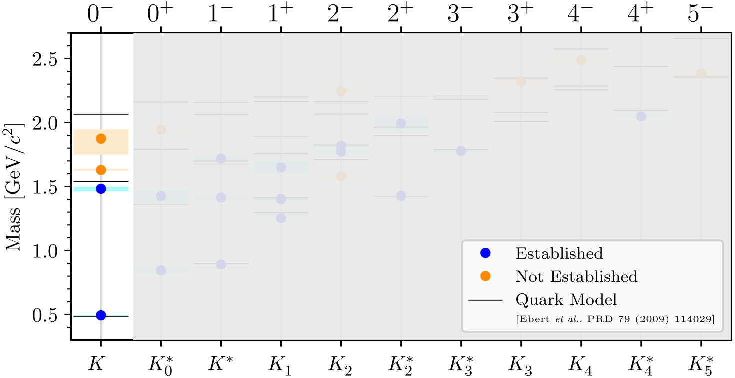

PDG (2022)

- $K(1460)$ and $K(1830)$
- "$K(1630)$"
  - Unexpectedly small width of only 16 MeV/c^2
  - J^P of "$K(1630)$" unclear

K Mesons

COMPASS $K^-\pi^-\pi^+$ data

- Peak at about $1.4\,\text{GeV}/c^2$
  - Established $K(1460)$
  - But, $m_{K\pi\pi} \lesssim 1.5\,\text{GeV}/c^2$ region weakly affected by known analysis artifacts
- Second peak at about $1.7\,\text{GeV}/c^2$
  - Excited K signal with mass $(1687 \pm 10\,^{+2}_{-67})\,\text{MeV}/c^2$ and $8.3\,\sigma$ statistical significance
  - Accompanied by rising phase
  - Measured width of $(140 \pm 20\,^{+50}_{-50})\,\text{MeV}/c^2$ larger than "$K(1630)$"
- Additional signal at about $2.0\,\text{GeV}/c^2$
  - $K(1830)$ signal with $5.4\,\sigma$ statistical significance
  - Most precise measurement of $K(1830)$ resonance parameters

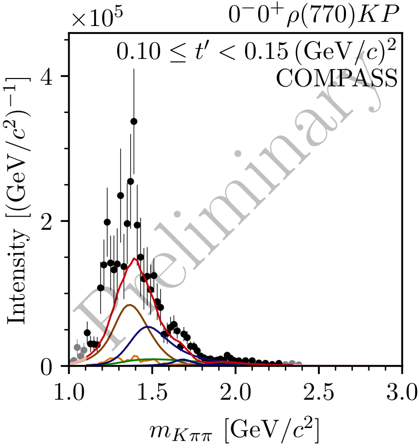

total resonance model, resonances, non-resonant, $\pi\pi\pi$ background, effective background

K Mesons

COMPASS $K^-\pi^-\pi^+$ data

- Peak at about 1.4 GeV$/c^2$
  - Established $K(1460)$
  - But, $m_{K\pi\pi} \lesssim 1.5\,\text{GeV}/c^2$ region weakly affected by known analysis artifacts
- Second peak at about 1.7 GeV$/c^2$
  - Excited K signal with mass $(1687 \pm 10\,^{+2}_{-67})\,\text{MeV}/c^2$ and $8.3\,\sigma$ statistical significance
  - Accompanied by rising phase
  - Measured width of $(140 \pm 20\,^{+50}_{-50})\,\text{MeV}/c^2$ larger than "$K(1630)$"
- Additional signal at about 2.0 GeV$/c^2$
  - $K(1830)$ signal with $5.4\,\sigma$ statistical significance
  - Most precise measurement of $K(1830)$ resonance parameters

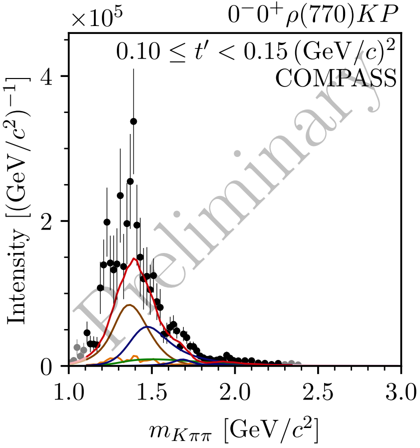

total resonance model, resonances, non-resonant, $\pi\pi\pi$ background, effective background

K Mesons

COMPASS $K^-\pi^-\pi^+$ data

- Peak at about $1.4\,\text{GeV}/c^2$
  - Established $K(1460)$
  - But, $m_{K\pi\pi} \lesssim 1.5\,\text{GeV}/c^2$ region weakly affected by known analysis artifacts
- Second peak at about $1.7\,\text{GeV}/c^2$
  - Excited K signal with mass $(1687 \pm 10\,^{+2}_{-67})\,\text{MeV}/c^2$ and $8.3\,\sigma$ statistical significance
  - Accompanied by rising phase
  - Measured width of $(140 \pm 20\,^{+50}_{-50})\,\text{MeV}/c^2$ larger than "$K(1630)$ "
- Additional signal at about $2.0\,\text{GeV}/c^2$
  - $K(1830)$ signal with $5.4\,\sigma$ statistical significance
  - Most precise measurement of $K(1830)$ resonance parameters

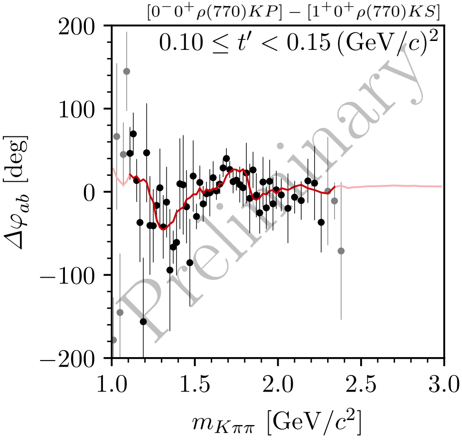

total resonance model, resonances, non-resonant, $\pi\pi\pi$ background, effective background

K Mesons

COMPASS $K^-\pi^-\pi^+$ data

- Peak at about 1.4 GeV/c^2
  - Established $K(1460)$
  - But, $m_{K\pi\pi} \lesssim 1.5\,\text{GeV}/c^2$ region weakly affected by known analysis artifacts
- Second peak at about 1.7 GeV/c^2
  - Excited K signal with mass $(1687 \pm 10\,^{+2}_{-67})\,\text{MeV}/c^2$ and $8.3\,\sigma$ statistical significance
  - Accompanied by rising phase
  - Measured width of $(140 \pm 20\,^{+50}_{-50})\,\text{MeV}/c^2$ larger than "$K(1630)$"
- Additional signal at about 2.0 GeV/c^2
  - $K(1830)$ signal with $5.4\,\sigma$ statistical significance
  - Most precise measurement of $K(1830)$ resonance parameters

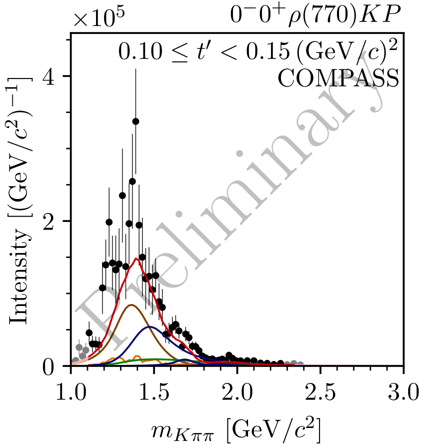

total resonance model, resonances, non-resonant, $\pi\pi\pi$ background, effective background

K Mesons

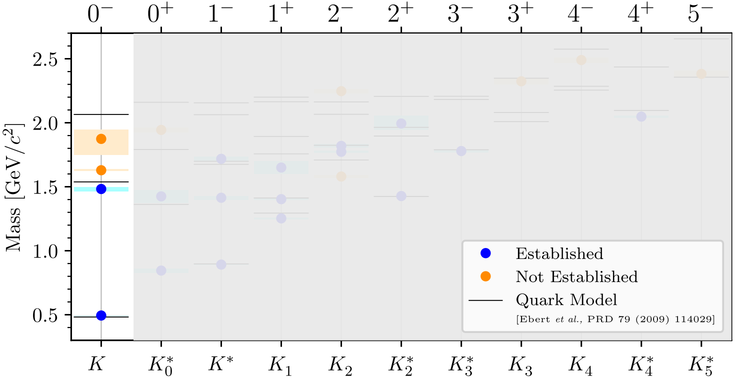

- Indications for 3 excited K from a single analysis
- Quark model predicts only two excited states: potentially $K(1460)$ and $K(1830)$
  - ➥ Supernumerary K signal at about 1690 MeV/c^2
  - ➥ Candidate for exotic non-$q\bar{q}$ state; other explanations possible ($K^*(892)\,\omega$ threshold nearby)

K Mesons

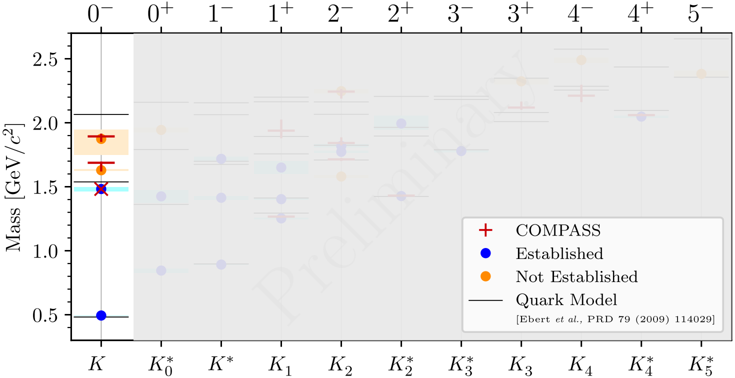

- Indications for 3 excited K from a single analysis
- Quark model predicts only two excited states: potentially $K(1460)$ and $K(1830)$
  - ➥ Supernumerary K signal at about 1690 MeV/c^2
  - ➥ Candidate for exotic non-$q\bar{q}$ state; other explanations possible ($K^*(892)\,\omega$ threshold nearby)

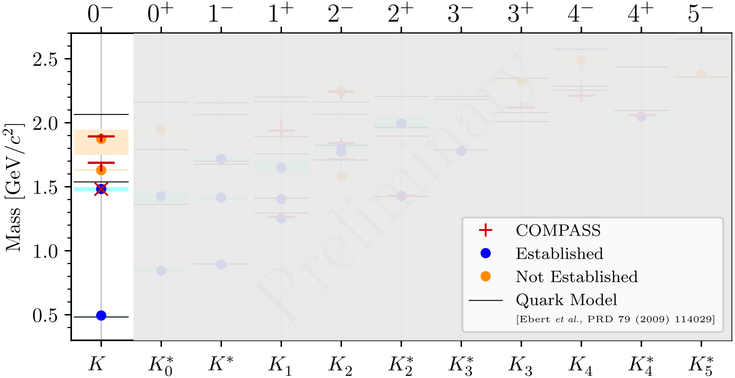

- Indications for 3 excited K from a single analysis
- Quark model predicts only two excited states: potentially $K(1460)$ and $K(1830)$
  - ➥ Supernumerary K signal at about 1690 MeV$/c^2$
  - ➥ Candidate for exotic non-$q\bar{q}$ state; other explanations possible ($K^*(892)\,\omega$ threshold nearby)

Limitations for Strange-Meson Spectroscopy at COMPASS

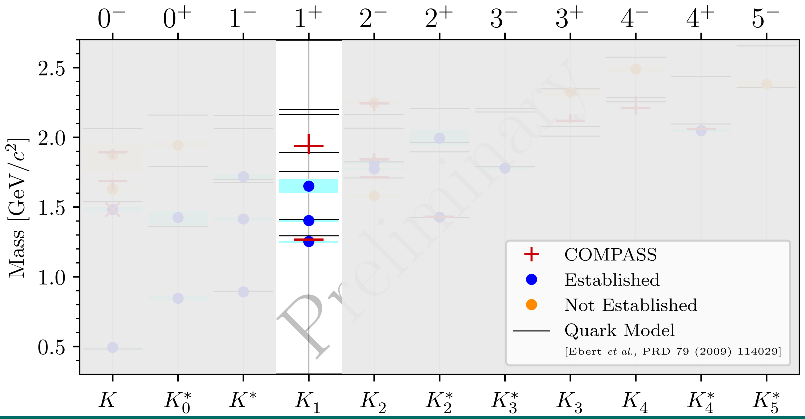

$K_1(1400)$

- Only $J^P = 1^+$ waves representing $\rho(770)K$ decay studied
- No significant $K(1400)$ signal, as expected

Limitations for Strange-Meson Spectroscopy at COMPASS

- Want to study K_1 states also in $K^*(892)\pi$ decays
- Very sensitive to systematic effects
- Event selection requires to identify one of the two negative particles
  - Limited acceptance due to limited kinematic range of final-state PID
  - Reduced differentiability of certain partial waves
  - Causes analysis artifacts in affected waves
- Only a sub-set of partial waves affected

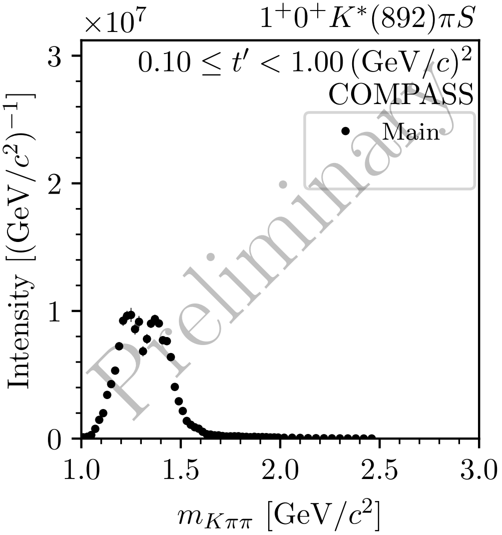

Limitations for Strange-Meson Spectroscopy at COMPASS

- Want to study K_1 states also in $K^*(892)\pi$ decays
- Very sensitive to systematic effects
- Event selection requires to identify one of the two negative particles
  - Limited acceptance due to limited kinematic range of final-state PID
  - Reduced differentiability of certain partial waves
  - Causes analysis artifacts in affected waves
- Only a sub-set of partial waves affected

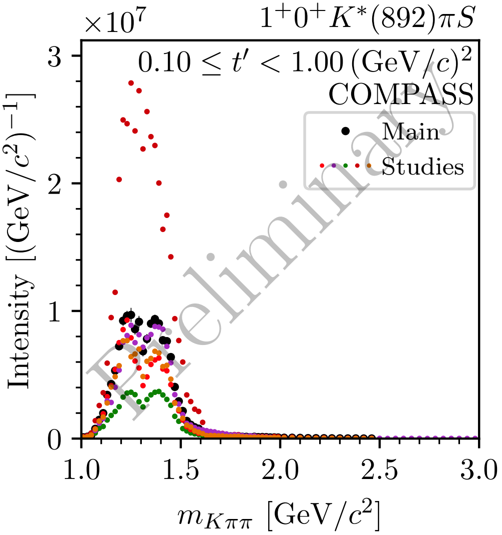

Limitations for Strange-Meson Spectroscopy at COMPASS

- Want to study K_1 states also in $K^*(892)\pi$ decays
- Very sensitive to systematic effects
- Event selection requires to identify one of the two negative particles
  - ➥ Limited acceptance due to limited kinematic range of final-state PID
  - ➥ Reduced differentiability of certain partial waves
  - ➥ Causes analysis artifacts in affected waves
- Only a sub-set of partial waves affected

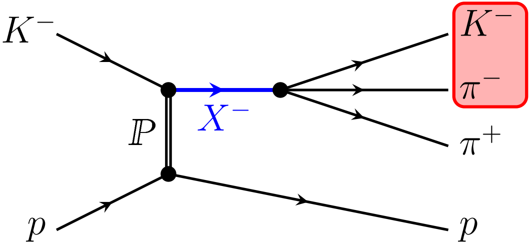

Limitations for Strange-Meson Spectroscopy at COMPASS

- Want to study K_1 states also in $K^*(892)\pi$ decays
- Very sensitive to systematic effects
- Event selection requires to identify one of the two negative particles
  - ➥ Limited acceptance due to limited kinematic range of final-state PID
  - ➥ Reduced differentiability of certain partial waves
  - ➥ Causes analysis artifacts in affected waves
- Only a sub-set of partial waves affected

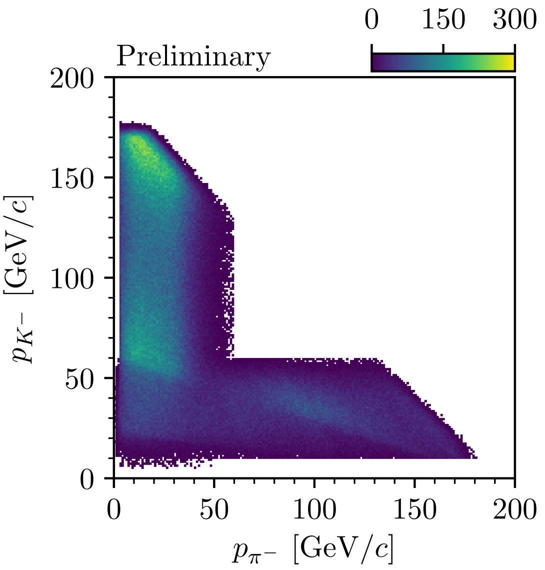

Limitations for Strange-Meson Spectroscopy at COMPASS

- Want to study K_1 states also in $K^*(892)\pi$ decays
- Very sensitive to systematic effects
- Event selection requires to identify one of the two negative particles
  - ➥ Limited acceptance due to limited kinematic range of final-state PID
  - ➥ Reduced differentiability of certain partial waves
  - ➥ Causes analysis artifacts in affected waves
- Only a sub-set of partial waves affected

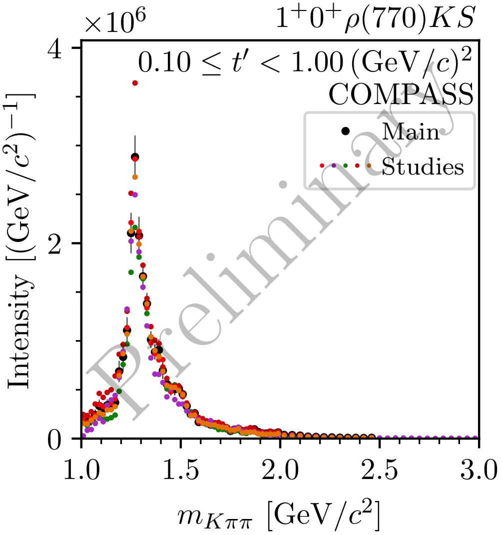

Limitations for Strange-Meson Spectroscopy at COMPASS

Main limiting factors

- Final-state particle identification
  - ➥ Analysis artifacts in some partial waves
  - ➥ Background from reactions like $\pi^- + p \to \pi^-\pi^-\pi^+ + p$
- Size of the data sample
  - Low kaon fraction in the beam ($\approx 2\,\%$)
  - Sample for strange mesons about 70 times smaller than sample used for non-strange mesons in published COMPASS $\pi^- + p \to \pi^-\pi^-\pi^+ + p$ analysis

High-Precision Strange-Meson Spectroscopy at AMBER

[see talk by B. Parsamyan]

AMBER

Apparatus for Meson and Baryon Experimental Research

Approved Phase-1 currently ongoing

[CERN-SPSC-2019-022]

- p-induced $\bar{p}$ production cross section
  - Input for cosmic ray studies and search for isospin asymmetric antiproton production
  - Measurements on various light targets completed [ICHEP talk by Davide Giordano]
- Proton charge-radius measurement
- Pion-induced Drell-Yan and charmonium production

Plans for Phase-2 beyond long shutdown 3 of LHC

[arXiv:1808.00848]

- Physics with high-intensity kaon beams
  - Strange-meson spectroscopy
    goal: $10\times$ larger data sample
  - Pion-induced Drell-Yan and charmonium production
  - ...
- Electromagnetic reactions: Meson charge radii
- ...

- Upgrade of final-state particle identification
  - Cover wide momentum range
  - Large and uniform acceptance
- Dedicated trigger for kaon-induced events
  - Triggerless DAQ
- Efficient beam-particle identification for high-purity sample
- High-resolution track reconstruction
- Efficient photon detection for access to final states with neutral particles

$p_{\mathrm{beam}} = 190\ \mathrm{GeV}/c$

Various options under study

- New detector for high-momentum particle identification
- Adjust the momentum range of the existing COMPASS RICH
- Reduce the beam momentum to better fit the current momentum coverage
  - However, lower fraction of K^- in the beam at lower momenta
  - Weaker momentum dependence for K^+ beam

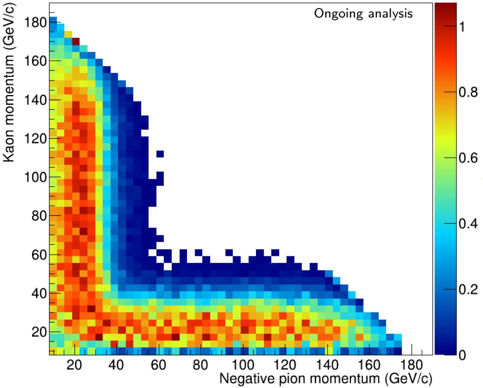

$p_{\text{beam}} = 150\,\text{GeV}/c$

Various options under study

- New detector for high-momentum particle identification
- Adjust the momentum range of the existing COMPASS RICH
- Reduce the beam momentum to better fit the current momentum coverage
  - However, lower fraction of K^- in the beam at lower momenta
  - Weaker momentum dependence for K^+ beam

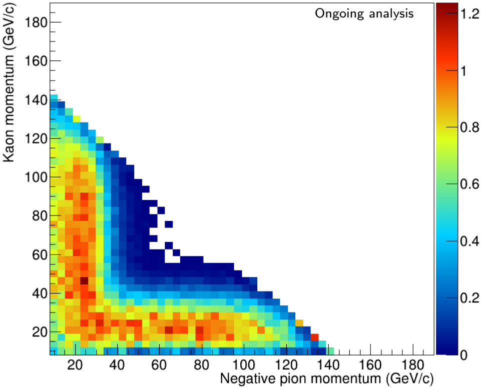

$p_{\mathrm{beam}} = 120\,\mathrm{GeV}/c$

Various options under study

- New detector for high-momentum particle identification
- Adjust the momentum range of the existing COMPASS RICH
- Reduce the beam momentum to better fit the current momentum coverage
  - However, lower fraction of K^- in the beam at lower momenta
  - Weaker momentum dependence for K^+ beam

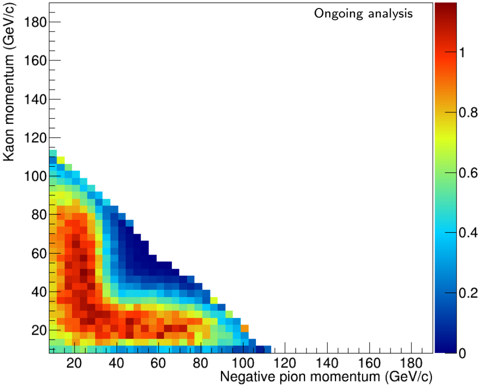

$p_{\mathrm{beam}} = 100\,\mathrm{GeV}/c$

Various options under study

- New detector for high-momentum particle identification
- Adjust the momentum range of the existing COMPASS RICH
- Reduce the beam momentum to better fit the current momentum coverage
  - However, lower fraction of K^- in the beam at lower momenta
  - Weaker momentum dependence for K^+ beam

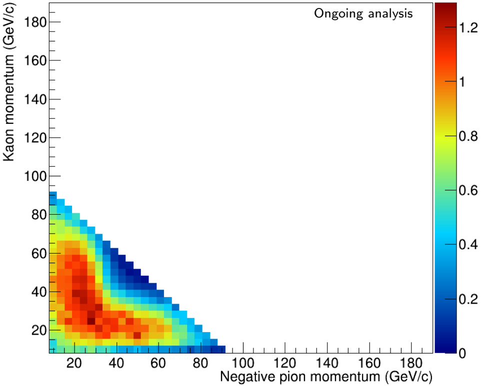

Various options under study

- New detector for high-momentum particle identification
- Adjust the momentum range of the existing COMPASS RICH
- Reduce the beam momentum to better fit the current momentum coverage
  - However, lower fraction of K^- in the beam at lower momenta
  - Weaker momentum dependence for K^+ beam

K^- beam

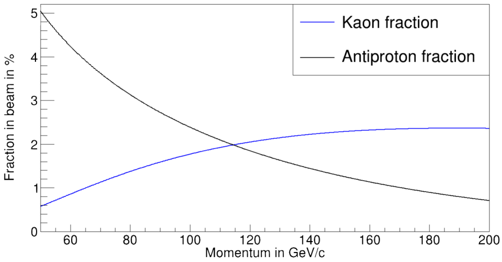

[F. Metzger, Physics Beyond Colliders Meeting]

Various options under study

- New detector for high-momentum particle identification
- Adjust the momentum range of the existing COMPASS RICH
- Reduce the beam momentum to better fit the current momentum coverage
  - However, lower fraction of K^- in the beam at lower momenta
  - Weaker momentum dependence for K^+ beam

K^+ beam

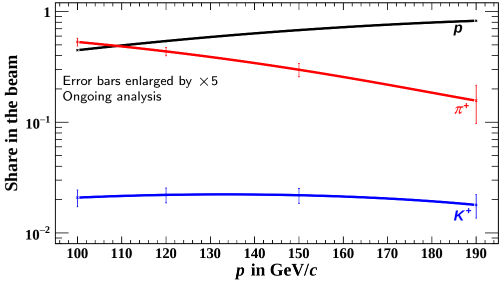

- Eliminate constraints and artifacts caused by limited final-state particle identification
  - ➥ Access to all decay modes in $K^-\pi^-\pi^+$ final state $\Rightarrow$ Study also $K^*(892)\pi$ decays
  - ➥ Access to all J^P sectors $\Rightarrow$ e.g. search for strange partner of the exotic $\pi_1(1600)$ in $J^P = 1^-$
  - ➥ Reduced systematic uncertainties
  - ➥ Access to other final states
- Increase size of the data sample by factor 30
  - ➥ Improved statistical precision
  - ➥ Observation of even smaller signals

Summary

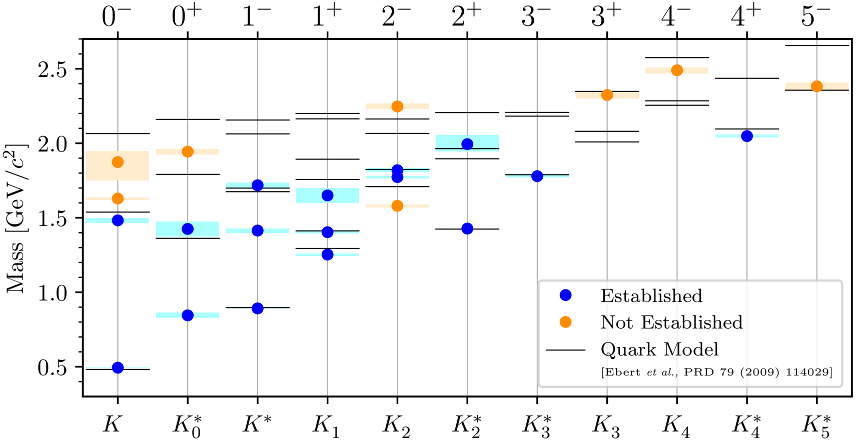

The Strange-Meson Spectrum

- Many strange mesons require further confirmation
- Search for strange partners of exotic non-strange light mesons

Summary

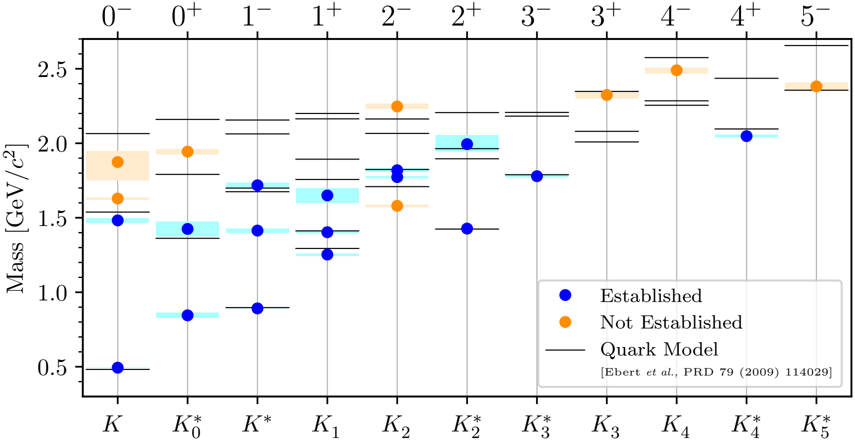

COMPASS

- World's largest data sample on $K^-\pi^-\pi^+$ $\Rightarrow$ Most detailed and comprehensive analysis
- First candidate for exotic strange-meson signal with $J^P = 0^-$

Summary

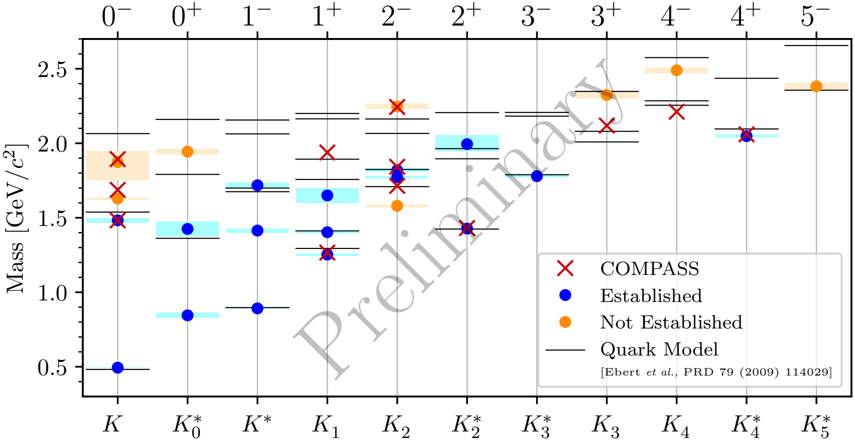

COMPASS

- World's largest data sample on $K^-\pi^-\pi^+$ $\Rightarrow$ Most detailed and comprehensive analysis
- First candidate for exotic strange-meson signal with $J^P = 0^-$

Summary

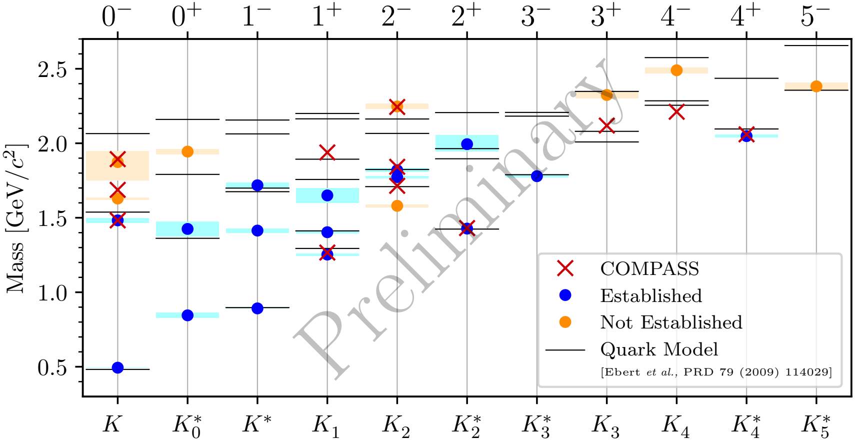

AMBER: Proposal for High-Precision Strange-Meson Spectroscopy

- Goal: Collect 20×10^6 $K^-\pi^-\pi^+$ events using high-energy kaon beam
- AMBER is open for interested collaborators to join

Backup

Outline

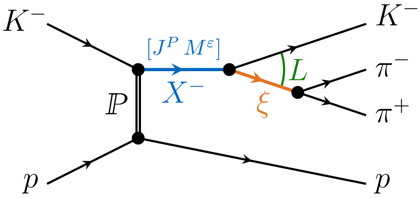

Partial wave

$$J^P M^\varepsilon \xi b L$$

- $J^P M^\varepsilon$: Spin, parity, and spin projection of X^-
- ξ: Isobar
- b: Bachelor particle. Here: Spectator K^-
- L: Angular momentum between bachelor and isobar

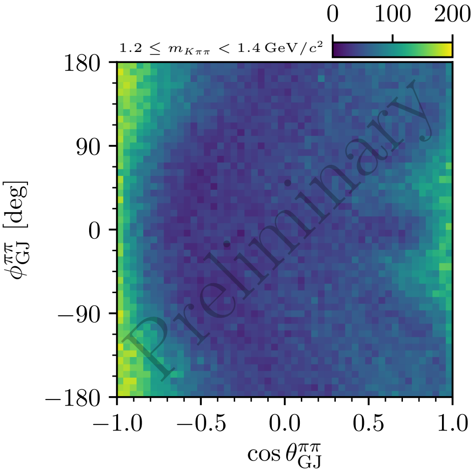

Partial-Wave Decomposition

Model intensity

$$\mathcal{I}(\tau, m_{K\pi\pi}, t') = \sum_{z} \left| \sum_{a \in \mathbb{W}_z(m_{K\pi\pi}, t')} \mathcal{T}_a^z(m_{K\pi\pi}, t') \Psi_a^z(\tau; m_{K\pi\pi}) \right|^2$$

- Model intensity distribution
  - in 5D $K^-\pi^-\pi^+$ phase-space
  - for a given $(m_{K\pi\pi}, t')$ cell
  - as incoherent sum over coherent sectors z
    - "Rank" of the partial-wave model = number of coherent sectors
- Ψ_a^z known, assuming the isobar model
- Wave set $\mathbb{W}_z(m_{K\pi\pi}, t')$ inferred from data using regularization-based model-selection techniques
- $\mathcal{T}_a^z$ extracted in maximum-likelihood fit, independently for each $(m_{K\pi\pi}, t')$ cell

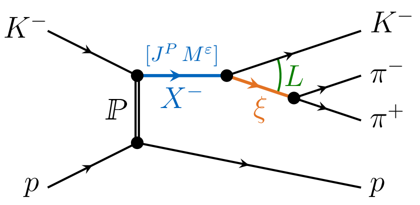

Spin-Density Matrix

$$\rho_{ab} = \sum_z \mathcal{T}_a^z \, [\mathcal{T}_b^z]^*$$

Model intensity

$$\mathcal{I}(\tau, m_{K\pi\pi}, t') = \sum_{z} \left| \sum_{a \in \mathbb{W}_z(m_{K\pi\pi}, t')} \mathcal{T}_a^z(m_{K\pi\pi}, t') \Psi_a^z(\tau; m_{K\pi\pi}) \right|^2$$

- Model intensity distribution
  - in 5D $K^-\pi^-\pi^+$ phase-space
  - for a given $(m_{K\pi\pi}, t')$ cell
  - as incoherent sum over coherent sectors z
    - "Rank" of the partial-wave model = number of coherent sectors
- Ψ_a^z known, assuming the isobar model
- Wave set $\mathbb{W}_z(m_{K\pi\pi}, t')$ inferred from data using regularization-based model-selection techniques
- $\mathcal{T}_a^z$ extracted in maximum-likelihood fit, independently for each $(m_{K\pi\pi}, t')$ cell

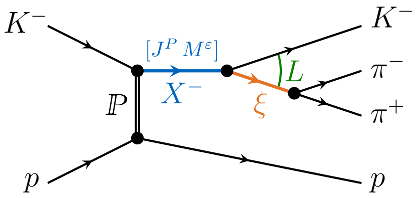

Spin-Density Matrix

$$\rho_{ab} = \sum_z \mathcal{T}_a^z \, [\mathcal{T}_b^z]^*$$

Partial-Wave Decomposition

Model intensity

$$\mathcal{I}(\tau, m_{K\pi\pi}, t') = \sum_{z} \left| \sum_{a \in \mathbb{W}_z(m_{K\pi\pi}, t')} \mathcal{T}_a^z(m_{K\pi\pi}, t') \Psi_a^z(\tau; m_{K\pi\pi}) \right|^2$$

- Model intensity distribution
  - in 5D $K^-\pi^-\pi^+$ phase-space
  - for a given $(m_{K\pi\pi}, t')$ cell
  - as incoherent sum over coherent sectors z
    - "Rank" of the partial-wave model = number of coherent sectors
- Ψ_a^z known, assuming the isobar model
- Wave set $\mathbb{W}_z(m_{K\pi\pi}, t')$ inferred from data using regularization-based model-selection techniques
- $\mathcal{T}_a^z$ extracted in maximum-likelihood fit, independently for each $(m_{K\pi\pi}, t')$ cell

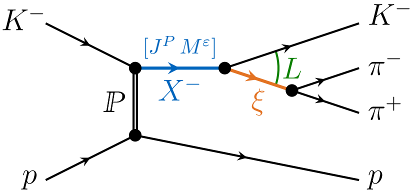

Spin-Density Matrix

$$\rho_{ab} = \sum_z \mathcal{T}_a^z \, [\mathcal{T}_b^z]^*$$

Approach

- Effectively take into account in partial-wave decomposition by incoherently adding additional coherent sectors z
  (Model background by $K^-\pi^-\pi^+$ partial waves)
  - ➥ Increasing the rank of the spin-density matrix ρ_{ab}
  - ➥ Signal not separated from background in partial-wave decomposition
  - ➥ Partial-wave amplitudes include background
- Model signal and background contributions in resonance-model fit using more constrained signal model
  - ➥ Separate signal from background

$$\mathcal{I}(\tau, m_{K\pi\pi}, t') = \sum_z \left| \sum_{a \in \mathbb{W}_z(m_{K\pi\pi}, t')} \mathcal{T}_a^z(m_{K\pi\pi}, t') \Psi_a^z(\tau; m_{K\pi\pi}) \right|^2$$

$$\rho_{ab} = \sum_z \mathcal{T}_a^z \, [\mathcal{T}_b^z]^*$$

Partial-Wave Decomposition

Treating the $\pi^-\pi^-\pi^+$ and Other Backgrounds

True physics intensity distribution

$$\mathcal{I}(\tau) = \left| \sum_{a}^{\text{waves}} \mathcal{T}_a \Psi_a(\tau) \right|^2$$

Experimentally measured intensity distribution

$$\mathcal{I}_{\text{measured}}(\tau) = \eta(\tau)\mathcal{I}(\tau)$$

- Take into account different processes $\mathfrak{p}$
  - Different model intensities $\mathcal{I}^{\mathfrak{p}}$
  - Different experimental acceptance $\eta^{\mathfrak{p}}$
  - Formulated in terms of different phase-space variables $\tau^{\mathfrak{p}}$
    - Jacobian terms $J(\tau^{K\pi\pi} \to \tau^{\mathfrak{p}})$ from variable transformation

True physics intensity distribution for process $\mathfrak{p}$

$$\mathcal{I}^{\mathfrak{p}}(\tau) = \left| \sum_a^{\text{waves}} \mathcal{T}_a^{\mathfrak{p}} \Psi_a^{\mathfrak{p}}(\tau) \right|^2$$

Experimentally measured intensity distribution

$$\mathcal{I}_{\text{measured}}(\tau) = \sum_{\mathfrak{p}} \eta^{\mathfrak{p}}(\tau)\, \mathcal{I}^{\mathfrak{p}}(\tau)$$

- Take into account different processes $\mathfrak{p}$
  - Different model intensities $\mathcal{I}^{\mathfrak{p}}$
  - Different experimental acceptance $\eta^{\mathfrak{p}}$
  - Formulated in terms of different phase-space variables $\tau^{\mathfrak{p}}$
    - Jacobian terms $J(\tau^{K\pi\pi} \to \tau^{\mathfrak{p}})$ from variable transformation

True physics intensity distribution for process $\mathfrak{p}$

$$\mathcal{I}^{\mathfrak{p}}(\tau^{\mathfrak{p}}) = \left| \sum_{a}^{\text{waves}} \mathcal{T}_a^{\mathfrak{p}} \, \Psi_a^{\mathfrak{p}}(\tau^{\mathfrak{p}}) \right|^2$$

Experimentally measured intensity distribution

$$\mathcal{I}_{\text{measured}}(\tau^{K\pi\pi}) = \sum_{\mathfrak{p}} \eta^{\mathfrak{p}}(\tau^{\mathfrak{p}}) \, \mathcal{I}^{\mathfrak{p}}(\tau^{\mathfrak{p}}) \, J(\tau^{K\pi\pi} \to \tau^{\mathfrak{p}})$$

- Take into account different processes $\mathfrak{p}$
  - Different model intensities $\mathcal{I}^{\mathfrak{p}}(\tau^{\mathfrak{p}})$
  - Different experimental acceptance $\eta^{\mathfrak{p}}(\tau^{\mathfrak{p}})$
  - Formulated in terms of different phase-space variables $\tau^{\mathfrak{p}}$
    - Jacobian terms $J(\tau^{K\pi\pi} \to \tau^{\mathfrak{p}})$ from variable transformation

True physics intensity distribution for process $\mathfrak{p}$

$$\mathcal{I}^{\mathfrak{p}}(\tau^{\mathfrak{p}}) = \left| \sum_{a}^{\text{waves}} \mathcal{T}_a^{\mathfrak{p}} \, \Psi_a^{\mathfrak{p}}(\tau^{\mathfrak{p}}) \right|^2$$

Experimentally measured intensity distribution

$$\mathcal{I}_{\text{measured}}(\tau^{K\pi\pi}) = \sum_{\mathfrak{p}} \eta^{\mathfrak{p}}(\tau^{\mathfrak{p}}) \, \mathcal{I}^{\mathfrak{p}}(\tau^{\mathfrak{p}}) \, J(\tau^{K\pi\pi} \to \tau^{\mathfrak{p}})$$

- $\mathcal{I}^{\pi\pi\pi}$ known by COMPASS analysis
- $\eta^{\pi\pi\pi}$ from detector simulation

- $\eta^{\pi\pi\pi}$ computationally expensive
- Different $m_{3\pi}$ bins enter one $m_{K\pi\pi}$ bin
- Other background channels: $K^-K^-K^+$, ...
  - $\mathcal{I}^{\mathfrak{p}}$ unknown
  - Unknown background channels

True physics intensity distribution for process $\mathfrak{p}$

$$\mathcal{I}^{\mathfrak{p}}(\tau^{\mathfrak{p}}) = \left|\sum_a^{\text{waves}} \mathcal{T}_a^{\mathfrak{p}}\,\Psi_a^{\mathfrak{p}}(\tau^{\mathfrak{p}})\right|^2$$

Experimentally measured intensity distribution

$$\mathcal{I}_{\text{measured}}(\tau^{K\pi\pi}) = \sum_{\mathfrak{p}} \eta^{\mathfrak{p}}(\tau^{\mathfrak{p}})\,\mathcal{I}^{\mathfrak{p}}(\tau^{\mathfrak{p}})\,J(\tau^{K\pi\pi} \to \tau^{\mathfrak{p}})$$

- $\mathcal{I}^{\pi\pi\pi}$ known by COMPASS analysis
- $\eta^{\pi\pi\pi}$ from detector simulation

- $\eta^{\pi\pi\pi}$ computationally expensive
- Different $m_{3\pi}$ bins enter one $m_{K\pi\pi}$ bin
- Other background channels: $K^-K^-K^+$, ...
  - $\mathcal{I}^{\mathfrak{p}}$ unknown
  - Unknown background channels

True physics intensity distribution for process $\mathfrak{p}$

$$\mathcal{I}^{\mathfrak{p}}(\tau^{\mathfrak{p}}) = \left|\sum_a^{\text{waves}} \mathcal{T}_a^{\mathfrak{p}}\, \Psi_a^{\mathfrak{p}}(\tau^{\mathfrak{p}})\right|^2$$

Experimentally measured intensity distribution

$$\mathcal{I}_{\text{measured}}(\tau^{K\pi\pi}) = \sum_{\mathfrak{p}} \eta^{\mathfrak{p}}(\tau^{\mathfrak{p}})\, \mathcal{I}^{\mathfrak{p}}(\tau^{\mathfrak{p}})\, J(\tau^{K\pi\pi} \to \tau^{\mathfrak{p}})$$

- $\mathcal{I}^{\pi\pi\pi}$ known by COMPASS analysis
- $\eta^{\pi\pi\pi}$ from detector simulation

- $\eta^{\pi\pi\pi}$ computationally expensive
- Different $m_{3\pi}$ bins enter one $m_{K\pi\pi}$ bin
- Other background channels: $K^-K^-K^+$, ...
  - $\mathcal{I}^{\mathfrak{p}}$ unknown
  - Unknown background channels

Approximate model for process $\mathfrak{p}$ by $K^-\pi^-\pi^+$ partial waves

$$\eta^{\mathfrak{p}}(\tau^{\mathfrak{p}}) \left| \sum_a^{\text{waves}} \mathcal{T}_a^{\mathfrak{p}} \, \Psi_a^{\mathfrak{p}}(\tau^{\mathfrak{p}}) \right|^2 \approx \eta^{K\pi\pi}(\tau^{K\pi\pi}) \left| \sum_a^{\text{waves}} \tilde{\mathcal{T}}_a^{\mathfrak{p}} \, \Psi_a^{K\pi\pi}(\tau^{K\pi\pi}) \right|^2$$

Total true physics intensity distribution

$$\mathcal{I}(\tau^{K\pi\pi}) = \sum_{\mathfrak{p}} \left| \sum_a^{\text{waves}} \mathcal{T}_a^{\mathfrak{p}} \, \Psi_a^{K\pi\pi}(\tau^{K\pi\pi}) \right|^2$$

Experimentally measured intensity distribution

$$\mathcal{I}_{\text{measured}}(\tau^{K\pi\pi}) = \eta^{K\pi\pi}(\tau^{K\pi\pi}) \, \mathcal{I}(\tau^{K\pi\pi})$$

- How well can $K^-\pi^-\pi^+$ partial waves approximate the distribution of process $\mathfrak{p}$
  - Is the set of $K^-\pi^-\pi^+$ partial waves sufficient?
    - ➡ Automatic wave-set selection using model-selection techniques

Approximate model for process $\mathfrak{p}$ by $K^-\pi^-\pi^+$ partial waves

$$\eta^{\mathfrak{p}}(\tau^{\mathfrak{p}}) \left| \sum_{a}^{\text{waves}} \mathcal{T}_a^{\mathfrak{p}} \, \Psi_a^{\mathfrak{p}}(\tau^{\mathfrak{p}}) \right|^2 \approx \eta^{K\pi\pi}(\tau^{K\pi\pi}) \left| \sum_{a}^{\text{waves}} \tilde{\mathcal{T}}_a^{\mathfrak{p}} \, \Psi_a^{K\pi\pi}(\tau^{K\pi\pi}) \right|^2$$

Total true physics intensity distribution

$$\mathcal{I}(\tau^{K\pi\pi}) = \sum_{\mathfrak{p}} \left| \sum_{a}^{\text{waves}} \mathcal{T}_a^{\mathfrak{p}} \, \Psi_a^{K\pi\pi}(\tau^{K\pi\pi}) \right|^2$$

Experimentally measured intensity distribution

$$\mathcal{I}_{\text{measured}}(\tau^{K\pi\pi}) = \eta^{K\pi\pi}(\tau^{K\pi\pi}) \, \mathcal{I}(\tau^{K\pi\pi})$$

- How well can $K^-\pi^-\pi^+$ partial waves approximate the distribution of process $\mathfrak{p}$
  - Is the set of $K^-\pi^-\pi^+$ partial waves sufficient?
    - ➥ Automatic wave-set selection using model-selection techniques

Approximate model for process $\mathfrak{p}$ by $K^-\pi^-\pi^+$ partial waves

$$\eta^{\mathfrak{p}}(\tau^{\mathfrak{p}}) \left| \sum_a^{\text{waves}} \mathcal{T}_a^{\mathfrak{p}} \Psi_a^{\mathfrak{p}}(\tau^{\mathfrak{p}}) \right|^2 \approx \eta^{K\pi\pi}(\tau^{K\pi\pi}) \left| \sum_a^{\text{waves}} \tilde{\mathcal{T}}_a^{\mathfrak{p}} \Psi_a^{K\pi\pi}(\tau^{K\pi\pi}) \right|^2$$

Total true physics intensity distribution

$$\mathcal{I}(\tau^{K\pi\pi}) = \sum_{a,b}^{\text{waves}} \Psi_a^{K\pi\pi}(\tau^{K\pi\pi})\, \rho_{a,b}\, [\Psi_b^{K\pi\pi}(\tau^{K\pi\pi})]^*$$

Spin-density matrix with rank $N_\mathrm{r} > 1$

$$\rho_{a,b} = \sum_{\mathfrak{p}}^{N_\mathrm{r}} \mathcal{T}_a^{\mathfrak{p}} [\mathcal{T}_b^{\mathfrak{p}}]^*$$

- How well can $K^-\pi^-\pi^+$ partial waves approximate the distribution of process $\mathfrak{p}$
  - Is the set of $K^-\pi^-\pi^+$ partial waves sufficient?
    - ➥ Automatic wave-set selection using model-selection techniques

Approximate model for process $\mathfrak{p}$ by $K^-\pi^-\pi^+$ partial waves

$$\eta^{\mathfrak{p}}(\tau^{\mathfrak{p}}) \left| \sum_a^{\text{waves}} \mathcal{T}_a^{\mathfrak{p}} \, \Psi_a^{\mathfrak{p}}(\tau^{\mathfrak{p}}) \right|^2 \approx \eta^{K\pi\pi}(\tau^{K\pi\pi}) \left| \sum_a^{\text{waves}} \tilde{\mathcal{T}}_a^{\mathfrak{p}} \, \Psi_a^{K\pi\pi}(\tau^{K\pi\pi}) \right|^2$$

Total true physics intensity distribution

$$\mathcal{I}(\tau^{K\pi\pi}) = \sum_{a,b}^{\text{waves}} \Psi_a^{K\pi\pi}(\tau^{K\pi\pi}) \, \rho_{a,b} \, [\Psi_b^{K\pi\pi}(\tau^{K\pi\pi})]^*$$

Spin-density matrix with rank $N_\text{r} > 1$

$$\rho_{a,b} = \sum_{\mathfrak{p}}^{N_\text{r}} \mathcal{T}_a^{\mathfrak{p}} [\mathcal{T}_b^{\mathfrak{p}}]^*$$

- How well can $K^-\pi^-\pi^+$ partial waves approximate the distribution of process $\mathfrak{p}$
  - Is the set of $K^-\pi^-\pi^+$ partial waves sufficient?
    - ➥ Automatic wave-set selection using model-selection techniques

Partial-Wave Decomposition

Treating the $\pi^-\pi^-\pi^+$ and Other Backgrounds

Approximate model for process $\mathfrak{p}$ by $K^-\pi^-\pi^+$ partial waves

$$\eta^{\mathfrak{p}}(\tau^{\mathfrak{p}}) \left| \sum_{a}^{\text{waves}} \mathcal{T}_a^{\mathfrak{p}} \, \Psi_a^{\mathfrak{p}}(\tau^{\mathfrak{p}}) \right|^2 \approx \eta^{K\pi\pi}(\tau^{K\pi\pi}) \left| \sum_{a}^{\text{waves}} \tilde{\mathcal{T}}_a^{\mathfrak{p}} \, \Psi_a^{K\pi\pi}(\tau^{K\pi\pi}) \right|^2$$

Total true physics intensity distribution

$$\mathcal{I}(\tau^{K\pi\pi}) = \sum_{a,b}^{\text{waves}} \Psi_a^{K\pi\pi}(\tau^{K\pi\pi}) \, \rho_{a,b} \, [\Psi_b^{K\pi\pi}(\tau^{K\pi\pi})]^*$$

Spin-density matrix with rank $N_\mathrm{r} > 1$

$$\rho_{a,b} = \sum_{\mathfrak{r}}^{N_\mathrm{r}} \mathcal{T}_a^{\mathfrak{r}} [\mathcal{T}_b^{\mathfrak{r}}]^*$$

- Experimentally measurable quantities are spin-density matrix elements
  - ➥ Transition amplitudes $\mathcal{T}_a^{\mathfrak{p}}$ are only effective parameters
  - ➥ Cannot determine $\mathcal{T}_a^{\mathfrak{p}}$ of individual processes
  - ➥ Cannot separate different processes

Approximate model for process $\mathfrak{p}$ by $K^-\pi^-\pi^+$ partial waves

$$\eta^{\mathfrak{p}}(\tau^{\mathfrak{p}}) \left| \sum_a^{\text{waves}} \mathcal{T}_a^{\mathfrak{p}} \Psi_a^{\mathfrak{p}}(\tau^{\mathfrak{p}}) \right|^2 \approx \eta^{K\pi\pi}(\tau^{K\pi\pi}) \left| \sum_a^{\text{waves}} \tilde{\mathcal{T}}_a^{\mathfrak{p}} \Psi_a^{K\pi\pi}(\tau^{K\pi\pi}) \right|^2$$

Total true physics intensity distribution

$$\mathcal{I}(\tau^{K\pi\pi}) = \sum_{a,b}^{\text{waves}} \Psi_a^{K\pi\pi}(\tau^{K\pi\pi})\, \rho_{a,b}\, [\Psi_b^{K\pi\pi}(\tau^{K\pi\pi})]^*$$

Spin-density matrix with rank $N_{\mathrm{r}} > 1$

$$\rho_{a,b} = \sum_{\mathfrak{r}}^{N_{\mathrm{r}}} \mathcal{T}_a^{\mathfrak{r}} [\mathcal{T}_b^{\mathfrak{r}}]^*$$

- Large number of fit parameters: $N_{\mathrm{para}} = N_{\mathrm{r}}(2N_{\mathrm{waves}} - N_{\mathrm{r}})$
- Sufficient rank of spin-density matrix must be determined
  - Rank two needed to describe pure $\pi^-\pi^-\pi^+$ Monte Carlo sample using $K^-\pi^-\pi^+$ partial waves
  - Used rank three to model $K^-\pi^-\pi^+$ sample

Data

720 k diffractively produced $K^-\pi^-\pi^+$ candidates

(I) Partial-Wave Decomposition

Partial Waves

Intensities and relative phases of the partial waves

(II) Resonance-Model Fit

Resonance Parameters

Masses and widths of the meson resonances

Resonance-Model Fit

- Spin-density matrix $\rho_{ab}(m_{K\pi\pi}, t')$ measured in partial-wave decomposition
- Model spin-density matrix in resonance-model fit

$$\hat{\rho}_{ab}(m_{K\pi\pi}, t') = \hat{\rho}_{ab}^{K\pi\pi}(m_{K\pi\pi}, t') + \hat{\rho}_{ab}^{3\pi}(m_{K\pi\pi}, t') + \hat{\rho}_{ab}^{\mathrm{Bkg}}(m_{K\pi\pi}, t')$$

Model transition amplitudes as coherent sum over various components

$$\hat{\mathcal{T}}_a^z(m_{K\pi\pi}, t') = \sum_{k\in\mathbb{S}_a} K(m_{K\pi\pi}, t')\, {}^k\mathcal{C}_a^{K\pi\pi}(t')\, \mathcal{D}_k(m_{K\pi\pi}; \zeta_k)$$

- Dynamic functions $\mathcal{D}_k(m_{K\pi\pi}; \zeta_k)$
  - For resonances: rel. Breit-Wigner
  - For non-resonant terms: $\mathcal{D}_k^{\mathrm{NR}}(m_{K\pi\pi}; a_k, c_k) = (m_{K\pi\pi} - m_{\mathrm{thr}})^{a_k}\, e^{-b(c_k)\,\tilde{q}_k^2(m_{K\pi\pi})}$
- "Coupling amplitudes": ${}^k\mathcal{C}_a^z(t')$
  - Independent coupling amplitude for each t' bin
- Kinematic factor $K(m_{K\pi\pi}, t')$
- Coherently summed over all assumed model components

Model transition amplitudes as coherent sum over various components

$$\hat{\mathcal{T}}_a^z(m_{K\pi\pi}, t') = \sum_{k\in\mathbb{S}_a} K(m_{K\pi\pi}, t')\,{}^k\mathcal{C}_a^{K\pi\pi}(t')\,\mathcal{D}_k(m_{K\pi\pi}; \zeta_k)$$

- Dynamic functions $\mathcal{D}_k(m_{K\pi\pi}; \zeta_k)$
  - For resonances: rel. Breit-Wigner
  - For non-resonant terms: $\mathcal{D}_k^{\mathrm{NR}}(m_{K\pi\pi}; a_k, c_k) = (m_{K\pi\pi} - m_{\mathrm{thr}})^{a_k}\, e^{-b(c_k)\,\tilde{q}_k^2(m_{K\pi\pi})}$
- "Coupling amplitudes": ${}^k\mathcal{C}_a^z(t')$
  - Independent coupling amplitude for each t' bin
- Kinematic factor $K(m_{K\pi\pi}, t')$
- Coherently summed over all assumed model components

Model transition amplitudes as coherent sum over various components

$$\hat{\mathcal{T}}_a^z(m_{K\pi\pi}, t') = \sum_{k \in \mathbb{S}_a} K(m_{K\pi\pi}, t')\, {}^k\mathcal{C}_a^{K\pi\pi}(t')\, \mathcal{D}_k(m_{K\pi\pi}; \zeta_k)$$

- Dynamic functions $\mathcal{D}_k(m_{K\pi\pi}; \zeta_k)$
  - For resonances: rel. Breit-Wigner
  - For non-resonant terms: $\mathcal{D}_k^{\mathrm{NR}}(m_{K\pi\pi}; a_k, c_k) = (m_{K\pi\pi} - m_{\mathrm{thr}})^{a_k}\, e^{-b(c_k)\, \tilde{q}_k^2(m_{K\pi\pi})}$
- "Coupling amplitudes": ${}^k\mathcal{C}_a^z(t')$
  - Independent coupling amplitude for each t' bin
- Kinematic factor $K(m_{K\pi\pi}, t')$
- Coherently summed over all assumed model components

Model transition amplitudes as coherent sum over various components

$$\hat{\mathcal{T}}_a^z(m_{K\pi\pi}, t') = \sum_{k\in\mathbb{S}_a} K(m_{K\pi\pi}, t')\, {}^k\mathcal{C}_a^{K\pi\pi}(t')\, \mathcal{D}_k(m_{K\pi\pi}; \zeta_k)$$

- Dynamic functions $\mathcal{D}_k(m_{K\pi\pi}; \zeta_k)$
  - For resonances: rel. Breit-Wigner
  - For non-resonant terms: $\mathcal{D}_k^{\mathrm{NR}}(m_{K\pi\pi}; a_k, c_k) = (m_{K\pi\pi} - m_{\mathrm{thr}})^{a_k} e^{-b(c_k)\,\tilde{q}_k^2(m_{K\pi\pi})}$
- “Coupling amplitudes”: ${}^k\mathcal{C}_a^z(t')$
  - Independent coupling amplitude for each t' bin
- Kinematic factor $K(m_{K\pi\pi}, t')$
- Coherently summed over all assumed model components

3π spin-density matrix

$$\hat{\rho}_{ab}^{\pi\pi\pi}(m_{K\pi\pi}, t') = \left|\mathcal{C}^{\pi\pi\pi}\right|^2 \rho_{ab}^{\pi\pi\pi}(m_{K\pi\pi}, t')$$

- $\rho_{ab}^{\pi\pi\pi}(m_{K\pi\pi}, t')$ obtained from PWD of $\pi^-\pi^-\pi^+$ pseudodata sample
  - $m_{K\pi\pi}$ dependence fixed
  - t' dependence fixed
  - Rel. strength between partial waves fixed (freed in a study)
- One global real-valued yield parameter $\left|\mathcal{C}^{\pi\pi\pi}\right|^2$

Background spin-density matrix

- Additional incoherent contribution form other processes: $K^- K^- K^+$, ...
- Transition amplitudes modeled by non-resonant parameterizations for each partial wave

$$\hat{\mathcal{T}}_a^{\mathrm{eBKG}}(m_{K\pi\pi}, t') = K(m_{K\pi\pi}, t')\, \mathcal{C}_a^{\mathrm{eBKG}}(t')\, \mathcal{D}_{k_a}^{\mathrm{eBKG}}(m_{K\pi\pi}; a_{k_a}, c_{k_a})$$

- χ^2 fit of the real and imaginary parts of the spin-density matrix
  - Taking into account correlations between spin-density matrix elements
  - Shape parameters (m_0, Γ_0, ...) and coupling amplitudes are free parameters
- For the main fit, we performed 2000 fit attempts with random start-parameter values for the shape parameters, e.g. mass and width parameters, and the coupling and branching amplitudes.
- Start-parameter ranges for the shape parameters are chosen according to previous measurements (see note)
- The best result is the one which yielded the smallest χ^2 value

- χ^2 fit of the real and imaginary parts of the spin-density matrix
  - Taking into account correlations between spin-density matrix elements
  - Shape parameters (m_0, Γ_0, ...) and coupling amplitudes are free parameters
- For the main fit, we performed 2000 fit attempts with random start-parameter values for the shape parameters, e.g. mass and width parameters, and the coupling and branching amplitudes.
- Start-parameter ranges for the shape parameters are chosen according to previous measurements (see note)
- The best result is the one which yielded the smallest χ^2 value

Wave-Set Selection

$$\mathcal{I}(\tau, m_{K\pi\pi}, t') = \left| \sum_{a \in \mathbb{W}(m_{K\pi\pi}, t')} \mathcal{T}_a(m_{K\pi\pi}, t') \Psi_a(\tau; m_{K\pi\pi}) \right|^2$$

Challenge: Find the "best" set of waves that describes the data

- If the wave set is too large
  - ➥ Starting to describe statistical fluctuations
- If waves that contribute to the data are missing
  - ➥ Intensity can be wrongly attributed to other waves
  - ➥ Model leakage

Wave-Set Selection

Infer wave set from data

- Systematically construct large set of allowed partial waves
  - ➥ "Wave pool"
- Fit wave pool to data
  - Impose penalty on $|\mathcal{T}_a|^2 \Rightarrow$ regularization
  - Suppress insignificant waves
- Select waves that significantly contribute to data
  - ➥ "Best" subset of waves that describe the data

Wave-Set Selection

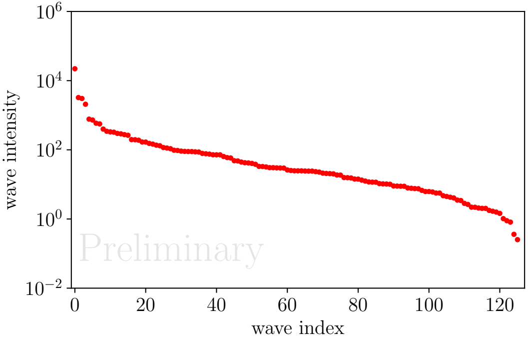

- $\pi^-\pi^-\pi^+$ Monte Carlo mock data set with 126 partial waves
- Fitting wave pool of 753 waves
  - ➥ Massive overfitting
  - ➥ Almost all waves pick up intensity

Courtesy F. Kaspar, TUM

Wave-Set Selection

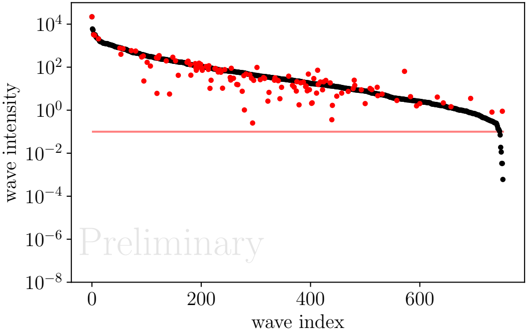

- $\pi^-\pi^-\pi^+$ Monte Carlo mock data set with 126 partial waves
- Fitting wave pool of 753 waves
  - ➥ Massive overfitting
  - ➥ Almost all waves pick up intensity

Courtesy F. Kaspar, TUM

$$\ln \mathcal{L}_{\text{fit}} = \ln \mathcal{L}_{\text{extended}} + \sum_{a}^{\text{waves}} \ln \mathcal{L}_{\text{reg}}(|\mathcal{T}_a|; \{c_{\text{para}}\})$$

LASSO/L1 regularization[1]

$$\ln \mathcal{L}_{\text{reg}}(|\mathcal{T}_a|; \lambda) = -\lambda |\mathcal{T}_a|$$

- Maximum at $|\mathcal{T}_a| = 0$
- Well established[2]
- "Smoothing" at $|\mathcal{T}_a| = 0$

$$|\mathcal{T}_a| \to \sqrt{|\mathcal{T}_a|^2 + \varepsilon}$$

[1] Robert Tibshirani. "Regression Shrinkage and Selection via the Lasso". In: Journal of the Royal Statistical Society. Series B 58.1 (1996)
[2] Baptiste Guegan et al. "Model selection for amplitude analysis". In: JINST 10.09 (2015), P09002

$$\ln \mathcal{L}_{\text{fit}} = \ln \mathcal{L}_{\text{extended}} + \sum_{a}^{\text{waves}} \ln \mathcal{L}_{\text{reg}}(|\mathcal{T}_a|; \{c_{\text{para}}\})$$

LASSO/L1 regularization[1]

$$\ln \mathcal{L}_{\text{reg}}(|\mathcal{T}_a|; \lambda) = -\lambda |\mathcal{T}_a|$$

- Maximum at $|\mathcal{T}_a| = 0$
- Well established[2]
- "Smoothing" at $|\mathcal{T}_a| = 0$

$$|\mathcal{T}_a| \to \sqrt{|\mathcal{T}_a|^2 + \varepsilon}$$

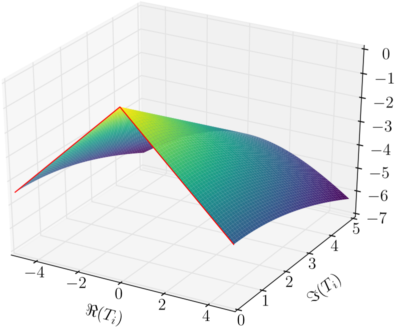

[1] Robert Tibshirani. "Regression Shrinkage and Selection via the Lasso". In: Journal of the Royal Statistical Society. Series B 58.1 (1996)
[2] Baptiste Guegan et al. "Model selection for amplitude analysis". In: JINST 10.09 (2015), P09002

$$\ln \mathcal{L}_{\text{fit}} = \ln \mathcal{L}_{\text{extended}} + \sum_{a}^{\text{waves}} \ln \mathcal{L}_{\text{reg}}(|\mathcal{T}_a|; \{c_{\text{para}}\})$$

LASSO/L1 regularization[1]

$$\ln \mathcal{L}_{\text{reg}}(|\mathcal{T}_a|; \lambda) = -\lambda |\mathcal{T}_a|$$

- Maximum at $|\mathcal{T}_a| = 0$
- Well established[2]
- "Smoothing" at $|\mathcal{T}_a| = 0$

$$|\mathcal{T}_a| \to \sqrt{|\mathcal{T}_a|^2 + \varepsilon}$$

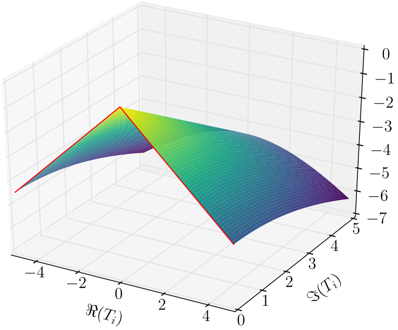

[1] Robert Tibshirani. "Regression Shrinkage and Selection via the Lasso". In: Journal of the Royal Statistical Society. Series B 58.1 (1996)
[2] Baptiste Guegan et al. "Model selection for amplitude analysis". In: JINST 10.09 (2015), P09002

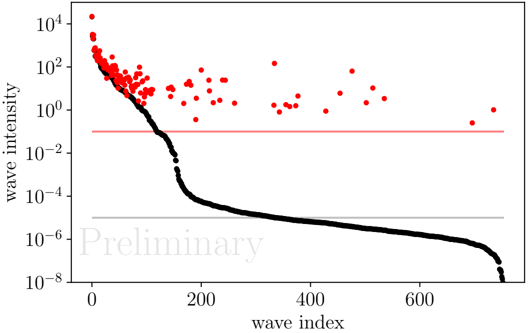

$\lambda = 0.3$

$\varepsilon = 10^{-5}$

- Bias also on large transition amplitudes
- Some additional waves
- Some waves missing

Courtesy F. Kaspar, TUM

Generalized Pareto[1]

$$\ln \mathcal{L}_{\mathrm{reg}}(|\mathcal{T}_a|; \Gamma, \zeta) = -\frac{1}{\zeta} \ln \left[1 + \zeta \frac{|\mathcal{T}_a|}{\Gamma}\right]$$

- Wave intensities spread over orders of magnitudes
- Use logarithmic prior
  - ➥ Heavy-tailed
  - ➥ Less bias on large waves
- LASSO-like for $|\mathcal{T}_a| \to 0$
- "Smoothing" at $|\mathcal{T}_a| = 0$

$$|\mathcal{T}_a| \to \sqrt{|\mathcal{T}_a|^2 + \varepsilon}$$

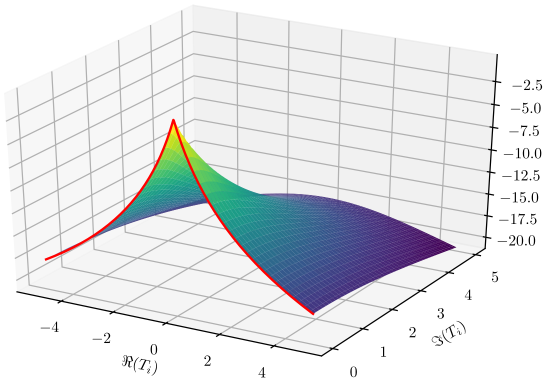

[1] Artin Armagan, David B. Dunson, and Jaeyong Lee. "Generalized double Pareto shrinkage". In: Statistica Sinica (2013). doi: 10.5705/ss.2011.048.

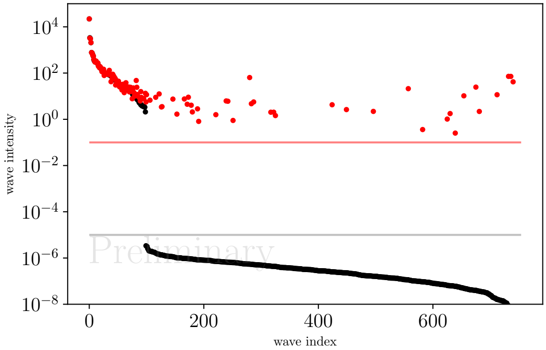

$\zeta = 0.5$

$\Gamma = 0.1$

$\varepsilon = 10^{-5}$

- Less bias on large transition amplitudes
- Clear kink in intensity distribution to smoothing scale $\Rightarrow$ Selection
- Less additional waves
- Some small waves missing

Courtesy F. Kaspar, TUM

“Cauchy”

$$\ln \mathcal{L}_{\mathrm{reg}}(|\mathcal{T}_a|;\Gamma) = -\ln\left[1 + \frac{|\mathcal{T}_a|^{2}}{\Gamma_a^2}\right]$$

- Logarithmic prior
- L2-like for $|\mathcal{T}_a| \to 0$

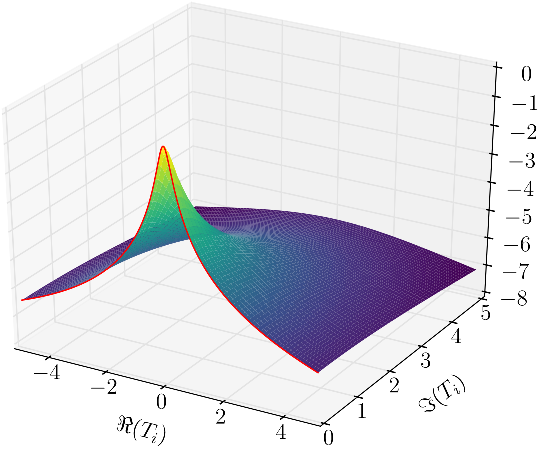

Wave-Set Selection
Regularization: Cauchy

$\Gamma = 0.2$

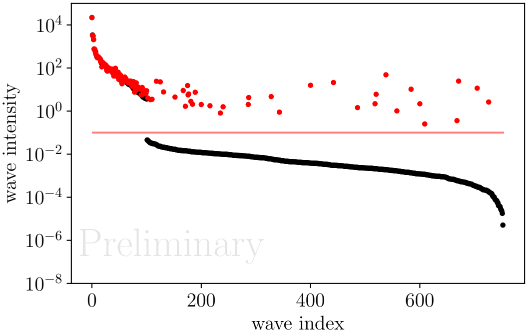

- Less bias on large transition amplitudes
- Clear kink in intensity distribution
- Few additional waves
- Few small waves missing

Courtesy F. Kaspar, TUM

Wave pool

- Spin $J \leq 7$
- Angular momentum $L \leq 7$
- Positive naturality of exchange particle
- 12 isobars
  - $[K\pi]_S^{K\pi}$, $[K\pi]_S^{K\eta}$, $K^*(892)$, $K^*(1680)$, $K_2^*(1430)$, $K_3^*(1780)$
  - $[\pi\pi]_S$, $f_0(980)$, $f_0(1500)$, $\rho(770)$, $f_2(1270)$, $\rho_3(1690)$

$\Rightarrow$ "Wave pool" of 596 waves

"only" 720 k events

Wave pool

- Spin $J \leq 7$
- Angular momentum $L \leq 7$
- Positive naturality of exchange particle
- 12 isobars
  - $[K\pi]_S^{K\pi}$, $[K\pi]_S^{K\eta}$, $K^*(892)$, $K^*(1680)$, $K_2^*(1430)$, $K_3^*(1780)$
  - $[\pi\pi]_S$, $f_0(980)$, $f_0(1500)$, $\rho(770)$, $f_2(1270)$, $\rho_3(1690)$

$\Rightarrow$ “Wave pool” of 596 waves

“only” 720 k events

Regularization

$$\ln \mathcal{L}_{\text{reg}}(|\mathcal{T}_a|;\Gamma) = -\ln\left[1 + \frac{|\mathcal{T}_a|^2}{\Gamma_a^2}\right]$$

- Use Cauchy regularization
- Scale of $|\mathcal{T}_a|$ depends on experimental acceptance
  - Apply penalty on expected number $\bar{N}_a$ of observed events

$$\Gamma_a = \frac{\Gamma}{\sqrt{\bar{\eta}_a}} \Rightarrow \frac{|\mathcal{T}_a|^2}{\Gamma_a^2} = \frac{\bar{N}_a}{\Gamma^2}$$

  - Γ is a universal parameter

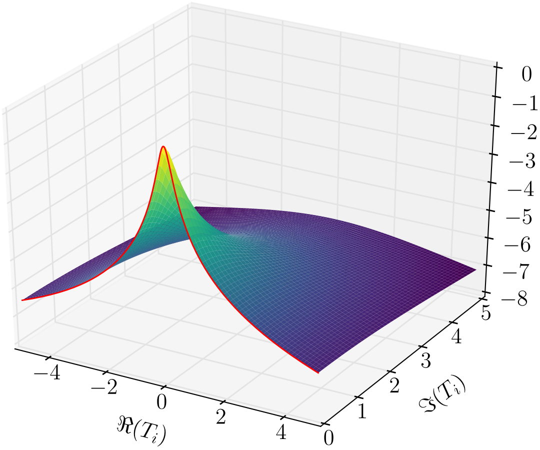

Regularization

$$\ln \mathcal{L}_{\mathrm{reg}}(|\mathcal{T}_a|; \Gamma) = -\ln\left[1 + \frac{|\mathcal{T}_a|^2}{\Gamma_a^2}\right]$$

- Use Cauchy regularization
- Scale of $|\mathcal{T}_a|$ depends on experimental acceptance
  - Apply penalty on expected number $\bar{N}_a$ of observed events

$$\Gamma_a = \frac{\Gamma}{\sqrt{\bar{\eta}_a}} \Rightarrow \frac{|\mathcal{T}_a|^2}{\Gamma_a^2} = \frac{\bar{N}_a}{\Gamma^2}$$

  - Γ is a universal parameter

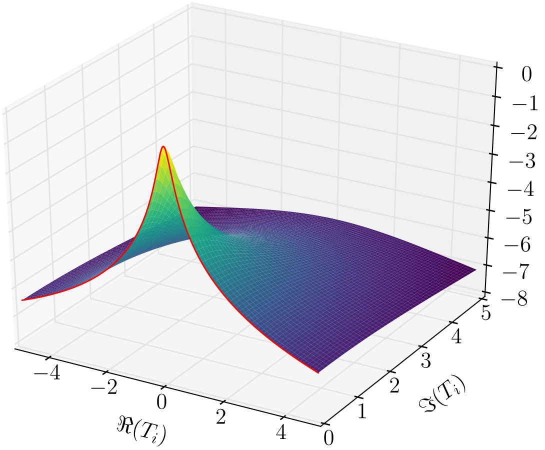

Regularization

$$\ln \mathcal{L}_{\text{reg}}(|\mathcal{T}_a|; \Gamma) = -\ln\left[1 + \frac{|\mathcal{T}_a|^2}{\Gamma_a^2}\right]$$

- Use Cauchy regularization
- Scale of $|\mathcal{T}_a|$ depends on experimental acceptance
  - Apply penalty on expected number $\bar{N}_a$ of observed events

$$\Gamma_a = \frac{\Gamma}{\sqrt{\bar{\eta}_a}} \quad \Rightarrow \quad \frac{|\mathcal{T}_a|^2}{\Gamma_a^2} = \frac{\bar{N}_a}{\Gamma^2}$$

  - Γ is a universal parameter

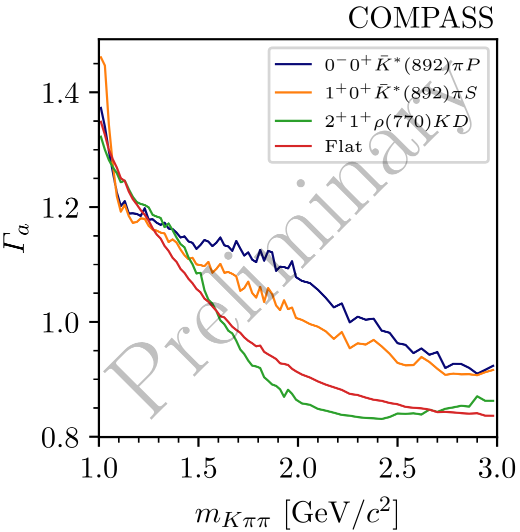

Regularization

$$\ln \mathcal{L}_{\text{reg}}(|\mathcal{T}_a|;\Gamma) = -\ln\left[1+\frac{|\mathcal{T}_a|^2}{\Gamma_a^2}\right]$$

- Use Cauchy regularization
- Scale of $|\mathcal{T}_a|$ depends on experimental acceptance
  - Apply penalty on expected number $\bar{N}_a$ of observed events

$$\Gamma_a = \frac{\Gamma}{\sqrt{\bar{\eta}_a}} \quad\Rightarrow\quad \frac{|\mathcal{T}_a|^2}{\Gamma_a^2} = \frac{\bar{N}_a}{\Gamma^2}$$

  - Γ is a universal parameter

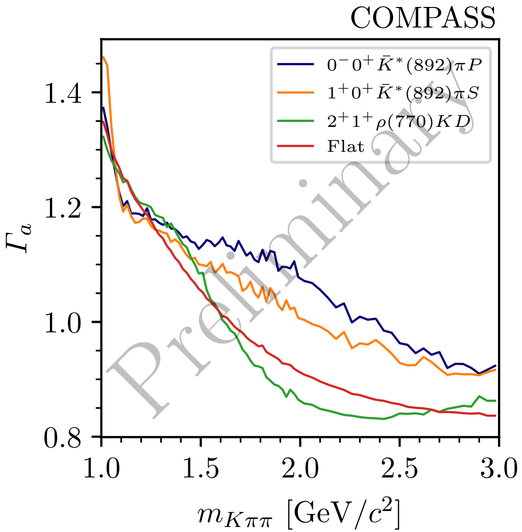

Wave-Set Selection

For the $K^-\pi^-\pi^+$ Final State

Imposing continuity of the wave set

- Wave-set inferred independently for each $(m_{K\pi\pi}, t')$ cell
- Impose continuity of the wave set in $m_{K\pi\pi}$ by adding additional regularization term

$$\ln \mathcal{L}_{\mathrm{cont}}(\{\mathcal{T}_a(m_{K\pi\pi}, t')\}; \lambda) = \sum_{j=i-3}^{j=i+3} \lambda \left| \mathcal{T}_a(m_{K\pi\pi}, t')(m_{K\pi\pi}^{j+1}) - \mathcal{T}_a(m_{K\pi\pi}, t')(m_{K\pi\pi}^{j}) \right|^2,$$

which suppresses fluctuations among neighboring $m_{K\pi\pi}$ bins

Wave-Set Selection

For the $K^-\pi^-\pi^+$ Final State

Wave-set size

- 5 to 90 waves per $(m_{K\pi\pi}, t')$ cell
- Larger wave set for larger binning in $m_{K\pi\pi}$
- Larger wave set in t' bins with more events

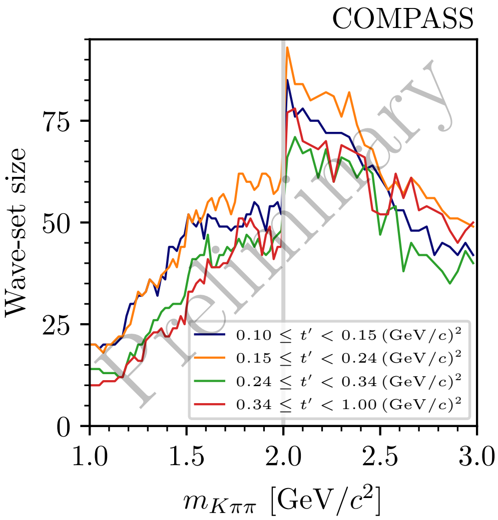

- Selection of large signals
- as well as of signals at per-mil level

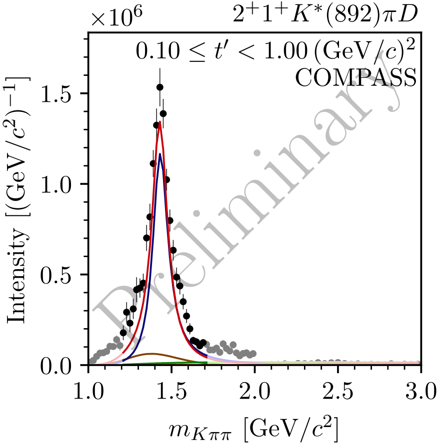

- Selection of large signals
- as well as of signals at per-mil level

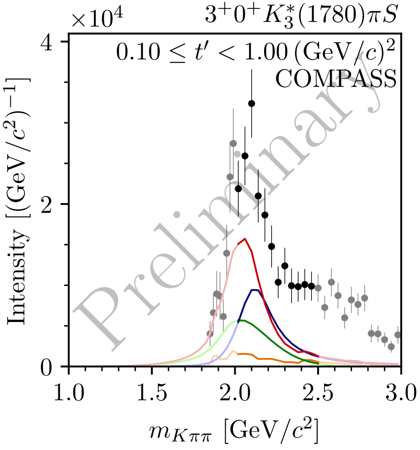

14-Wave Resonance-Model Fit

Searching for Exotic Strange Mesons with $J^P = 0^-$

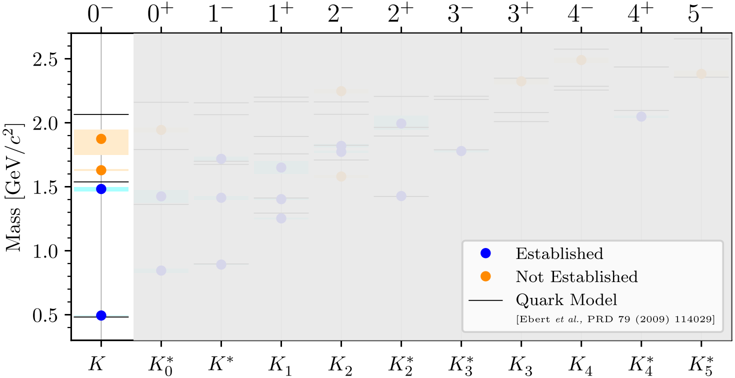

PDG (2022)

- $K(1460)$ and $K(1830)$
- $K(1630)$
  - Unexpectedly small width of only 16 MeV$/c^2$
  - J^P of $K(1630)$ unclear

14-Wave Resonance-Model Fit

Searching for Exotic Strange Mesons with $J^P = 0^-$

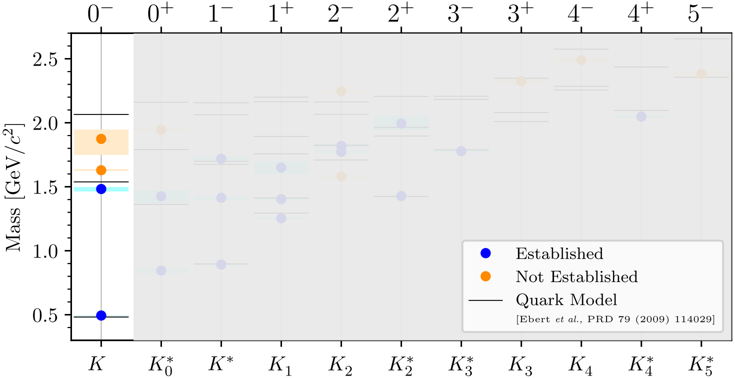

PDG (2022)

- $K(1460)$ and $K(1830)$
- $K(1630)$
  - Unexpectedly small width of only 16 MeV$/c^2$
  - J^P of $K(1630)$ unclear

COMPASS $K^-\pi^-\pi^+$ data

- Peak at about 1.4 GeV/c^2
  - Potentially from established $K(1460)$
  - But, $m_{K\pi\pi} \lesssim 1.5$ GeV/c^2 region affected by analysis artifacts
- Second peak at about 1.7 GeV/c^2
  - $K(1630)$ signal with 8.3 σ statistical significance
  - Accompanied by rising phase
- Weak signal at about 2.0 GeV/c^2
  - $K(1830)$ signal with 5.4 σ statistical significance

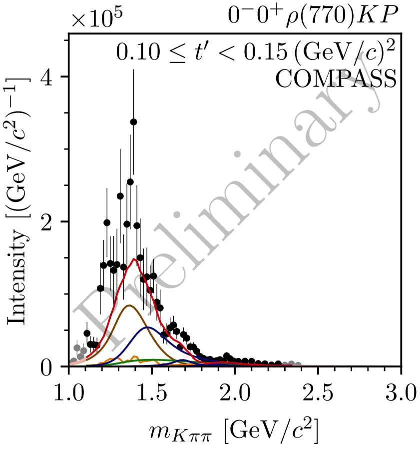

total resonance model, resonances, non-resonant, $\pi\pi\pi$ background, effective background

COMPASS $K^-\pi^-\pi^+$ data

- Peak at about $1.4\,\mathrm{GeV}/c^2$
  - Potentially from established $K(1460)$
  - But, $m_{K\pi\pi} \lesssim 1.5\,\mathrm{GeV}/c^2$ region affected by analysis artifacts
- Second peak at about $1.7\,\mathrm{GeV}/c^2$
  - $K(1630)$ signal with $8.3\,\sigma$ statistical significance
  - Accompanied by rising phase
- Weak signal at about $2.0\,\mathrm{GeV}/c^2$
  - $K(1830)$ signal with $5.4\,\sigma$ statistical significance

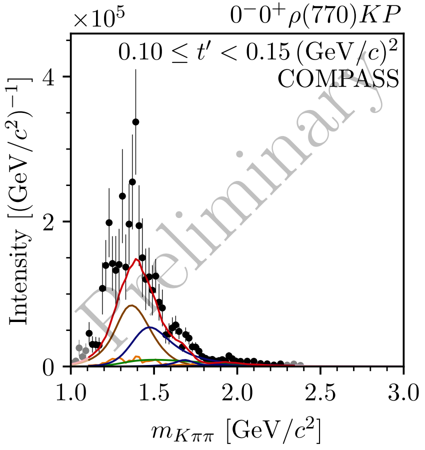

total resonance model, resonances, non-resonant, $\pi\pi\pi$ background, effective background

COMPASS $K^-\pi^-\pi^+$ data

- Peak at about 1.4 GeV/c^2
  - Potentially from established $K(1460)$
  - But, $m_{K\pi\pi} \lesssim 1.5$ GeV/c^2 region affected by analysis artifacts
- Second peak at about 1.7 GeV/c^2
  - $K(1630)$ signal with 8.3 σ statistical significance
  - Accompanied by rising phase
- Weak signal at about 2.0 GeV/c^2
  - $K(1830)$ signal with 5.4 σ statistical significance

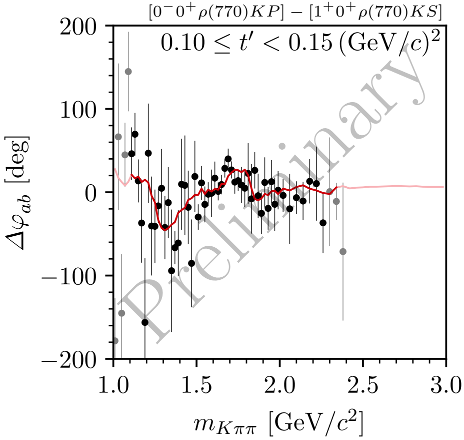

total resonance model, resonances, non-resonant, $\pi\pi\pi$ background, effective background

COMPASS $K^-\pi^-\pi^+$ data

- Peak at about 1.4 GeV/c^2
  - Potentially from established $K(1460)$
  - But, $m_{K\pi\pi} \lesssim 1.5$ GeV/c^2 region affected by analysis artifacts
- Second peak at about 1.7 GeV/c^2
  - $K(1630)$ signal with 8.3 σ statistical significance
  - Accompanied by rising phase
- Weak signal at about 2.0 GeV/c^2
  - $K(1830)$ signal with 5.4 σ statistical significance

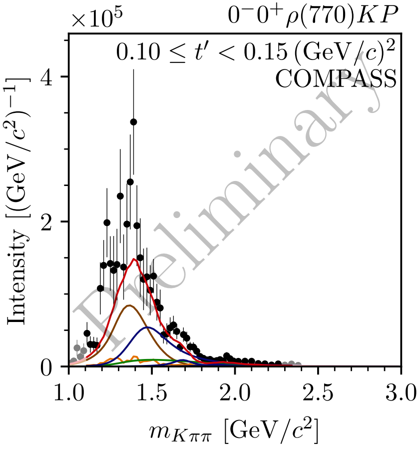

total resonance model, resonances, non-resonant, $\pi\pi\pi$ background, effective background

14-Wave Resonance-Model Fit

Searching for Exotic Strange Mesons with $J^P = 0^-$

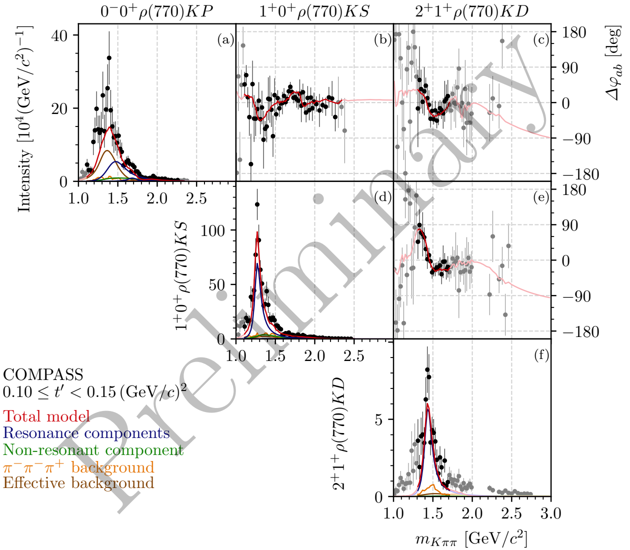

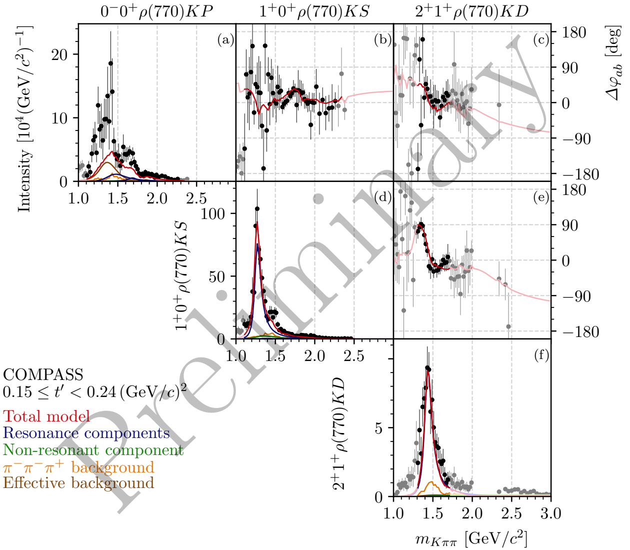

$0^-0^+\rho(770)KP$
$1^+0^+\rho(770)KS$
$2^+1^+\rho(770)KD$
(a)
(b)
(c)
(d)
(e)
(f)
Intensity $[10^4 (\text{GeV}/c^2)^{-1}]$
$1^+0^+\rho(770)KS$
$2^+1^+\rho(770)KD$
$\Delta\varphi_{ab}$ [deg]
$m_{K\pi\pi}$ $[\text{GeV}/c^2]$
COMPASS
$0.15 \leq t' < 0.24\,(\text{GeV}/c)^2$
Total model
Resonance components
Non-resonant component
$\pi^-\pi^-\pi^+$ background
Effective background
Preliminary

14-Wave Resonance-Model Fit

Searching for Exotic Strange Mesons with $J^P = 0^-$

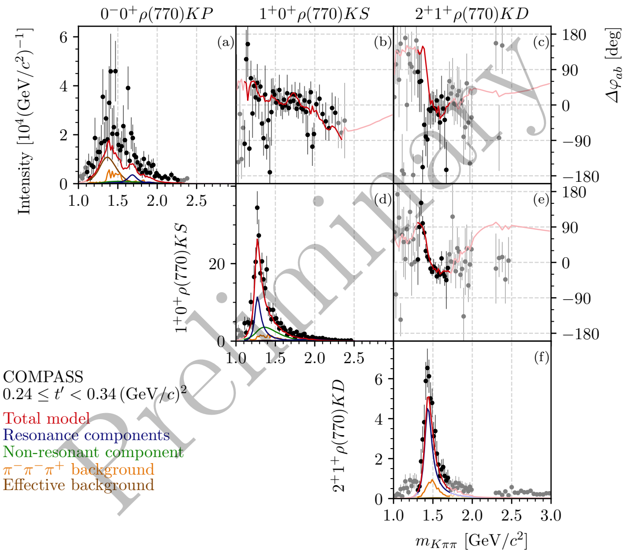

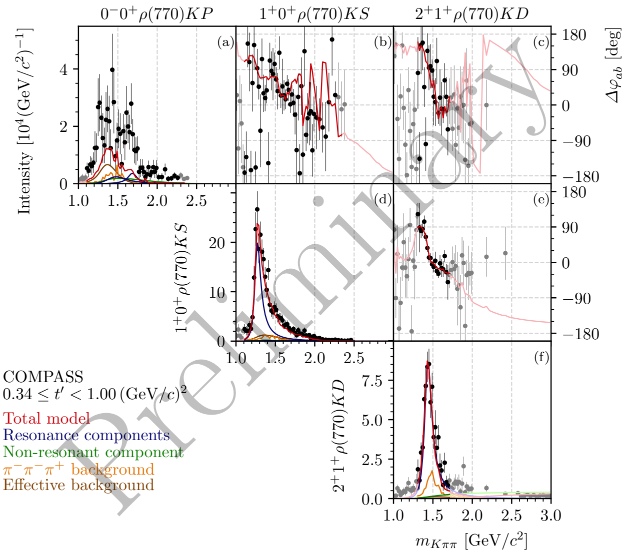

$0^-0^+\rho(770)KP$
$1^+0^+\rho(770)KS$
$2^+1^+\rho(770)KD$
(a)
(b)
(c)
(d)
(e)
(f)
Intensity $[10^4(\mathrm{GeV}/c^2)^{-1}]$
$\Delta\varphi_{ab}$ [deg]
$1^+0^+\rho(770)KS$
$2^+1^+\rho(770)KD$
$m_{K\pi\pi}$ $[\mathrm{GeV}/c^2]$
COMPASS
$0.34 \leq t' < 1.00\,(\mathrm{GeV}/c)^2$
Total model
Resonance components
Non-resonant component
$\pi^-\pi^-\pi^+$ background
Effective background
Preliminary

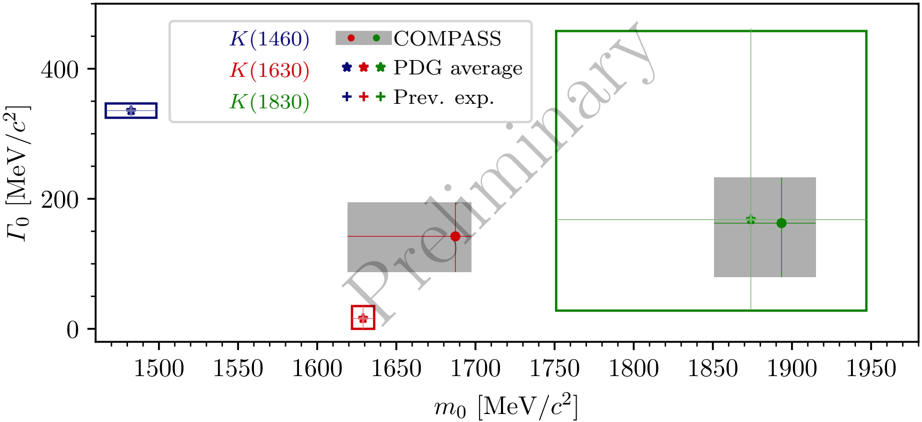

- $K(1830)$ parameters in good agreement with LCHb measurement [PRL 118 (2017) 022003]
- Realistic $K(1630)$ width of about 140 MeV/c^2

14-Wave Resonance-Model Fit

Searching for Exotic Strange Mesons with $J^P = 0^-$

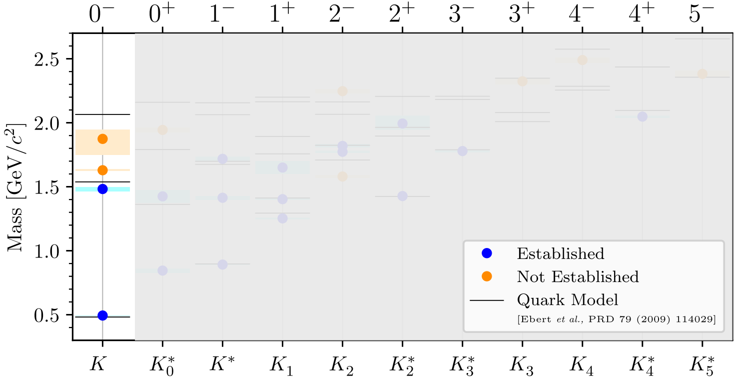

- Indications for 3 excited K from a single analysis
- Quark-model predicts only two excited states: potentially $K(1460)$ and $K(1830)$
  - ➥ $K(1630)$ supernumerary signal
  - ➥ Candidate for exotic non-$q\bar{q}$ state; other explanations possible ($K^*(892)\,\omega$ threshold nearby)

14-Wave Resonance-Model Fit

Searching for Exotic Strange Mesons with $J^P = 0^-$

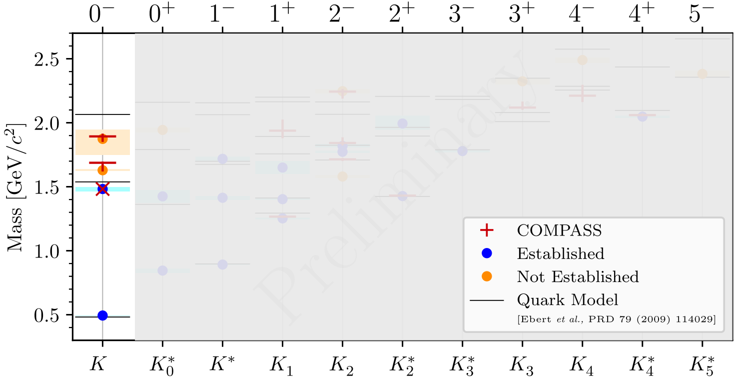

- Indications for 3 excited K from a single analysis
- Quark-model predicts only two excited states: potentially $K(1460)$ and $K(1830)$
  - ➥ $K(1630)$ supernumerary signal
  - ➥ Candidate for exotic non-$q\bar{q}$ state; other explanations possible ($K^*(892)\,\omega$ threshold nearby)

14-Wave Resonance-Model Fit

Searching for Exotic Strange Mesons with $J^P = 0^-$

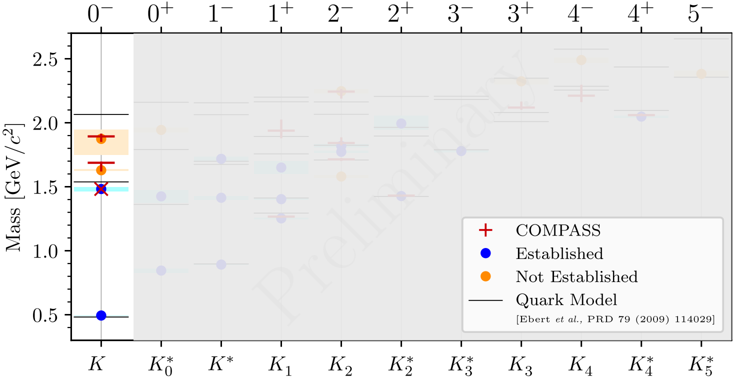

- Indications for 3 excited K from a single analysis
- Quark-model predicts only two excited states: potentially $K(1460)$ and $K(1830)$
  - ➥ $K(1630)$ supernumerary signal
  - ➥ Candidate for exotic non-$q\bar{q}$ state; other explanations possible ($K^*(892)\ \omega$ threshold nearby)

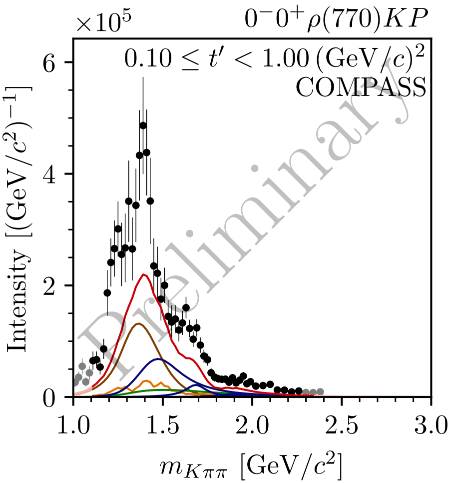

$\times 10^5$
$0^- 0^+ \rho(770) K P$
$0.10 \leq t' < 1.00\,(\text{GeV}/c)^2$
COMPASS
Preliminary
Intensity $[(\text{GeV}/c^2)^{-1}]$
6
4
2
0
1.0
1.5
2.0
2.5
3.0
$m_{K\pi\pi}$ $[\text{GeV}/c^2]$

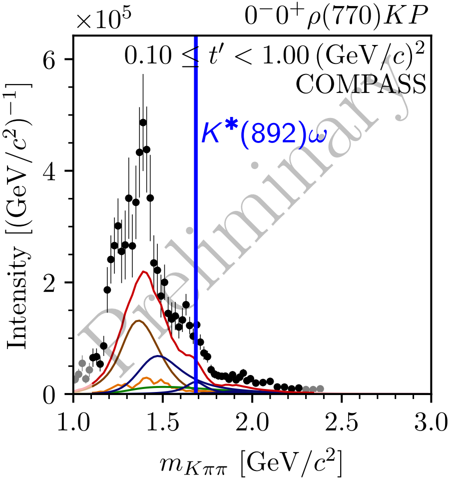
$\times 10^5$
$0^-0^+\rho(770)KP$
$0.10 \leq t' < 1.00\,(\mathrm{GeV}/c)^2$
COMPASS
$K^*(892)\omega$
Preliminary
Intensity $[(\mathrm{GeV}/c^2)^{-1}]$
0
2
4
6
1.0
1.5
2.0
2.5
3.0
$m_{K\pi\pi}$ $[\mathrm{GeV}/c^2]$

$K^-\pi^-\pi^+$ from ACCMOR

- Potential $K(1630)$ signal already in ACCMOR analysis

$K^-\pi^-\pi^+$ from LHCb

- Measurement of $D^0 \to K^\mp\pi^\pm\pi^\pm\pi^\mp$ at LHCb
  - Study strange mesons in $K\pi\pi$ subsystem
  - MIPWA of $J^P = 0^-$ amplitude
  - Potential signal above 1.6 GeV/c^2
  - Limited by kinematic range

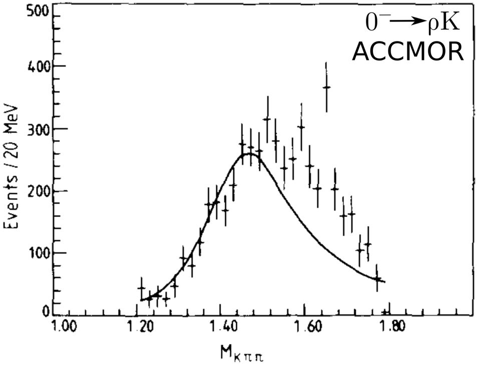

WA03 (CERN), 200 000 events, ACCMOR, Nucl. Phys. B **187** (1981)

$K^-\pi^-\pi^+$ from ACCMOR

- Potential $K(1630)$ signal already in ACCMOR analysis

$K^-\pi^-\pi^+$ from LHCb

- Measurement of $D^0 \to K^\mp\pi^\pm\pi^\pm\pi^\mp$ at LHCb
  - Study strange mesons in $K\pi\pi$ subsystem
  - MIPWA of $J^P = 0^-$ amplitude
  - Potential signal above 1.6 GeV/c^2
  - Limited by kinematic range

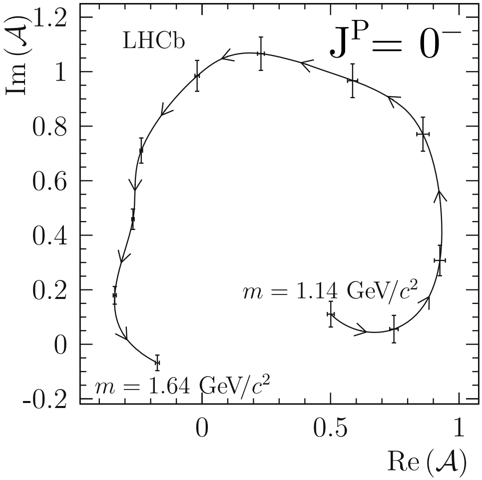

LHCb, 893 000 events, Eur. Phys. J. C **78** (2018)

$K^-\pi^-\pi^+$ from ACCMOR

- Potential $K(1630)$ signal already in ACCMOR analysis

$K^-\pi^-\pi^+$ from LHCb

- Measurement of $D^0 \to K^\mp\pi^\pm\pi^\pm\pi^\mp$ at LHCb
  - Study strange mesons in $K\pi\pi$ subsystem
  - MIPWA of $J^P = 0^-$ amplitude
  - Potential signal above 1.6 GeV/c^2
  - Limited by kinematic range

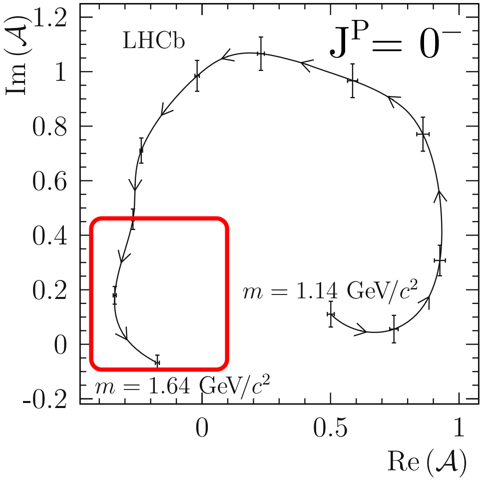

LHCb, 893 000 events, Eur. Phys. J. C **78** (2018)

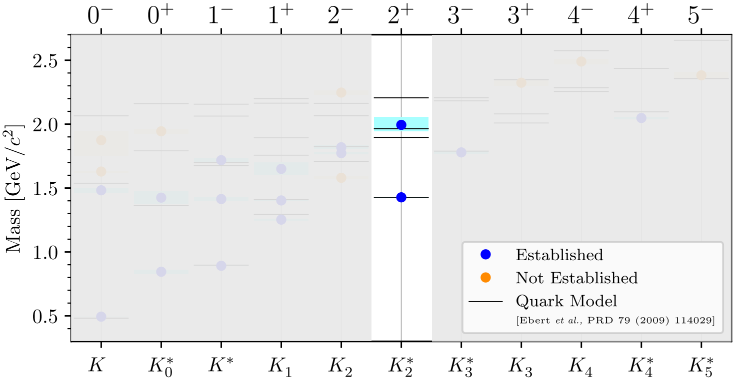

PDG

(2022)

- $K_2^*(1430)$ well known resonance

14-Wave Resonance-Model Fit

Partial Waves with $J^P = 2^+$

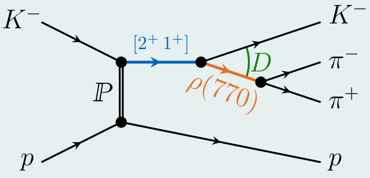

- Signal in $K_2^*(1430)$ mass region
- In different decays
  - $\rho(770)\,K\,D$
  - $K^*(892)\,\pi\,D$
- In agreement with previous measurements
- Cleaner signal in COMPASS data

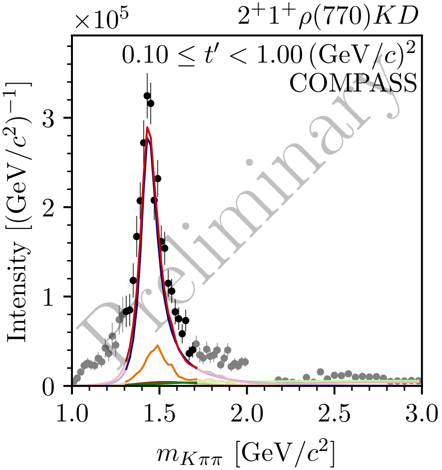

total resonance model, resonances, non-resonant, $\pi\pi\pi$ background, effective background

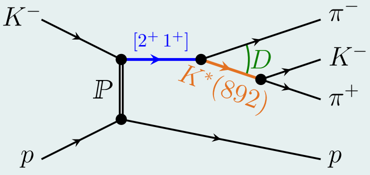

- Signal in $K_2^*(1430)$ mass region
- In different decays
  - $\rho(770)\,K\,D$
  - $K^*(892)\,\pi\,D$
- In agreement with previous measurements
- Cleaner signal in COMPASS data

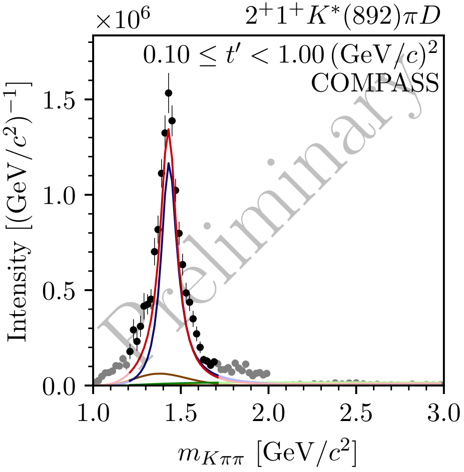

total resonance model, resonances, non-resonant, $\pi\,\pi\,\pi$ background, effective background

14-Wave Resonance-Model Fit

Partial Waves with $J^P = 2^+$

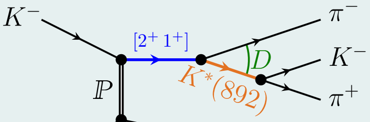

- Signal in $K_2^*(1430)$ mass region
- In different decays
  - $\rho(770)\,K\,D$
  - $K^*(892)\,\pi\,D$
- In agreement with previous measurements
- Cleaner signal in COMPASS data

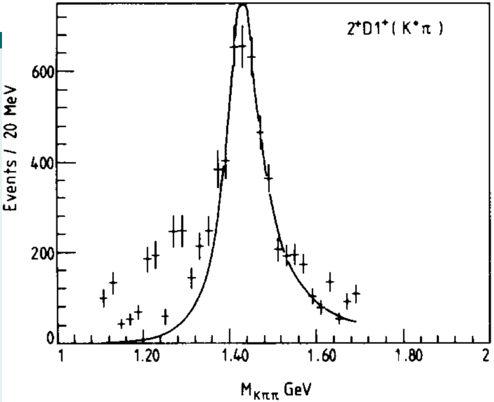

WA03 (CERN), 200 000 events, ACCMOR, Nucl. Phys. B **187** (1981)

14-Wave Resonance-Model Fit
Partial Waves with $J^P = 2^+$

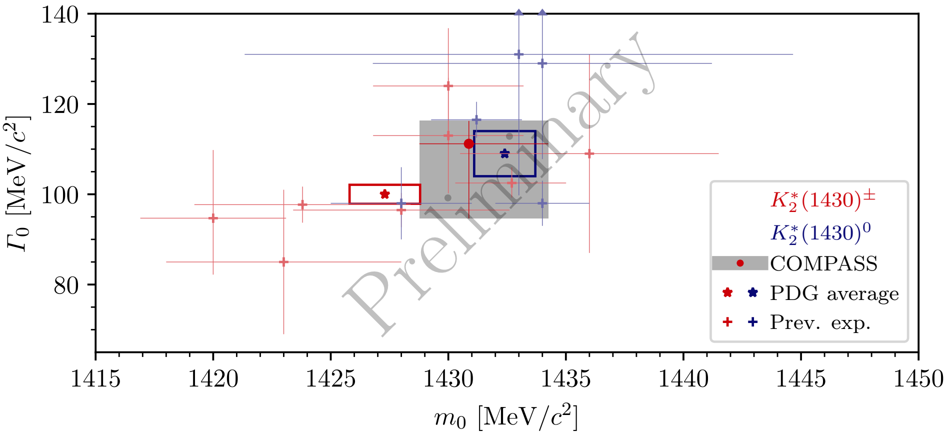

- $K_2^*(1430)$ parameters consistent with previous observations
- Better agreement with PDG average values for neutral $K_2^*(1430)$

14-Wave Resonance-Model Fit

Partial Waves with $J^P = 2^-$

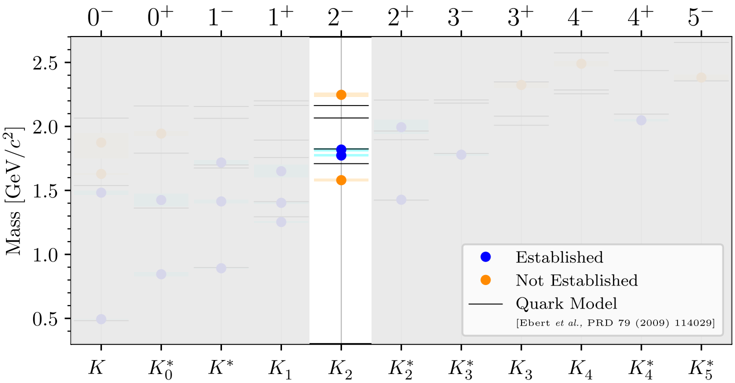

PDG (2022)

- Established $K_2(1770)$ and $K_2(1820)$
- $K_2(2250)$ need further confirmation

14-Wave Resonance-Model Fit

Partial Waves with $J^P = 2^-$

- Simultaneously fit 4 waves with $J^P = 2^-$
- $1.8\,\mathrm{GeV}/c^2$ peak modeled by $K_2(1770)$, $K_2(1820)$
- High-mass shoulder modeled by $K_2(2250)$
- Different intensity spectra and large phase motions among 2^- waves

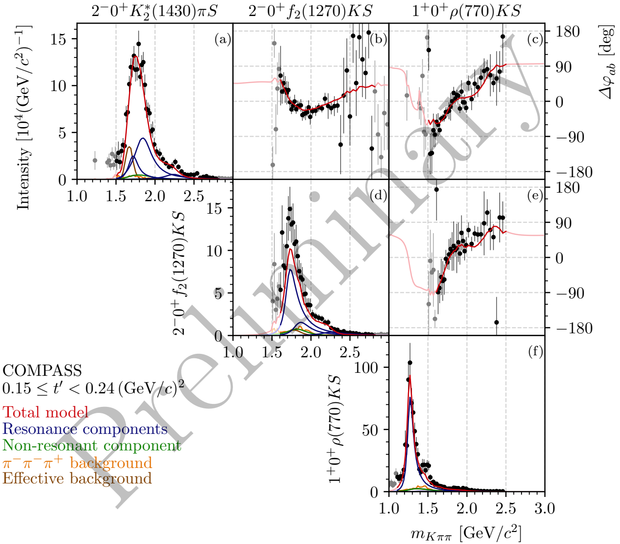

- Simultaneously fit 4 waves with $J^P = 2^-$
- 1.8 GeV/c^2 peak modeled by $K_2(1770)$, $K_2(1820)$
- High-mass shoulder modeled by $K_2(2250)$
- Different intensity spectra and large phase motions among 2^- waves

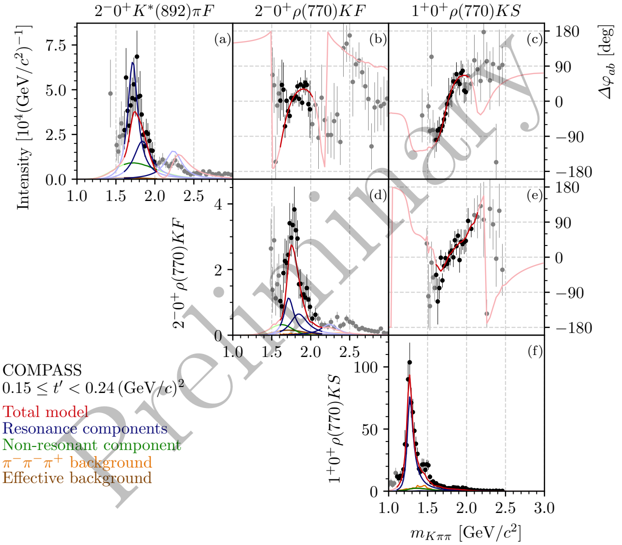

14-Wave Resonance-Model Fit

Partial Waves with $J^P = 2^-$

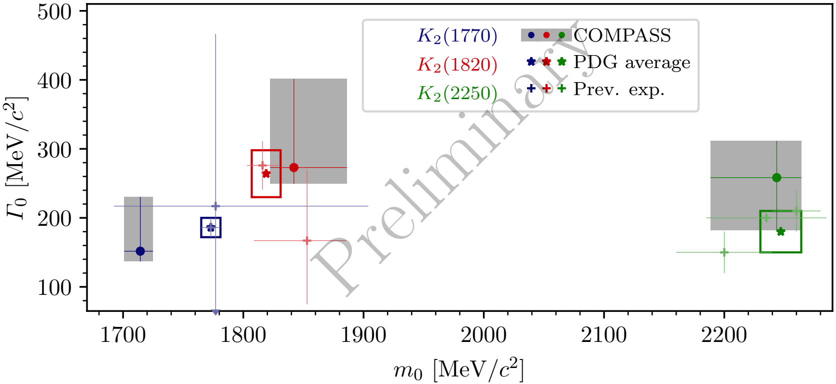

$K_2(1770)$ and $K_2(1820)$

- Two states were considered by only three measurements ACCMOR, LASS, LHCb
- Only LHCb measurement could confirm two states ($3\,\sigma$ statistical significance)
- We observe two sates with $11\,\sigma$ statistical significance

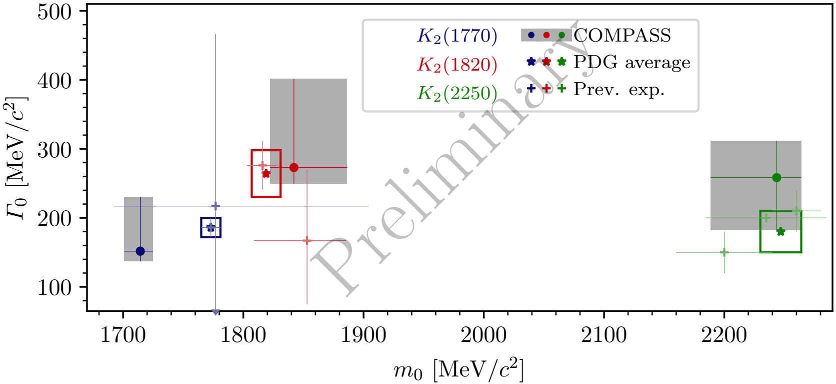

$K_2(2250)$

- Studied so far mainly in $\overset{(-)}{\Lambda}\overset{(-)}{p}$ final states
- First simultaneous measurement of $K_2(1770)$, $K_2(1820)$, and $K_2(2250)$
- Resonance parameters consistent with previous observations

14-Wave Resonance-Model Fit

Partial Waves with $J^P = 2^-$

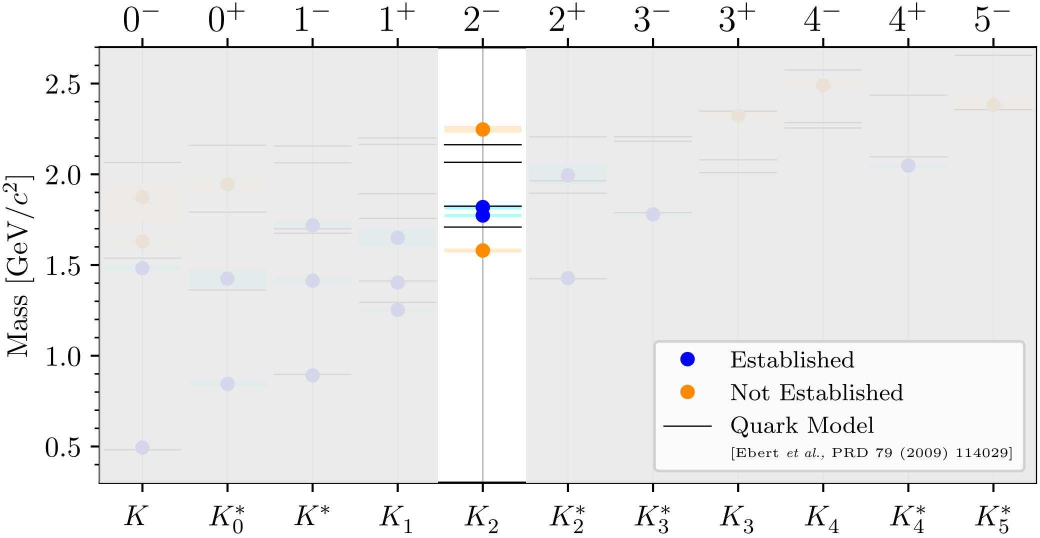

14-Wave Resonance-Model Fit

Partial Waves with $J^P = 2^-$

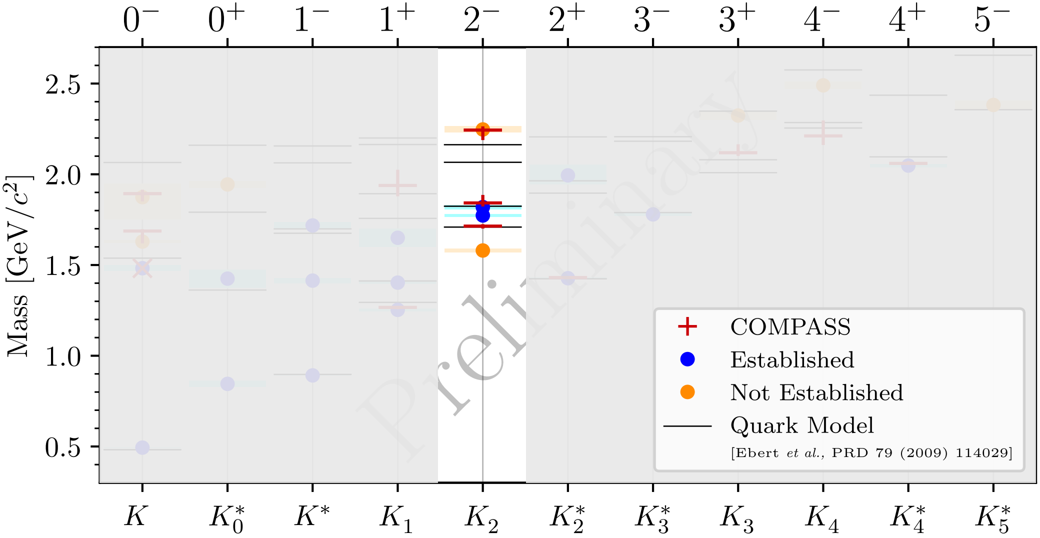

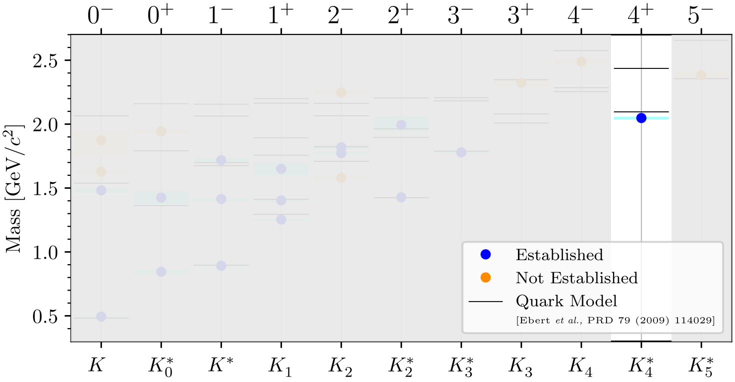

PDG

(2022)

- $K_4^*(2045)$ known resonance

- Signal $K_4^*(2045)$ signal in $K^*(892)\,\pi$ and $\rho(770)\,K$ decays

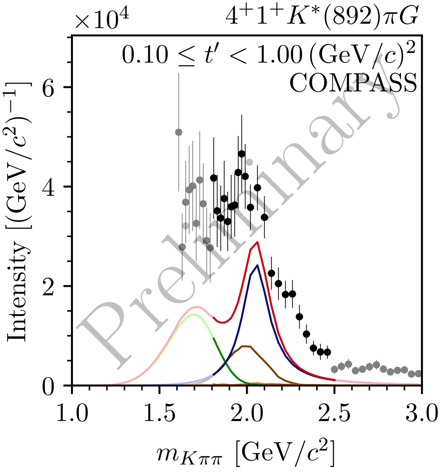

total resonance model, resonances, non-resonant, $\pi\pi\pi$ background, effective background

14-Wave Resonance-Model Fit

Partial Waves with $J^P = 4^+$

- Signal $K_4^*(2045)$ signal in $K^*(892)\,\pi$ and $\rho(770)\,K$ decays

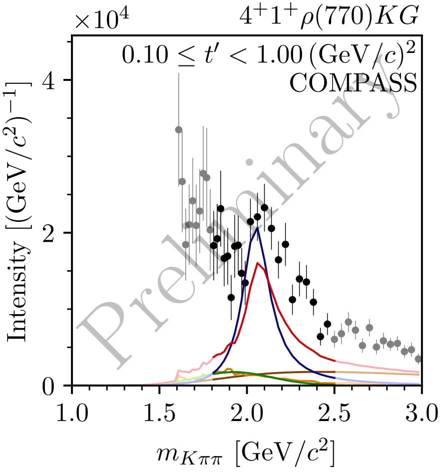

total resonance model, resonances, non-resonant, $\pi\pi\pi$ background, effective background

- Signal $K_4^*(2045)$ signal in $K^*(892)\,\pi$ and $\rho(770)\,K$ decays

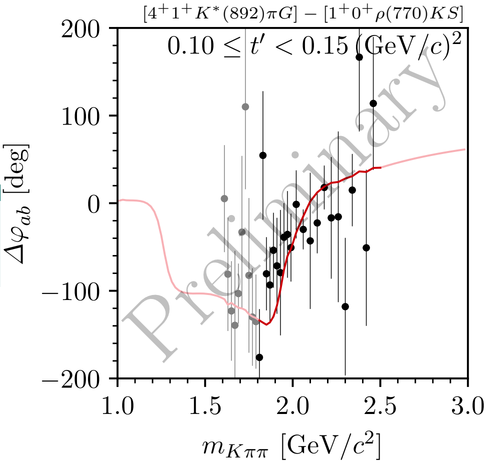

total resonance model, resonances, non-resonant, $\pi\pi\pi$ background, effective background

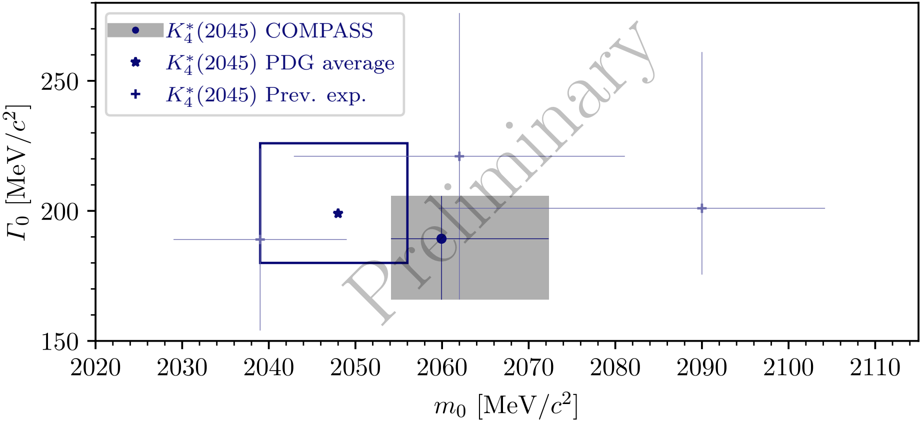

$K_4^*(2045)$ COMPASS
$K_4^*(2045)$ PDG average
$K_4^*(2045)$ Prev. exp.
Preliminary
250
200
150
Γ_0 [MeV/c^2]
2020
2030
2040
2050
2060
2070
2080
2090
2100
2110
m_0 [MeV/c^2]

14-Wave Resonance-Model Fit

Partial Waves with $J^P = 4^+$

- Imperfect description of magnitude of intensity,
- Also, real and imaginary parts of interference terms described well, including their magnitude
- Intensities and real and imaginary parts of interference terms not directly related as $\mathrm{Rank}[\rho_{ab}] > 1$ $|\rho_{ab}| \neq \sqrt{|\rho_{aa}|\,|\rho_{bb}|}$
  - ➥ Analysis artifacts in intensities of small waves, which are the least constrained by data

- Results validated by Monte Carlo input-output and systematic studies
- Imperfections considered in systematic uncertainties
- Results in agreement with previous experiments

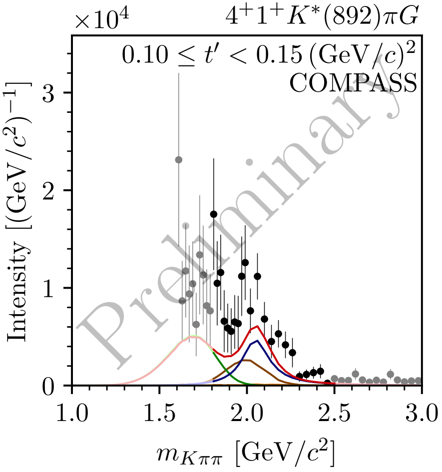

total resonance model, resonances, non-resonant, $\pi\pi\pi$ background, effective background

- Imperfect description of magnitude of intensity, , while relative phase described well
- Also, real and imaginary parts of interference terms described well, including their magnitude
- Intensities and real and imaginary parts of interference terms not directly related as $\mathrm{Rank}[\rho_{ab}] > 1$ $|\rho_{ab}| \neq \sqrt{|\rho_{aa}|\,|\rho_{bb}|}$
  - ➥ Analysis artifacts in intensities of small waves, which are the least constrained by data

- Results validated by Monte Carlo input-output and systematic studies
- Imperfections considered in systematic uncertainties
- Results in agreement with previous experiments

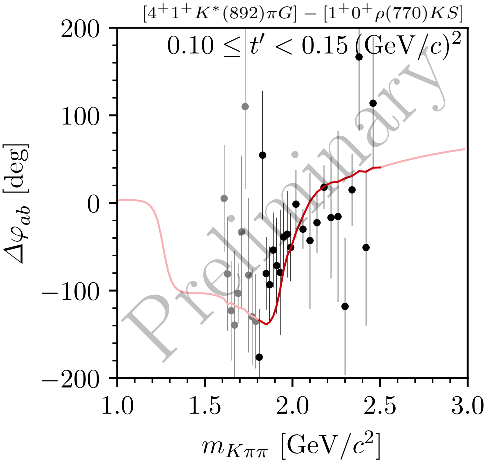

total resonance model, resonances, non-resonant, $\pi\pi\pi$ background, effective background

- Imperfect description of magnitude of intensity, , while relative phase described well
- Also, real and imaginary parts of interference terms described well, including their magnitude
- Intensities and real and imaginary parts of interference terms not directly related as $\mathrm{Rank}[\rho_{ab}] > 1$
  $|\rho_{ab}| \neq \sqrt{|\rho_{aa}|\,|\rho_{bb}|}$
  - ➥ Analysis artifacts in intensities of small waves, which are the least constrained by data

- Results validated by Monte Carlo input-output and systematic studies
- Imperfections considered in systematic uncertainties
- Results in agreement with previous experiments

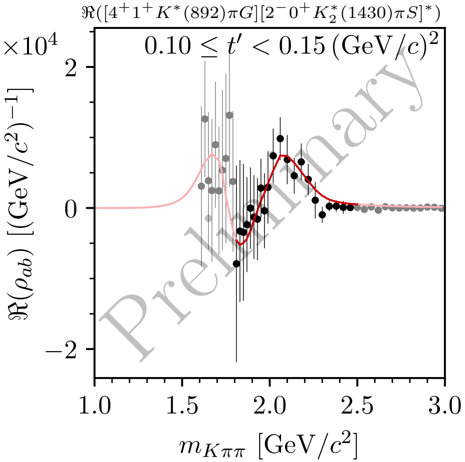

total resonance model, resonances, non-resonant, $\pi\pi\pi$ background, effective background

- Imperfect description of magnitude of intensity, , while relative phase described well
- Also, real and imaginary parts of interference terms described well, including their magnitude
- Intensities and real and imaginary parts of interference terms not directly related as $\mathrm{Rank}[\rho_{ab}] > 1$ $|\rho_{ab}| \neq \sqrt{|\rho_{aa}|\,|\rho_{bb}|}$
  - ➥ Analysis artifacts in intensities of small waves, which are the least constrained by data

- Results validated by Monte Carlo input-output and systematic studies
- Imperfections considered in systematic uncertainties
- Results in agreement with previous experiments

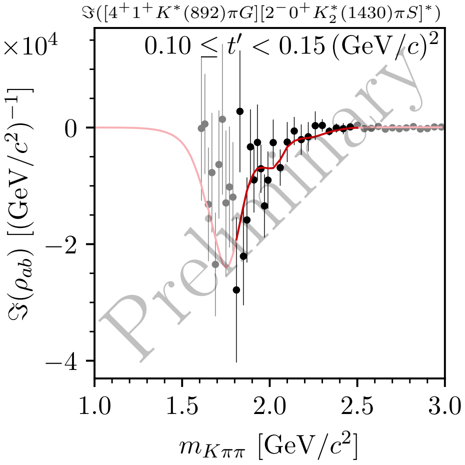

total resonance model, resonances, non-resonant, $\pi\pi\pi$ background, effective background

14-Wave Resonance-Model Fit

Partial Waves with $J^P = 4^+$

- Imperfect description of magnitude of intensity, , while relative phase described well
- Also, real and imaginary parts of interference terms described well, including their magnitude
- Intensities and real and imaginary parts of interference terms not directly related as $\mathrm{Rank}[\rho_{ab}] > 1$ $|\rho_{ab}| \neq \sqrt{|\rho_{aa}|\,|\rho_{bb}|}$
  - ➥ Analysis artifacts in intensities of small waves, which are the least constrained by data

- Results validated by Monte Carlo input-output and systematic studies
- Imperfections considered in systematic uncertainties
- Results in agreement with previous experiments

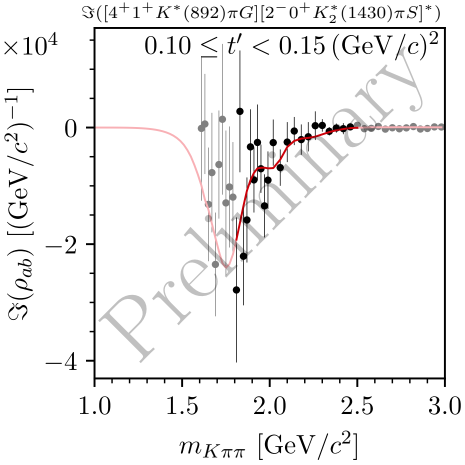

total resonance model, resonances, non-resonant, $\pi\pi\pi$ background, effective background

14-Wave Resonance-Model Fit

Partial Waves with $J^P = 4^+$

- Imperfect description of magnitude of intensity, , while relative phase described well
- Also, real and imaginary parts of interference terms described well, including their magnitude
- Intensities and real and imaginary parts of interference terms not directly related as $\mathrm{Rank}[\rho_{ab}] > 1$
  $|\rho_{ab}| \neq \sqrt{|\rho_{aa}|\,|\rho_{bb}|}$
  - ➥ Analysis artifacts in intensities of small waves, which are the least constrained by data

- Results validated by Monte Carlo input-output and systematic studies
- Imperfections considered in systematic uncertainties
- Results in agreement with previous experiments

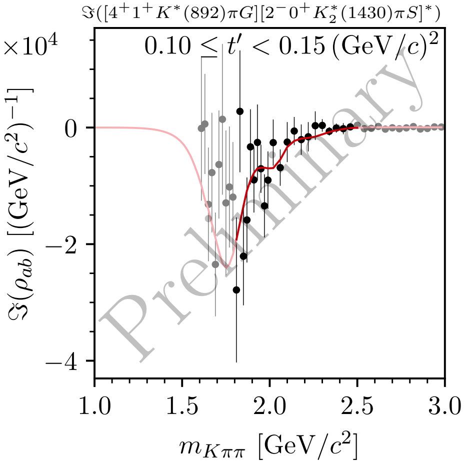

total resonance model, resonances, non-resonant, $\pi\pi\pi$ background, effective background

14-Wave Resonance-Model Fit
Partial Waves with $J^P = 4^+$

- Imperfect description of magnitude of intensity, , while relative phase described well
- Also, real and imaginary parts of interference terms described well, including their magnitude
- Intensities and real and imaginary parts of interference terms not directly related as $\mathrm{Rank}[\rho_{ab}] > 1$
  $|\rho_{ab}| \neq \sqrt{|\rho_{aa}|\,|\rho_{bb}|}$
  - ➥ Analysis artifacts in intensities of small waves, which are the least constrained by data

- Results validated by Monte Carlo input-output and systematic studies
- Imperfections considered in systematic uncertainties
- Results in agreement with previous experiments

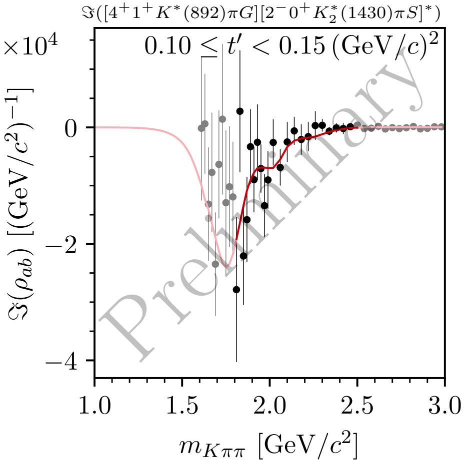

total resonance model, resonances, non-resonant, $\pi\pi\pi$ background, effective background

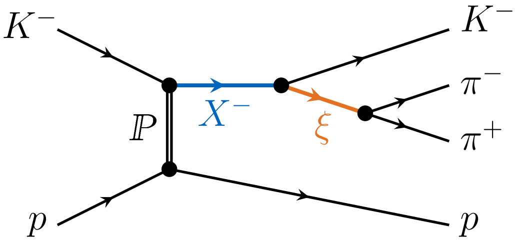

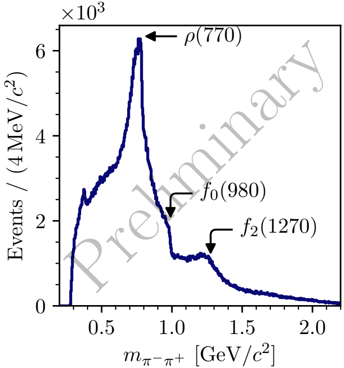

- Also structure in $\pi^-\pi^+$ and $K^-\pi^+$ subsystems
  - ➥ Successive 2-body decay via $\pi^-\pi^+$ / $K^-\pi^+$ resonance called isobar
- Also structure in angular distributions

Kinematic Distribution of $K^-\pi^-\pi^+$ Events
Subsystem

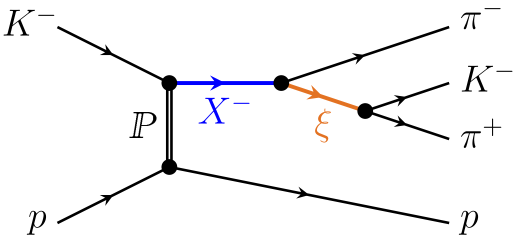

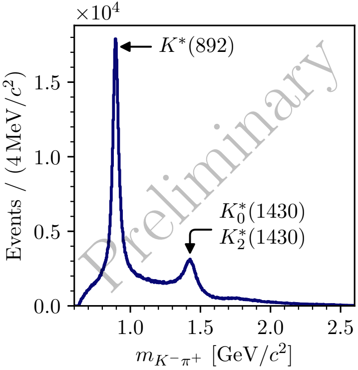

- Also structure in $\pi^-\pi^+$ and $K^-\pi^+$ subsystems
  - ➥ Successive 2-body decay via $\pi^-\pi^+$ / $K^-\pi^+$ resonance called isobar
- Also structure in angular distributions

Kinematic Distribution of $K^-\pi^-\pi^+$ Events

Subsystem

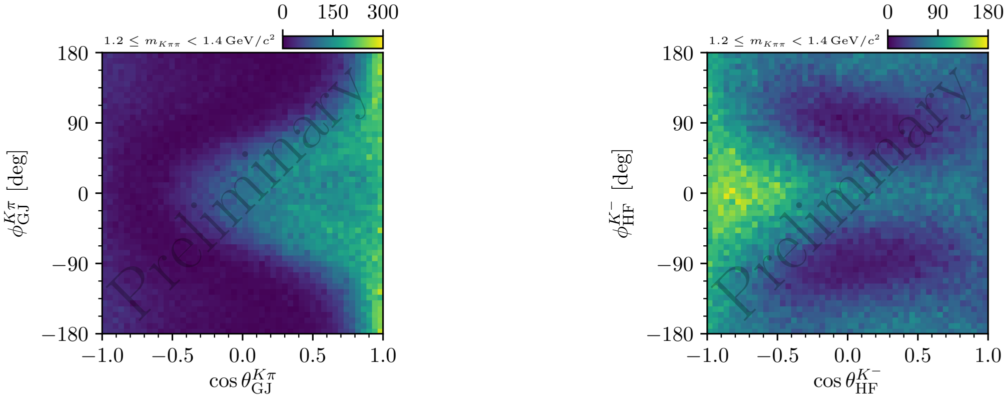

- Also structure in $\pi^-\pi^+$ and $K^-\pi^+$ subsystems
  - ➥ Successive 2-body decay via $\pi^-\pi^+$ / $K^-\pi^+$ resonance called isobar
- Also structure in angular distributions

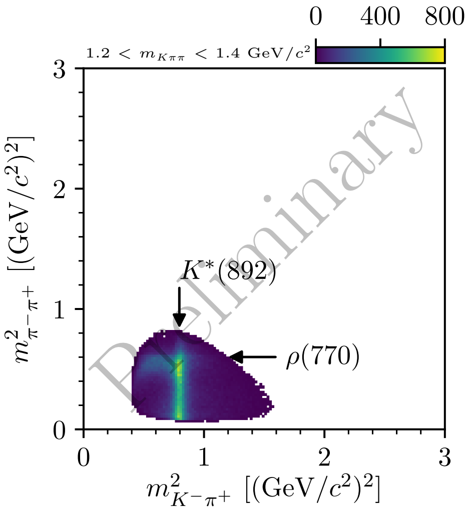

0 400 800
$1.2 < m_{K\pi\pi} < 1.4\ \mathrm{GeV}/c^2$
$K^*(892)$
$\rho(770)$
Preliminary
$m^2_{\pi^-\pi^+}$ [(GeV/c^2)^2]
$m^2_{K^-\pi^+}$ [(GeV/c^2)^2]
0
1
2
3

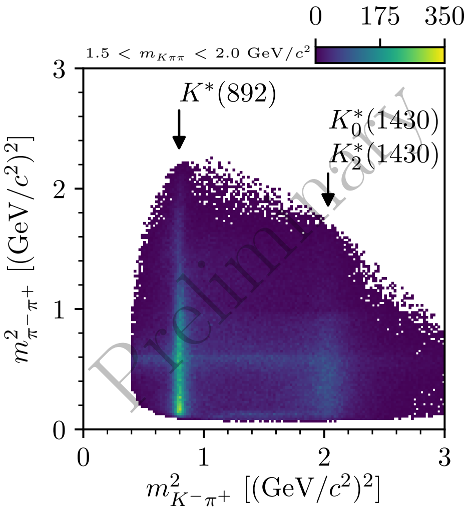

0 175 350
$1.5 < m_{K\pi\pi} < 2.0\ \mathrm{GeV}/c^2$
$K^*(892)$
$K_0^*(1430)$
$K_2^*(1430)$
Preliminary
$m^2_{\pi^-\pi^+}$ [(GeV/c^2)^2]
$m^2_{K^-\pi^+}$ [(GeV/c^2)^2]
0
1
2
3

Kinematic Distribution of $K^-\pi^-\pi^+$ Events

$m_{K^-\pi^-}$

- No dominant resonant structures

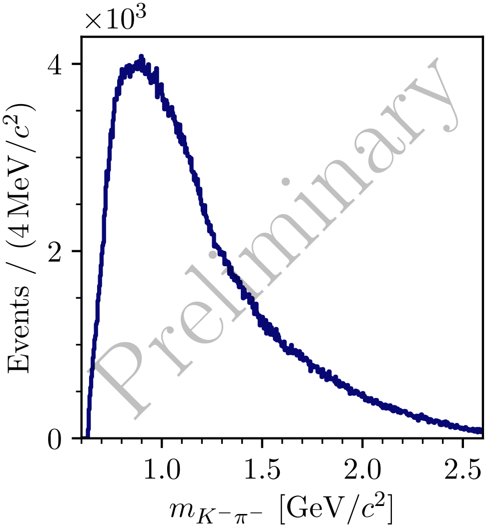

- Exponential shape
- Shallower for larger t'

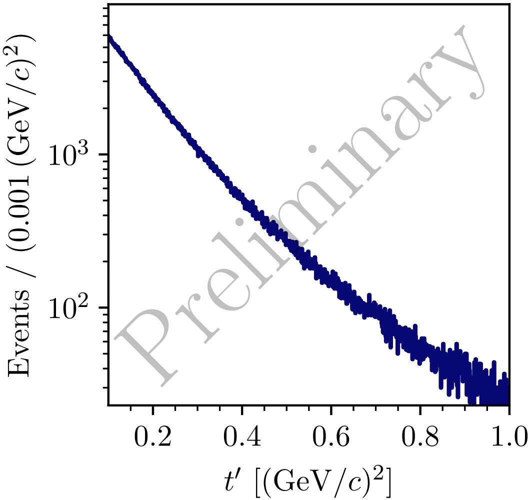

Kinematic Distribution of $K^-\pi^-\pi^+$ Events
Exclusivity

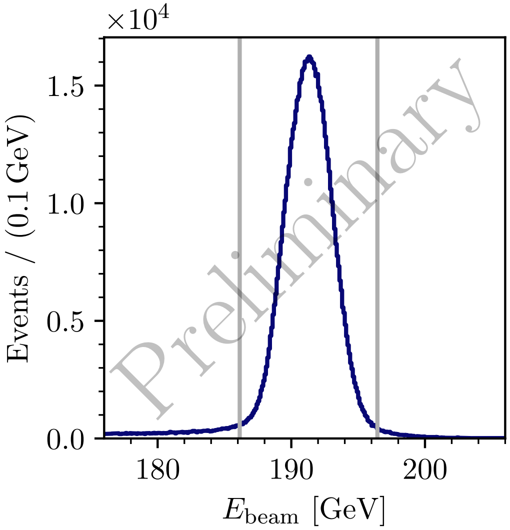

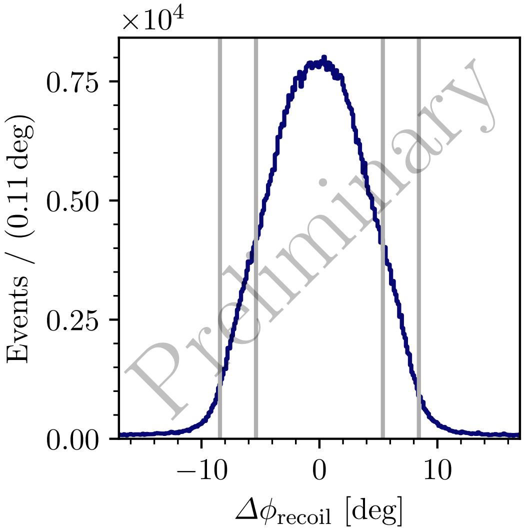

Kinematic Distribution of $K^-\pi^-\pi^+$ Events
Exclusivity

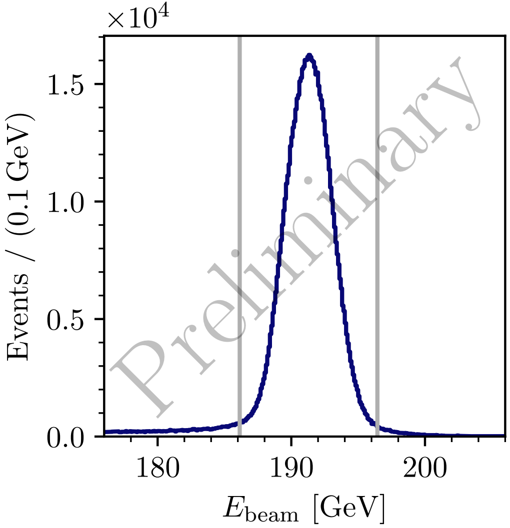

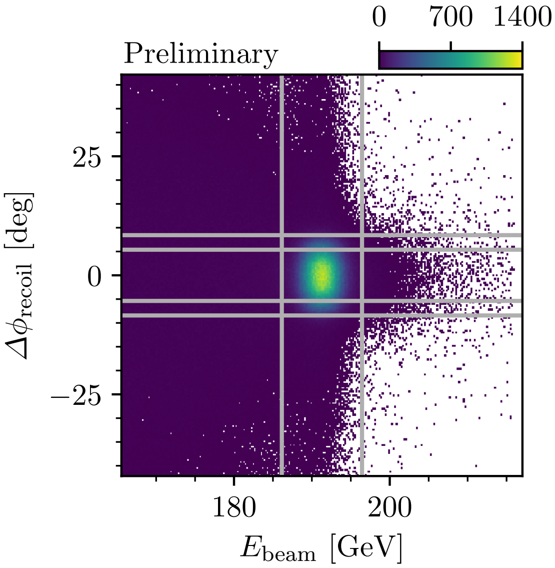

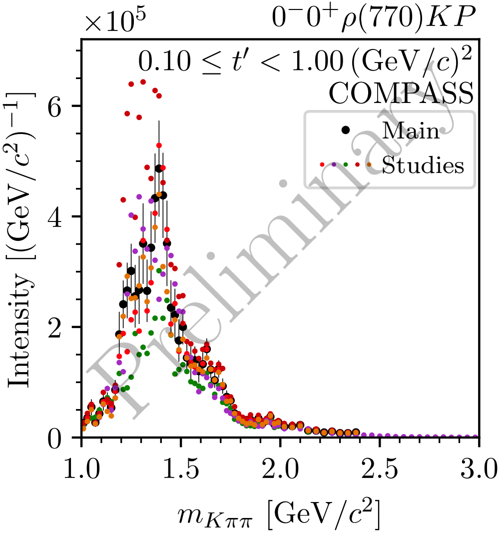

$\times 10^5$
$0^-0^+\rho(770)KP$
$0.10 \leq t' < 1.00\,(\mathrm{GeV}/c)^2$
COMPASS
Main
Studies
Preliminary
Intensity $[(\mathrm{GeV}/c^2)^{-1}]$
$m_{K\pi\pi}$ $[\mathrm{GeV}/c^2]$
0
2
4
6
1.0
1.5
2.0
2.5
3.0

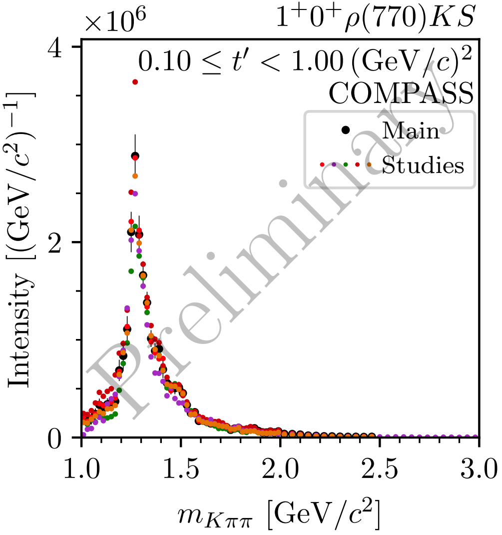
$\times 10^6$
$1^+0^+\rho(770)KS$
$0.10 \leq t' < 1.00\,(\mathrm{GeV}/c)^2$
COMPASS
Main
Studies
Preliminary
Intensity $[(\mathrm{GeV}/c^2)^{-1}]$
$m_{K\pi\pi}$ $[\mathrm{GeV}/c^2]$
0
2
4
1.0
1.5
2.0
2.5
3.0

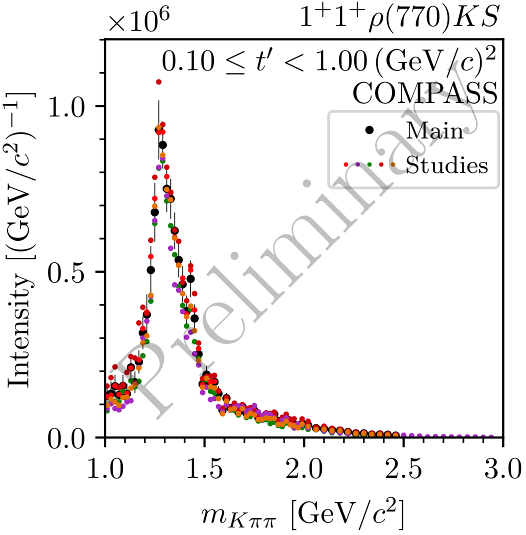
$\times 10^6$
$1^+1^+\rho(770)KS$
$0.10 \leq t' < 1.00\,(\mathrm{GeV}/c)^2$
COMPASS
Main
Studies
Preliminary
Intensity $[(\mathrm{GeV}/c^2)^{-1}]$
1.0
0.5
0.0
1.0
1.5
2.0
2.5
3.0
$m_{K\pi\pi}$ $[\mathrm{GeV}/c^2]$

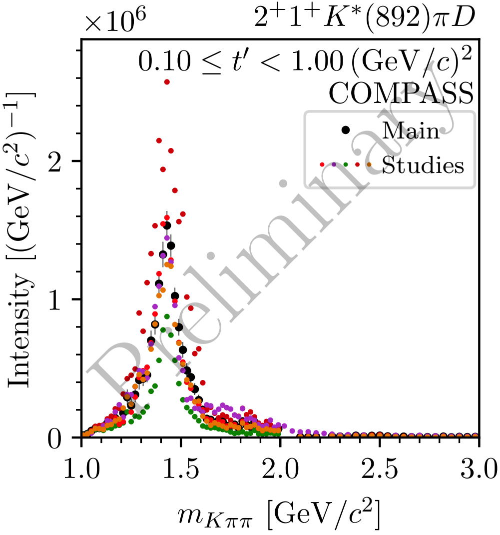
$\times 10^6$
$2^+1^+K^*(892)\pi D$
$0.10 \leq t' < 1.00\,(\mathrm{GeV}/c)^2$
COMPASS
Main
Studies
Preliminary
Intensity $[(\mathrm{GeV}/c^2)^{-1}]$
0
1
2
1.0
1.5
2.0
2.5
3.0
$m_{K\pi\pi}\ [\mathrm{GeV}/c^2]$

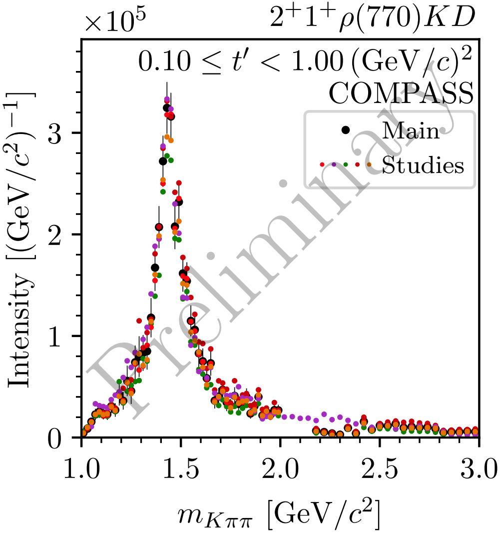
$\times 10^5$
$2^+1^+\rho(770)KD$
$0.10 \leq t' < 1.00\,(\mathrm{GeV}/c)^2$
COMPASS
Main
Studies
Preliminary
Intensity $[(\mathrm{GeV}/c^2)^{-1}]$
0
1
2
3
1.0
1.5
2.0
2.5
3.0
$m_{K\pi\pi}$ $[\mathrm{GeV}/c^2]$

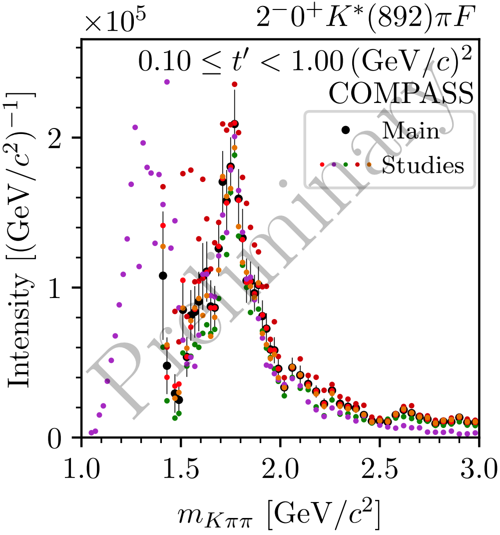

$\times 10^5$
$2^- 0^+ K^*(892)\pi F$
$0.10 \leq t' < 1.00\,(\text{GeV}/c)^2$
COMPASS
Main
Studies
Preliminary
Intensity $[(\text{GeV}/c^2)^{-1}]$
$m_{K\pi\pi}$ $[\text{GeV}/c^2]$
0
1
2
1.0
1.5
2.0
2.5
3.0

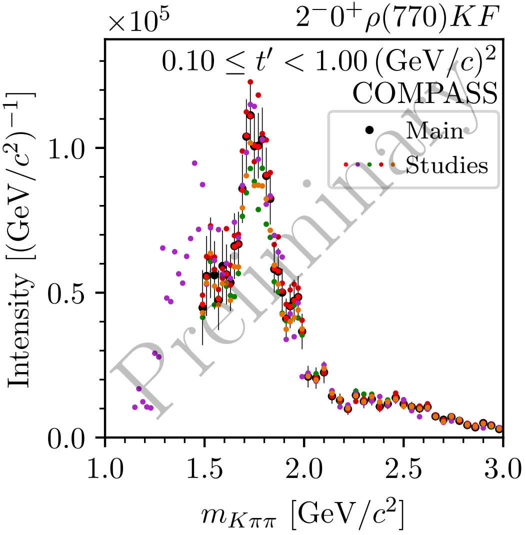
$\times 10^5$
$2^-0^+\rho(770)KF$
$0.10 \leq t' < 1.00\,(\mathrm{GeV}/c)^2$
COMPASS
Main
Studies
Preliminary
Intensity $[(\mathrm{GeV}/c^2)^{-1}]$
1.0
0.5
0.0
1.0
1.5
2.0
2.5
3.0
$m_{K\pi\pi}$ $[\mathrm{GeV}/c^2]$

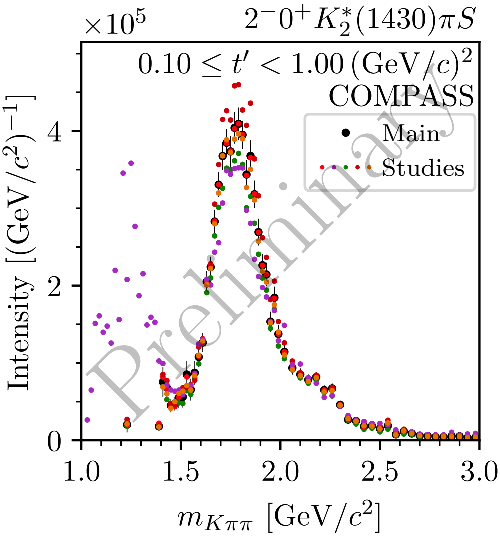
$\times 10^5$
$2^-0^+K_2^*(1430)\pi S$
$0.10 \leq t' < 1.00\,(\mathrm{GeV}/c)^2$
COMPASS
Main
Studies
Preliminary
Intensity $[(\mathrm{GeV}/c^2)^{-1}]$
0
2
4
1.0
1.5
2.0
2.5
3.0
$m_{K\pi\pi}\ [\mathrm{GeV}/c^2]$

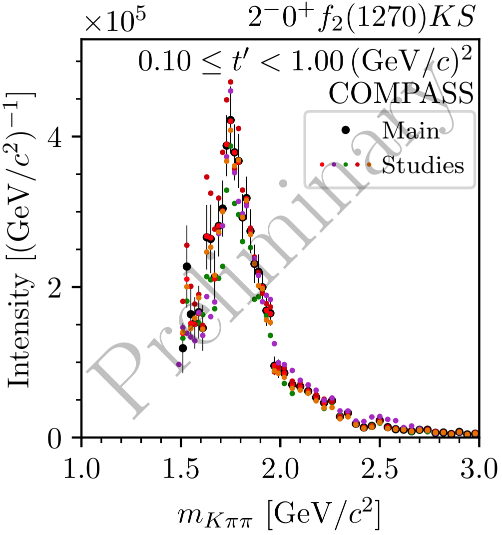
$2^-0^+ f_2(1270) K S$
$\times 10^5$
$0.10 \leq t' < 1.00\,(\text{GeV}/c)^2$
COMPASS
Main
Studies
Preliminary
Intensity $[(\text{GeV}/c^2)^{-1}]$
0
2
4
1.0
1.5
2.0
2.5
3.0
$m_{K\pi\pi}$ $[\text{GeV}/c^2]$

Systematic Studies of the Partial-Wave Decomposition
14 Waves

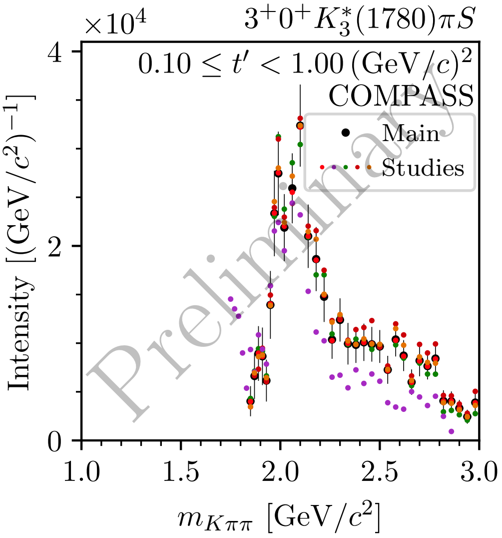

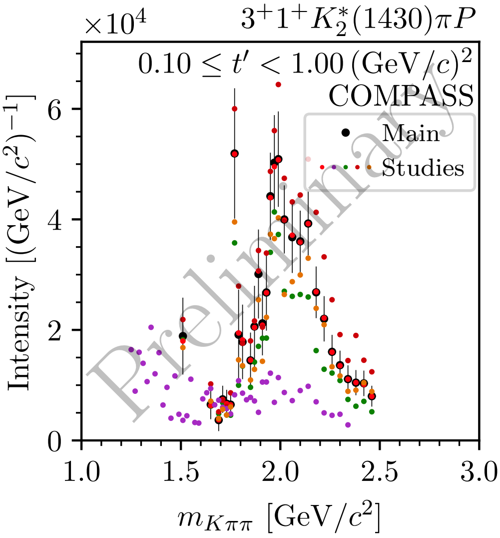
$\times 10^4$
$3^+1^+K_2^*(1430)\pi P$
$0.10 \leq t' < 1.00\,(\mathrm{GeV}/c)^2$
COMPASS
Main
Studies
Preliminary
Intensity $[(\mathrm{GeV}/c^2)^{-1}]$
0
2
4
6
1.0
1.5
2.0
2.5
3.0
$m_{K\pi\pi}$ $[\mathrm{GeV}/c^2]$

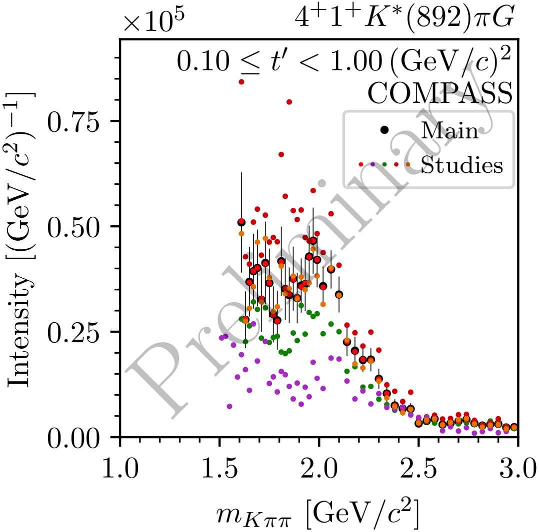

$4^+1^+K^*(892)\pi G$
$\times 10^5$
$0.10 \leq t' < 1.00\,(\text{GeV}/c)^2$
COMPASS
Main
Studies
Preliminary
Intensity $[(\text{GeV}/c^2)^{-1}]$
0.00
0.25
0.50
0.75
1.0
1.5
2.0
2.5
3.0
$m_{K\pi\pi}$ $[\text{GeV}/c^2]$

Systematic Studies of the Partial-Wave Decomposition
14 Waves

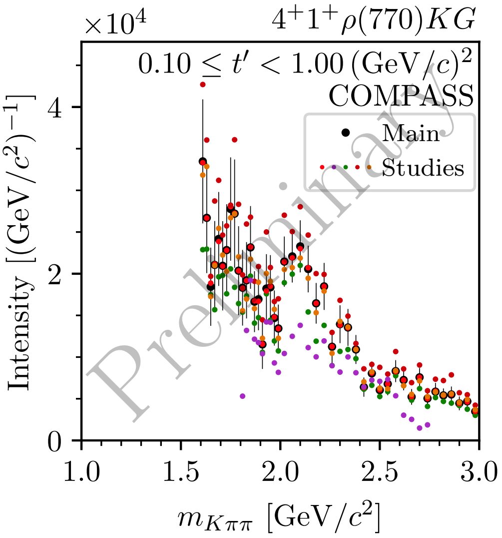

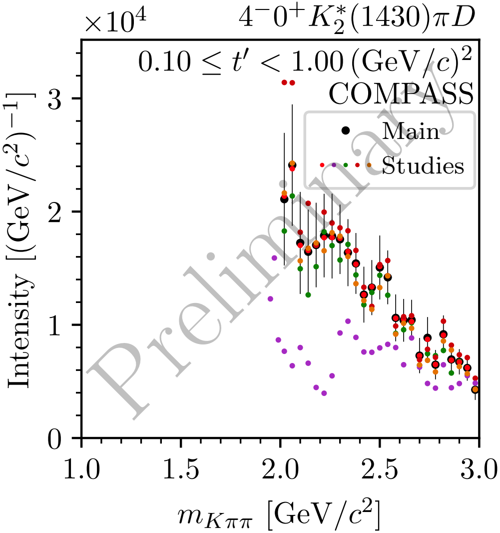
$\times 10^4$
$4^- 0^+ K_2^*(1430)\pi D$
$0.10 \leq t' < 1.00\,(\text{GeV}/c)^2$
COMPASS
Main
Studies
Preliminary
Intensity $[(\text{GeV}/c^2)^{-1}]$
$m_{K\pi\pi}$ $[\text{GeV}/c^2]$
0
1
2
3
1.0
1.5
2.0
2.5
3.0

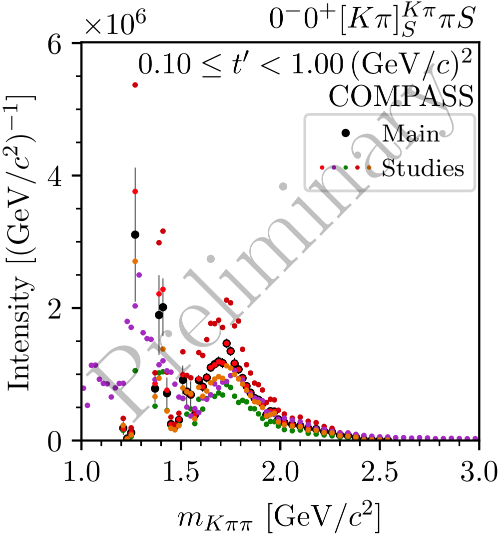
$\times 10^6$
$0^-0^+[K\pi]^{K\pi}_S \pi S$
$0.10 \leq t' < 1.00\,(\mathrm{GeV}/c)^2$
COMPASS
Main
Studies
Preliminary
6
4
2
0
1.0
1.5
2.0
2.5
3.0
Intensity $[(\mathrm{GeV}/c^2)^{-1}]$
$m_{K\pi\pi}$ $[\mathrm{GeV}/c^2]$

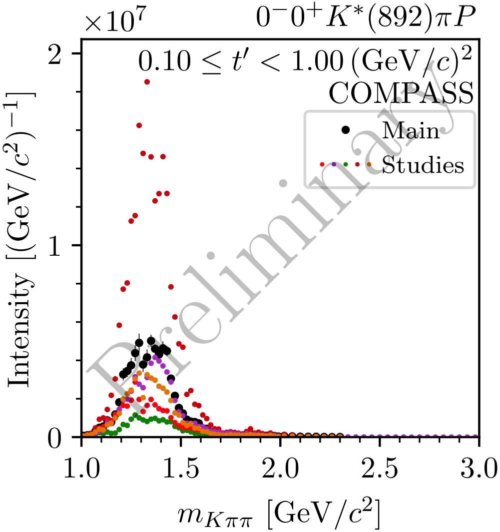
$\times 10^7$
$0^-0^+K^*(892)\pi P$
$0.10 \leq t' < 1.00\,(\mathrm{GeV}/c)^2$
COMPASS
Main
Studies
Preliminary
Intensity $[(\mathrm{GeV}/c^2)^{-1}]$
$m_{K\pi\pi}$ $[\mathrm{GeV}/c^2]$
0
1
2
1.0
1.5
2.0
2.5
3.0

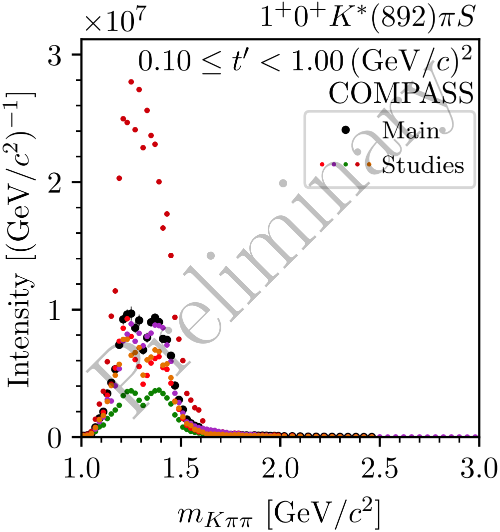
$\times 10^7$
$1^+0^+K^*(892)\pi S$
$0.10 \leq t' < 1.00\,(\mathrm{GeV}/c)^2$
COMPASS
Main
Studies
Preliminary
Intensity $[(\mathrm{GeV}/c^2)^{-1}]$
$m_{K\pi\pi}$ $[\mathrm{GeV}/c^2]$
0
1
2
3
1.0
1.5
2.0
2.5
3.0

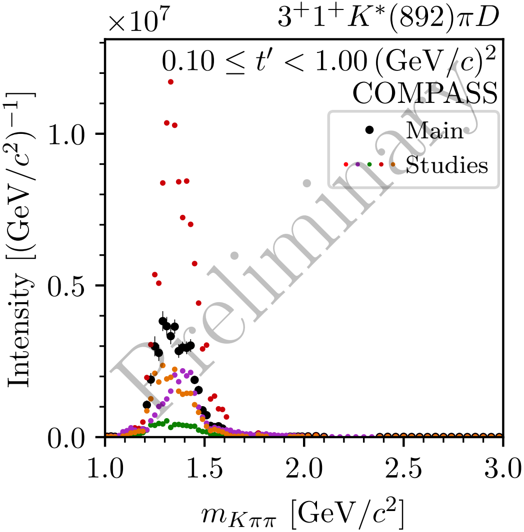
$3^+1^+K^*(892)\pi D$
$\times 10^7$
$0.10 \leq t' < 1.00\,(\mathrm{GeV}/c)^2$
COMPASS
Main
Studies
Preliminary
Intensity $[(\mathrm{GeV}/c^2)^{-1}]$
$m_{K\pi\pi}$ $[\mathrm{GeV}/c^2]$
0.0
0.5
1.0
1.0
1.5
2.0
2.5
3.0

Leakage Effect

- Unexpected low-mass enhancement in $3^+ 1^+$ $K^*(892)\,\pi\, D$ wave
- Similar to dominant 1^+ wave
- Sensitive to systematic effects
- Decay amplitudes of different J^P are orthogonal
- Event selection requires to identify one of the two negative particles
  - Limited acceptance due to limited kinematic range of final-state PID
- Loss of orthogonality taking acceptance into account
  - Reduced differentiability of certain partial waves
- Only a sub-set of partial waves affected

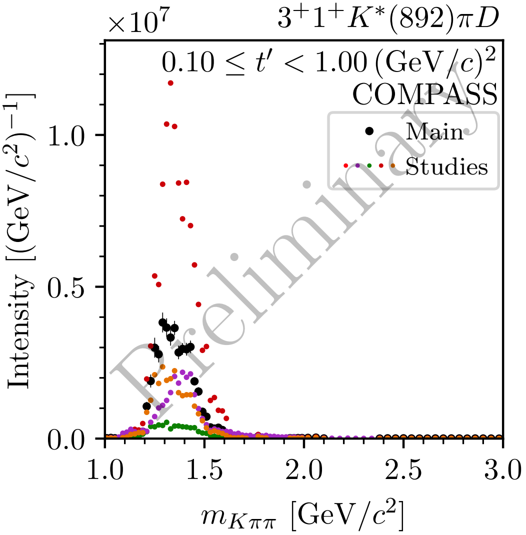

Leakage Effect

- Unexpected low-mass enhancement in $3^+ 1^+$ $K^*(892)\,\pi\,D$ wave
- Similar to dominant 1^+ wave
- Sensitive to systematic effects
- Decay amplitudes of different J^P are orthogonal
- Event selection requires to identify one of the two negative particles
  - Limited acceptance due to limited kinematic range of final-state PID
- Loss of orthogonality taking acceptance into account
  - ➡ Reduced differentiability of certain partial waves
- Only a sub-set of partial waves affected

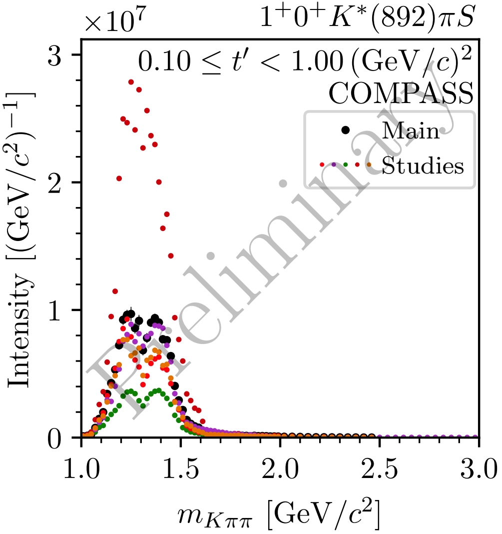

Leakage Effect

- Unexpected low-mass enhancement in $3^+ 1^+ K^*(892) \pi D$ wave
- Similar to dominant 1^+ wave
- Sensitive to systematic effects
- Decay amplitudes of different J^P are orthogonal
- Event selection requires to identify one of the two negative particles
  - Limited acceptance due to limited kinematic range of final-state PID
- Loss of orthogonality taking acceptance into account
  - ➡ Reduced differentiability of certain partial waves
- Only a sub-set of partial waves affected

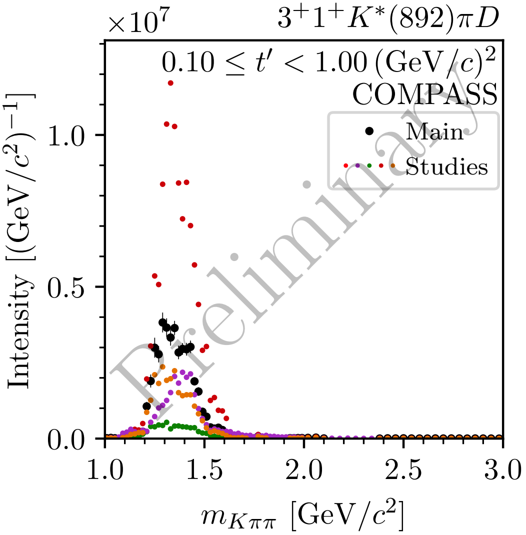

Leakage Effect

- Unexpected low-mass enhancement in $3^+ 1^+ K^*(892)\,\pi\, D$ wave
- Similar to dominant 1^+ wave
- Sensitive to systematic effects
- Decay amplitudes of different J^P are orthogonal
- Event selection requires to identify one of the two negative particles
  - Limited acceptance due to limited kinematic range of final-state PID
- Loss of orthogonality taking acceptance into account
  - ➥ Reduced differentiability of certain partial waves
- Only a sub-set of partial waves affected

$$I_{a,b} = \int \mathrm{d}\varphi_3(\tau)\; \Psi_a(\tau)\Psi_b^*(\tau)$$

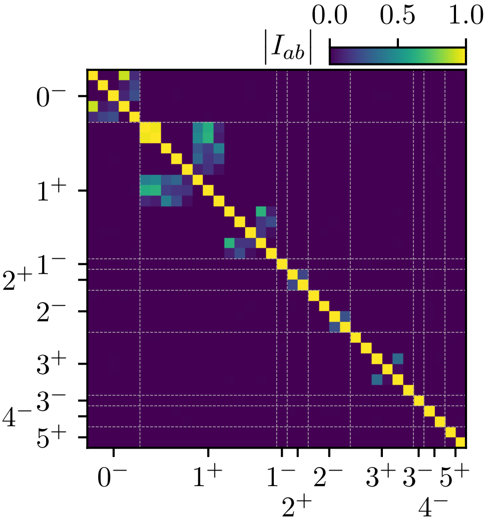

Leakage Effect

- Unexpected low-mass enhancement in $3^+ 1^+$ $K^*(892)\,\pi\ D$ wave
- Similar to dominant 1^+ wave
- Sensitive to systematic effects
- Decay amplitudes of different J^P are orthogonal
- Event selection requires to identify one of the two negative particles
  - Limited acceptance due to limited kinematic range of final-state PID
- Loss of orthogonality taking acceptance into account
  - ➡ Reduced differentiability of certain partial waves
- Only a sub-set of partial waves affected

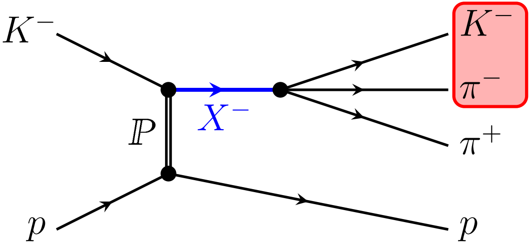

Leakage Effect

- Unexpected low-mass enhancement in $3^+ 1^+ K^*(892) \pi D$ wave
- Similar to dominant 1^+ wave
- Sensitive to systematic effects
- Decay amplitudes of different J^P are orthogonal
- Event selection requires to identify one of the two negative particles
  - Limited acceptance due to limited kinematic range of final-state PID
- Loss of orthogonality taking acceptance into account
  - ➡ Reduced differentiability of certain partial waves
- Only a sub-set of partial waves affected

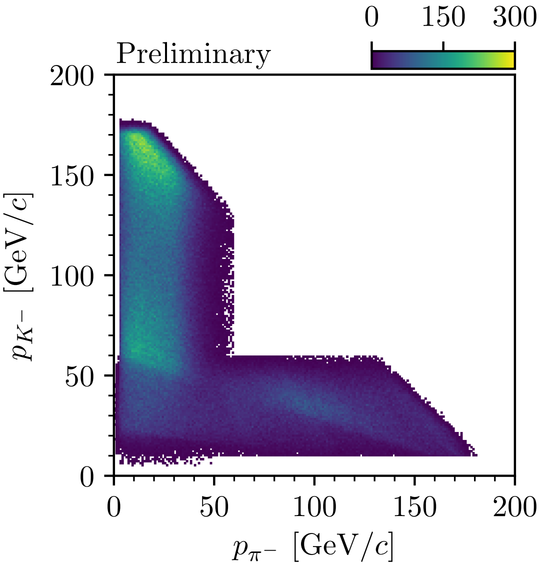

Leakage Effect

- Unexpected low-mass enhancement in $3^+ 1^+ K^*(892)\,\pi\, D$ wave
- Similar to dominant 1^+ wave
- Sensitive to systematic effects
- Decay amplitudes of different J^P are orthogonal
- Event selection requires to identify one of the two negative particles
  - Limited acceptance due to limited kinematic range of final-state PID
- Loss of orthogonality taking acceptance into account
  - ➥ Reduced differentiability of certain partial waves
- Only a sub-set of partial waves affected

$$\bar{I}_{a,b} = \int \mathrm{d}\varphi_3(\tau)\; \eta(\tau)\, \Psi_a(\tau)\Psi_b^*(\tau)$$

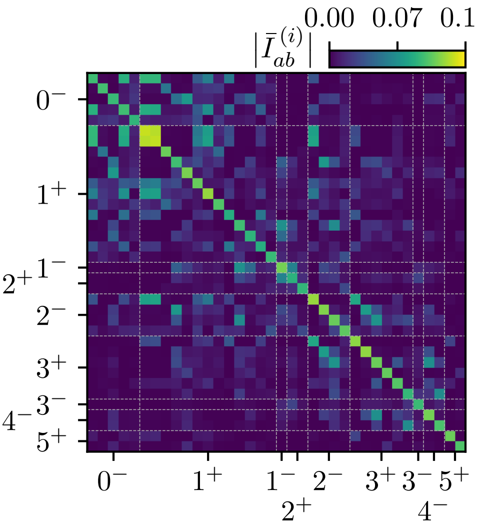

Leakage Effect

- Unexpected low-mass enhancement in $3^+ 1^+$ $K^*(892)\,\pi\, D$ wave
- Similar to dominant 1^+ wave
- Sensitive to systematic effects
- Decay amplitudes of different J^P are orthogonal
- Event selection requires to identify one of the two negative particles
  - Limited acceptance due to limited kinematic range of final-state PID
- Loss of orthogonality taking acceptance into account
  - ➡ Reduced differentiability of certain partial waves
- Only a sub-set of partial waves affected

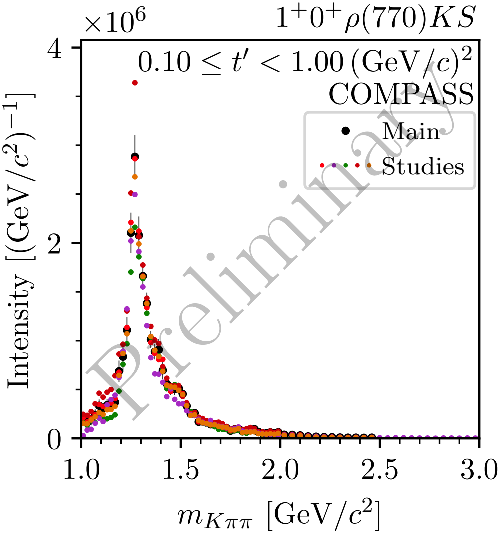

Leakage Effect

- Unexpected low-mass enhancement in $3^+ 1^+$ $K^*(892)\,\pi\, D$ wave
- Similar to dominant 1^+ wave
- Sensitive to systematic effects
- Decay amplitudes of different J^P are orthogonal
- Event selection requires to identify one of the two negative particles
  - Limited acceptance due to limited kinematic range of final-state PID
- Loss of orthogonality taking acceptance into account
  - ➥ Reduced differentiability of certain partial waves
- Only a sub-set of partial waves affected

Incoherent $\pi^-\pi^-\pi^+$ Background

- $K^-\pi^-\pi^+$ and $\pi^-\pi^-\pi^+$ similar experimental footprint
- Distinguishable only by
  - Beam particle identification
  - Final-state particle identification
- Excellent beam PID:
  - Expect small contamination from beam π^-
- Final-state PID does not suppress $\pi^-\pi^-\pi^+$ background
  - ➥ Non-negligible $\pi^-\pi^-\pi^+$ background in $K^-\pi^-\pi^+$ sample of about 7 %
  - ➥ Dominant background in $K^-\pi^-\pi^+$ sample

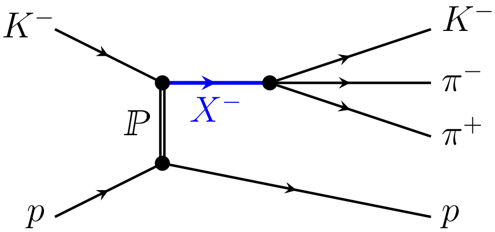

Incoherent $\pi^-\pi^-\pi^+$ Background

- $K^-\pi^-\pi^+$ and $\pi^-\pi^-\pi^+$ similar experimental footprint
- Distinguishable only by
  - Beam particle identification
  - Final-state particle identification
- Excellent beam PID:
  - Expect small contamination from beam π^-
- Final-state PID does not suppress $\pi^-\pi^-\pi^+$ background
  - ➥ Non-negligible $\pi^-\pi^-\pi^+$ background in $K^-\pi^-\pi^+$ sample of about 7 %
  - ➥ Dominant background in $K^-\pi^-\pi^+$ sample

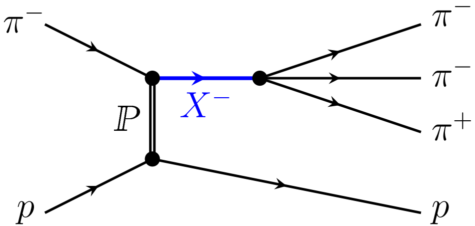

Incoherent $\pi^-\pi^-\pi^+$ Background

- $K^-\pi^-\pi^+$ and $\pi^-\pi^-\pi^+$ similar experimental footprint
- Distinguishable only by
  - Beam particle identification
  - Final-state particle identification
- Excellent beam PID:
  - Expect small contamination from beam π^-
- Final-state PID does not suppress $\pi^-\pi^-\pi^+$ background
  - ➥ Non-negligible $\pi^-\pi^-\pi^+$ background in $K^-\pi^-\pi^+$ sample of about 7 %
  - ➥ Dominant background in $K^-\pi^-\pi^+$ sample

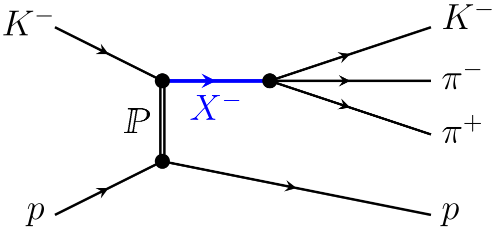

- $K^-\pi^-\pi^+$ and $\pi^-\pi^-\pi^+$ similar experimental footprint
- Distinguishable only by
  - Beam particle identification
  - Final-state particle identification
- Excellent beam PID:
  - Expect small contamination from beam π^-
- Final-state PID does not suppress $\pi^-\pi^-\pi^+$ background
  - ➥ Non-negligible $\pi^-\pi^-\pi^+$ background in $K^-\pi^-\pi^+$ sample of about 7 %
  - ➥ Dominant background in $K^-\pi^-\pi^+$ sample

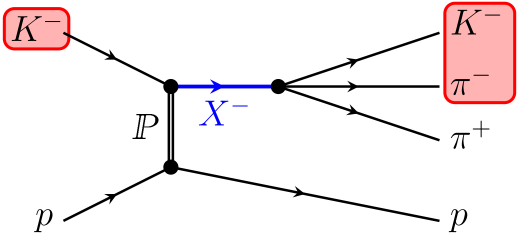

- Well established model for $\pi^- + p \to \pi^-\pi^-\pi^+ + p$
  - From very same data set
  - Measured with high precision
  - Acceptance corrected
- Generate $\pi^-\pi^-\pi^+$ Monte Carlo sample
- Mis-interpret $\pi^-\pi^-\pi^+$ Monte Carlo events as $K^-\pi^-\pi^+$
  - Apply wrong mass assumption
  - Same event reconstruction and selection as for $K^-\pi^-\pi^+$
- Perform partial-wave decomposition of mis-interpreted $\pi^-\pi^-\pi^+$ Monte Carlo sample
  - Using the same PWA model as for measured $K^-\pi^-\pi^+$ sample

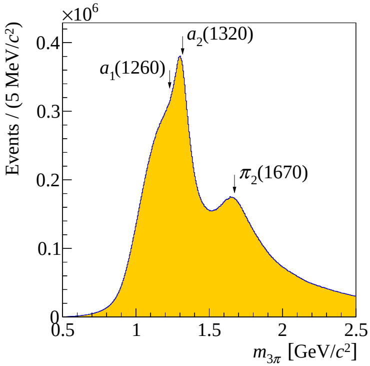

Incoherent $\pi^-\pi^-\pi^+$ Background

[Phys. Rev. D 95 (2017) 032004]

- Well established model for $\pi^- + p \to \pi^-\pi^-\pi^+ + p$
  - From very same data set
  - Measured with high precision
  - Acceptance corrected
- Generate $\pi^-\pi^-\pi^+$ Monte Carlo sample
- Mis-interpret $\pi^-\pi^-\pi^+$ Monte Carlo events as $K^-\pi^-\pi^+$
  - Apply wrong mass assumption
  - Same event reconstruction and selection as for $K^-\pi^-\pi^+$
- Perform partial-wave decomposition of mis-interpreted $\pi^-\pi^-\pi^+$ Monte Carlo sample
  - Using the same PWA model as for measured $K^-\pi^-\pi^+$ sample

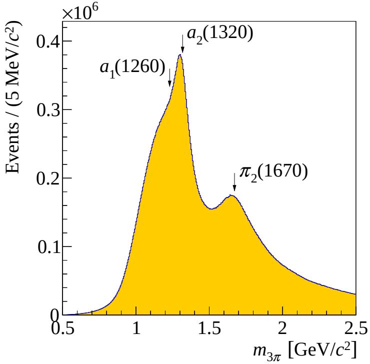

Incoherent $\pi^-\pi^-\pi^+$ Background

[Phys. Rev. D 95 (2017) 032004]

- Well established model for $\pi^- + p \to \pi^-\pi^-\pi^+ + p$
  - From very same data set
  - Measured with high precision
  - Acceptance corrected
- Generate $\pi^-\pi^-\pi^+$ Monte Carlo sample
- Mis-interpret $\pi^-\pi^-\pi^+$ Monte Carlo events as $K^-\pi^-\pi^+$
  - Apply wrong mass assumption
  - Same event reconstruction and selection as for $K^-\pi^-\pi^+$
- Perform partial-wave decomposition of mis-interpreted $\pi^-\pi^-\pi^+$ Monte Carlo sample
  - Using the same PWA model as for measured $K^-\pi^-\pi^+$ sample

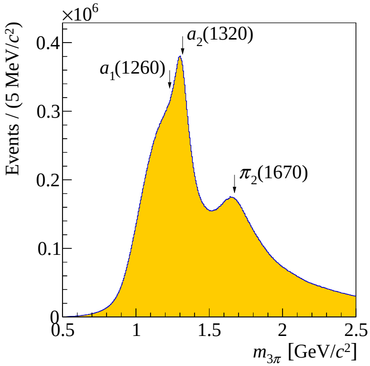

Incoherent $\pi^-\pi^-\pi^+$ Background

[Phys. Rev. D 95 (2017) 032004]

- Well established model for $\pi^- + p \to \pi^-\pi^-\pi^+ + p$
  - From very same data set
  - Measured with high precision
  - Acceptance corrected
- Generate $\pi^-\pi^-\pi^+$ Monte Carlo sample
- Mis-interpret $\pi^-\pi^-\pi^+$ Monte Carlo events as $K^-\pi^-\pi^+$
  - Apply wrong mass assumption
  - Same event reconstruction and selection as for $K^-\pi^-\pi^+$
- Perform partial-wave decomposition of mis-interpreted $\pi^-\pi^-\pi^+$ Monte Carlo sample
  - Using the same PWA model as for measured $K^-\pi^-\pi^+$ sample

➥ Study $\pi^-\pi^-\pi^+$ background in individual $K^-\pi^-\pi^+$ partial waves

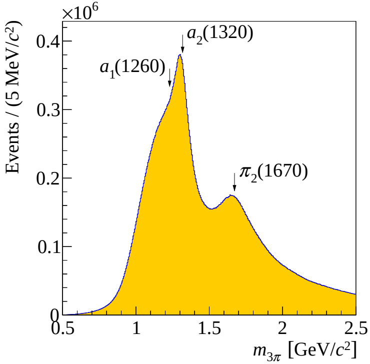

Incoherent $\pi^-\pi^-\pi^+$ Background

- Significant contribution to waves with $\rho(770)$ isobar
- $\pi^-\pi^-\pi^+$ produces peaking structures
- Largest relative contribution to $2^+ 1^+ \rho(770)\, K\, D$ wave
- Small contribution to waves with $K^*(892)$ isobar
- Also significant contribution to waves with $f_2(1270)$ and $K_2^*(1430)$ isobars
- No contribution to flat wave

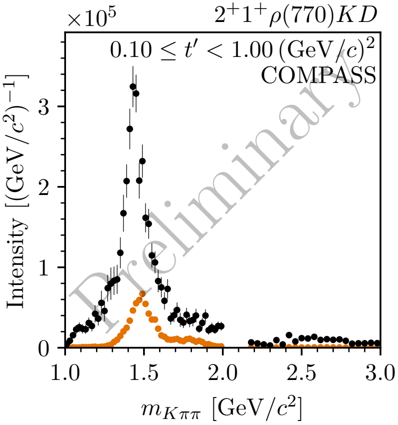

$K^-\pi^-\pi^+$ data, $\pi^-\pi^-\pi^+$ pseudo data

Incoherent $\pi^-\pi^-\pi^+$ Background

- Significant contribution to waves with $\rho(770)$ isobar
- $\pi^-\pi^-\pi^+$ produces peaking structures
- Largest relative contribution to $2^+\,1^+\,\rho(770)\,K\,D$ wave
- Small contribution to waves with $K^*(892)$ isobar
- Also significant contribution to waves with $f_2(1270)$ and $K_2^*(1430)$ isobars
- No contribution to flat wave

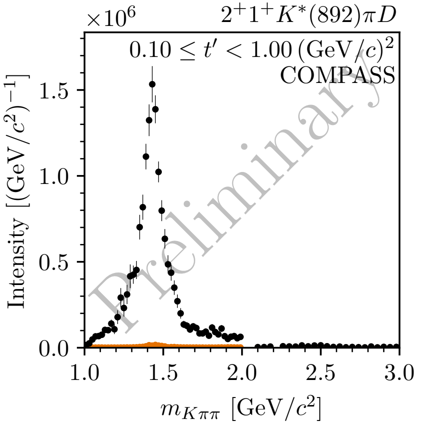

$K^-\pi^-\pi^+$ data, $\pi^-\pi^-\pi^+$ pseudo data

Incoherent $\pi^-\pi^-\pi^+$ Background

- Significant contribution to waves with $\rho(770)$ isobar
- $\pi^-\pi^-\pi^+$ produces peaking structures
- Largest relative contribution to $2^+1^+\rho(770)KD$ wave
- Small contribution to waves with $K^*(892)$ isobar
- Also significant contribution to waves with $f_2(1270)$ and $K_2^*(1430)$ isobars
- No contribution to flat wave

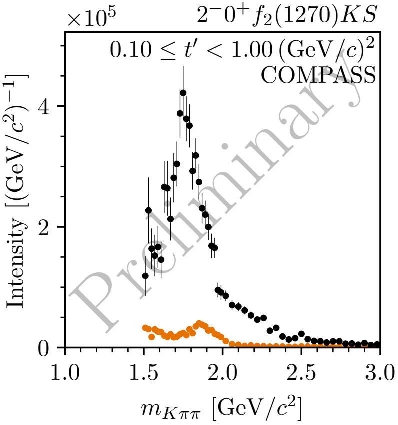

$K^-\pi^-\pi^+$ data, $\pi^-\pi^-\pi^+$ pseudo data

Incoherent $\pi^-\pi^-\pi^+$ Background

- Significant contribution to waves with $\rho(770)$ isobar
- $\pi^-\pi^-\pi^+$ produces peaking structures
- Largest relative contribution to $2^+ 1^+ \rho(770) K D$ wave
- Small contribution to waves with $K^*(892)$ isobar
- Also significant contribution to waves with $f_2(1270)$ and $K_2^*(1430)$ isobars
- No contribution to flat wave

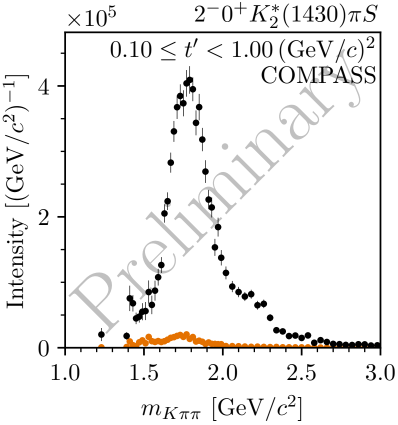

$K^-\pi^-\pi^+$ data, $\pi^-\pi^-\pi^+$ pseudo data

Incoherent $\pi^-\pi^-\pi^+$ Background

- Significant contribution to waves with $\rho(770)$ isobar
- $\pi^-\pi^-\pi^+$ produces peaking structures
- Largest relative contribution to $2^+1^+\rho(770)\,K\,D$ wave
- Small contribution to waves with $K^*(892)$ isobar
- Also significant contribution to waves with $f_2(1270)$ and $K_2^*(1430)$ isobars
- No contribution to flat wave

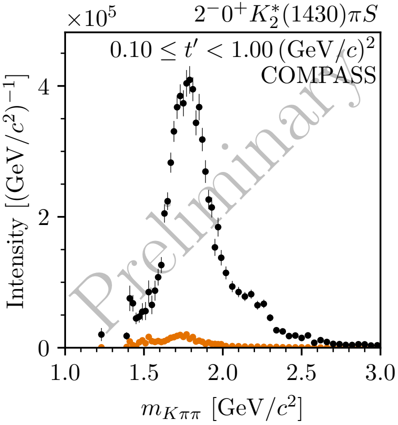

$K^-\pi^-\pi^+$ data, $\pi^-\pi^-\pi^+$ pseudo data

Incoherent $\pi^-\pi^-\pi^+$ Background

- 238-wave set can describe main features of $\pi^-\pi^-\pi^+$ pseudodata sufficiently well
- Largest deviation for $K^-\pi^+$ isobar system at thigh $m_{K\pi\pi}$

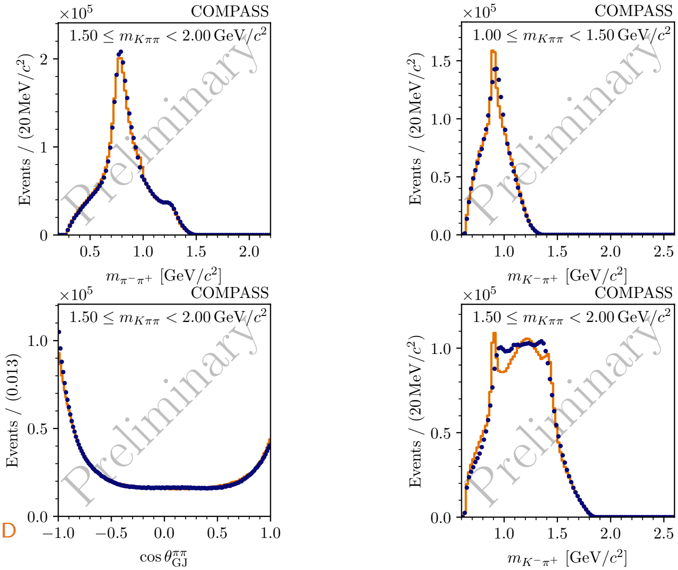

$\pi^-\pi^-\pi^+$ pseudo data,
prediction (weighted-MC) of $K^-\pi^-\pi^+$ PWD to $\pi^-\pi^-\pi^+$ pseudo data